The Geological Society of America
Field Guide 41

Pleistocene megaflood landscapes of the Channeled Scabland

Victor R. Baker*
Department of Hydrology and Atmospheric Sciences, The University of Arizona, Tucson, Arizona 85721-0011, USA

Bruce N. Bjornstad
Ice Age Floodscapes, Richland, Washington 99354, USA

David R. Gaylord
School of the Environment, Washington State University, Pullman, Washington 99164-2812, USA

Gary A. Smith
Organization, Information, and Learning Sciences, MSC05 3020, University of New Mexico, Albuquerque, New Mexico 87131, USA

Scott E. Meyer
Office of Water Programs, California State University Sacramento, Sacramento, California 95819-6025, USA

Petteri Alho
Department of Geography, Turku University, Turku, Fl-20014, Finland

Roy M. Breckenridge
Idaho Geological Survey, University of Idaho, Moscow, Idaho 83843, USA

Mark R. Sweeney
Earth Sciences Department, University of South Dakota, Vermillion, South Dakota 57069, USA

Marek Zreda
Department of Hydrology and Atmospheric Sciences, The University of Arizona, Tucson, Arizona 85721-0011, USA

ABSTRACT

The Channeled Scabland of east-central Washington comprises a complex of anastomosing fluvial channels that were eroded by Pleistocene megaflooding into the basalt bedrock and overlying sediments of the Columbia Plateau and Columbia Basin regions of eastern Washington State, U.S.A. The cataclysmic flooding produced huge coulees (dry river courses), cataracts, streamlined loess hills, rock basins, butte-and-basin scabland, potholes, inner channels, broad gravel deposits, and immense gravel bars. Giant current ripples (fluvial dunes) developed in the coarse gravel bedload. In the 1920s, J Harlen Bretz established the cataclysmic flooding origin for the Channeled Scabland, and Joseph Thomas Pardee subsequently demonstrated that the megaflooding derived

*baker@email.arizona.edu

Baker, V.R., Bjornstad, B.N., Gaylord, D.R., Smith, G.A., Meyer, S.E., Alho, P., Breckenridge, R.M., Sweeney, M.R., and Zreda, M., 2016, Pleistocene megaflood landscapes of the Channeled Scabland, *in* Lewis, R.S., and Schmidt, K.L., eds., Exploring the Geology of the Inland Northwest: Geological Society of America Field Guide 41, p. 1–73, doi:10.1130/2016.0041(01).

from the margins of the Cordilleran Ice Sheet, notably from ice-dammed glacial Lake Missoula, which had formed in western Montana and northern Idaho. More recent research, to be discussed on this field trip, has revealed the complexity of megaflooding and the details of its history.

To understand the scabland one has to throw away textbook treatments of river work.

—J. Hoover Mackin, as quoted in Bretz et al. (1956, p. 960)

INTRODUCTION

Overview of This Guide

The Channeled Scabland of the Columbia River Basin is home to the best-studied examples of landscapes created by catastrophic flooding, as well as the effects of associated eolian, glacial, and mass-wasting processes. These terrains provide exceptional analogs for the study of similar landscapes that are increasingly being recognized in other parts of the world (Baker, 2013; Komatsu et al., 2015), as well as on the planet Mars (Baker, 1982; Baker et al., 2015). The late Pleistocene megaflood landforms of the Channeled Scabland include both erosional and depositional forms. Deposits associated with the latter provided source materials for very interesting eolian features located throughout the region. Because we will see many of these features along the field-trip route, this guide describes the eolian landscapes in some detail.

The formal field trip starts in Spokane, Washington. We will spend three days with two overnights, ending in Moscow, Idaho. An optional pre-trip focused on the Spokane area is highly recommended. This involves a half-day excursion emphasizing late Quaternary megaflood-influenced sedimentary deposits associated with glacial Lake Columbia. There is an extended description of this area by D. Gaylord, S. Meyer, and R. Breckenridge. An extended description of low-energy megaflood deposits is authored by G. Smith and can be found near the end of the regular field-trip log. Eolian features also receive an extended description for Day 2 of the regular trip in a mini section by D. Gaylord and M. Sweeney.

Portions of this guide were modified and updated from other Geological Society of America guidebook chapters that involved the authors. These include Webster et al. (1976), Baker (1977, 1987b, 1989), Bjornstad et al. (2007), and Keszthelyi et al. (2009). Additional guidebooks and guidebook papers of relevance include Baker and Nummedal (1978), Waitt (1994), Waitt et al. (2009), Bjornstad (2006a), and Bjornstad and Kiver (2012).

Geologic and Geographic Setting (Baker)

The Columbia River Basin is situated in eastern Washington. To the north and east stand the Rocky Mountains, uplifted during the Laramide orogeny. The basin lies east of the Cascade Mountain Range, which is located where a volcanic arc has persisted since ca. 50 Ma, culminating in a chain of immense Quaternary volcanoes. It also lies just north of the Basin and Range province, which was produced by the ongoing extension of western North America.

The basin proper is often referred to as a plateau since much of it stands ~500 m or more above sea level. However, because it is surrounded by higher topography on all sides, we prefer to call it a "basin." Its northern and western boundaries are demarked by the Columbia River. The Snake River runs close to the southern boundary.

Columbia River Basalt Group (Baker; Modified from Keszthelyi et al., 2009)

The Miocene Columbia River Basalt Group is the youngest and best-preserved continental flood basalt province on Earth (Fig. 1). It is composed of four stratigraphic units (e.g., Tolan et al., 1989; Reidel et al., 2013). The oldest, the Imnaha Basalt, erupted at ca. 17.5 Ma. Now mostly exposed near the southern margin of the province, many of these flows were canyon confined as the lava inundated the preexisting topography. Approximately 87% of the Columbia River Basalt Group's volume is within the next unit, the 17–15.5 Ma Grand Ronde Basalt. The Wanapum Basalt records the waning stages of the main lava pulse through ca. 14.5 Ma. The Saddle Mountains Basalt includes a series of late stage eruptions that ended at ca. 6 Ma.

The Columbia River Basalt Group contains hundreds of lava flows, each 20–100 m thick. The lava pile is generally ~1 km thick, but reaches ~3.5 km in the center of the basin. Most of the lavas are basaltic andesites with 53–57.5 wt% SiO_2 (e.g., Hooper, 1997). These high silica contents may indicate significant crustal contamination. The nature of the mantle source is less clear, with three to four different components required to explain the isotopic data. The dense interiors of most of the lava flows are very chemically homogenous, allowing much of the stratigraphy to be deciphered through a combination of geochemistry and paleomagnetism. However, when examined in detail, there are vertical variations in chemistry within some lava flows (e.g., Reidel and Fecht, 1987; Reidel, 2005).

The vents for these lava flows are found along the southeastern margin of the province. They were fed by long dikes, generally 10–100 m wide (e.g., Swanson et al., 1975). While a lava pond

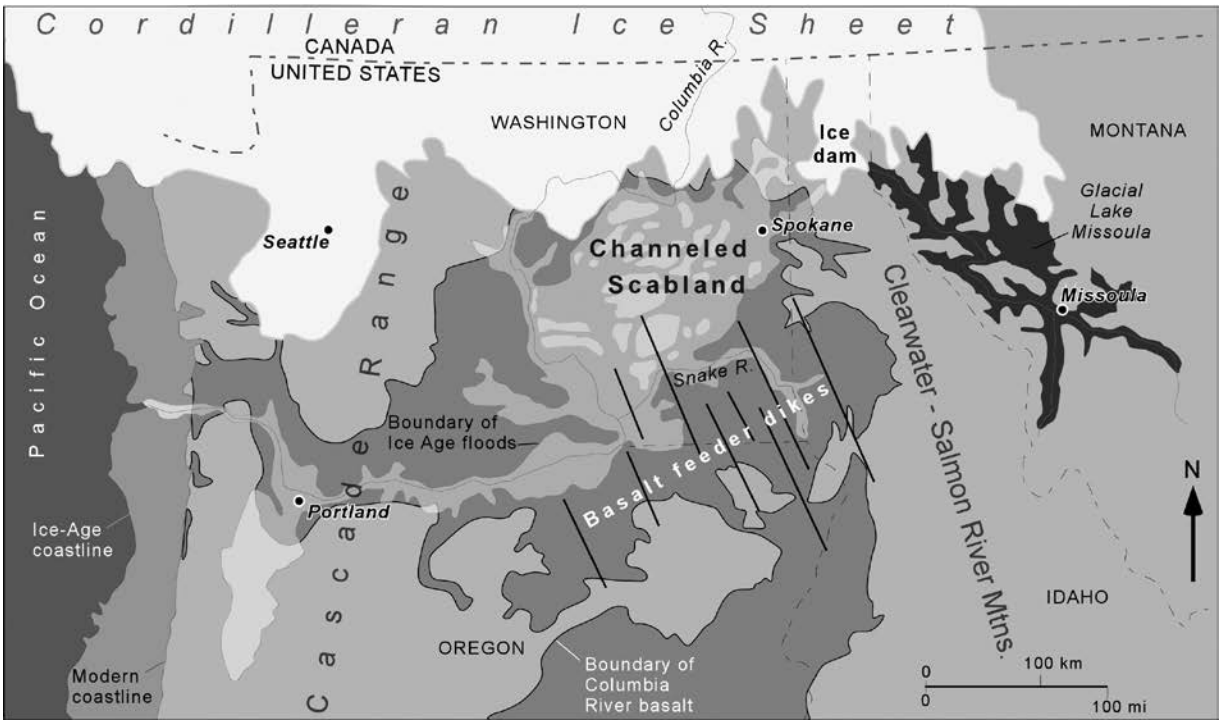

Figure 1. Distribution of Miocene Columbia River Basalt Group rocks in relation to Pleistocene megafloods in the Pacific Northwest.

has been found (Reidel and Tolan, 1992), the near-vent areas are dominated by vast areas covered by spatter. The spatter can be seen transitioning into lava flows, providing direct evidence that the flows were generally fountain fed. Very low shields probably existed, but no prominent volcanic edifices were constructed. Instead, fissures >100 km long appear to have been the main vent feature. However, it is likely that only some tens of kilometers were fountaining along these fissures at any given time (e.g., Self et al., 1997).

Initial models for the emplacement of these flood lava flows indicated massive turbulent floods with eruption durations on the order of weeks (Shaw and Swanson, 1970). This follows inevitably if one assumes that the lava was emplaced as a single ~30-m-thick sheet. The volumetric eruption flux needed for such a scenario would be of the order 10^6 m^3/s (for comparison, the current Kilauea eruption produces ~3 m^3/s and the largest basaltic eruption witnessed by humans, the 1783–1784 Laki eruption in Iceland, peaked at a few thousand m^3/s). Thermal modeling shows that such turbulent floods would allow lava to be transported hundreds of kilometers without significant cooling (Keszthelyi et al., 2006).

However, the field observations suggest a very different mode of emplacement. The pahoehoe surfaces of, and the vesicle distributions within, many of the lavas in the Columbia River Basalt Group are identical to those in Hawaiian inflated pahoehoe flows (e.g., Self et al., 1996; Thordarson and Self, 1998). While the overall thickness of the Columbia River Basalt Group lavas is typically an order of magnitude greater than the Hawaiian examples, it seems that the same process produced both. Examples in Iceland, intermediate in size between the Hawaiian and Columbia River Basalt Group lavas, support the idea that the flows were produced relatively slowly with lava moving under a thick insulating crust. The duration of the emplacement of individual lobes can be estimated from the time needed to produce the observed crust atop the active flows, with most Columbia River Basalt Group major flow lobes taking months to a few years to form. Each eruption has several lobes, and thus an eruption duration of about a decade seems to have been typical. This longer eruption duration implies an average effusion rate of some thousands of m^3/s (e.g., Self et al., 1996; Thordarson and Self, 1998).

An important variant on the classic inflated pahoehoe model was recognized during the investigation of Icelandic analogs to Martian flood lavas (Keszthelyi et al., 2004). These flows have thick, insulating but brecciated flow tops. The breccia is composed of broken pieces of pahoehoe instead of the spinose clinker characteristic of classic Hawaiian aa. These "rubbly" pahoehoe flows appear to have formed when surges passed through an inflating pahoehoe sheet flow. The estimated flux during these surges is of the order 10^4–10^5 m^3/s. The discovery of such lava flows in the Columbia River Basalt Group suggests that some flows may have been emplaced more rapidly than the classic inflated pahoehoe, but even these eruptions probably lasted some years.

The Columbia River Basalt not only provides excellent sites to study the emplacement of flood lavas, but also to investigate a

wide variety of lava-water interactions. Pillow lavas and hyaloclastites involve the most water, having formed when lava entered large bodies of water. Typically, the pillows and hyaloclastites are found in deltas with foreset beds that were built as the lava pushed into the water (e.g., Fuller, 1932). Most deltas are capped with subaerial lavas that formed after the delta built above the water surface. Entablature-style jointing is also diagnostic of extensive water cooling. The thick Columbia River Basalt Group lava flows can have multiple tiers of entablature and colonnade jointing, recording multiple episodes of inundation by water (e.g., Long and Wood, 1986). The structural particulars of the flows (Fig. 2) are of great importance for their influences on megaflooding erosion processes. Colonnade zones are preferentially subject to plucking-type erosion, while entablature zones commonly are preserved as erosionally resistant layers.

J Harlen Bretz and the Channeled Scabland (Baker)

The Channeled Scabland in east-central Washington State was named and described by J Harlen Bretz in a series of papers during the 1920s and 1930s. The description from Bretz (1928, p. 446) makes one marvel at what could be accepted for publication in the peer-reviewed scientific literature of the time:

> No one with an eye for landforms can cross eastern Washington in daylight without encountering and being impressed by the "scabland." Like great scars marring the otherwise fair face to the plateau are these elongated tracts of bare, black rock carved into mazes of buttes and canyons. Everybody on the plateau knows scabland. … The popular name is a metaphor. The scablands are wounds only partially healed—great wounds in the epidermis of soil with which Nature protects the underlying rock. … The region is unique: let the observer take wings of the morning to the uttermost parts of the earth: he will nowhere find its likeness.

Bretz defined "scablands" as lowlands diversified by a multiplicity of irregular channels and rock basins eroded into basalt. The Channeled Scabland is a spectacular complex of anastomosing channels, cataracts, streamlined loess "islands," rock basins, broad gravel deposits, and immense gravel bars. Field relations among many of these features, most notably the multiple levels of divide crossings, the cataracts, gravel bars, and rock basins led Bretz to propose that an immense cataclysmic flood had swept across the Columbia Plateau in late Pleistocene time (Bretz, 1923; Bretz et al., 1956). So much floodwater crossed the plateau that it completely filled the preexisting valleys, allowing water to spill across the intervening divides. In this way, the pre-flood valleys were transformed into a complex of dividing and rejoining channel ways (Fig. 3).

Bretz was born Harley Bretz (the "J Harlen" came later) on 2 September 1882, in the small farming town of Saranac in central Michigan. He had a childhood interest in many aspects of natural science, and majored in biology at Albion College in Albion, Michigan. After graduating, he taught biology for a brief period in Flint, Michigan. In 1907, he and his wife Fanny (whom he met at Albion) moved to Seattle, Washington, where Bretz taught at three different high schools over the next several years. During the long summers, he explored the local glacial geology. His mapping of Pleistocene surficial deposits at a scale of 1 inch to 6 miles eventually covered the entire Puget Sound region from Centralia and Chehalis to the Canadian border.

Bretz recalled (1978, personal commun.) that around 1909, while he was teaching high school science in Seattle, he became intrigued by an unusual landform on the newly published Quincy topographic sheet of the U.S. Geological Survey. The map clearly shows what we now know as the Potholes Cataract (seen at Stop 9 on Day 2 of this field trip) of the western Quincy Basin (Fig. 4). Bretz wondered how this now-dry ancient waterfall could have been formed without an obvious river course leading to it. His questions to geology faculty members at the University of Washington provided no satisfactory answer, and this question apparently stuck in his mind as he worked on glacial geological studies of the Puget Sound region. The results earned Bretz a Ph.D. in geology from the University of Chicago in 1913.

In reviewing the Ph.D. dissertation, Bretz's supervisor, Rollin D. Salisbury, asked about the name on the author line, 'J Harlen Bretz,' "Shouldn't the full name be spelled out?" Bretz purportedly replied that "J" was the entire first name and thus could not be abbreviated. To this Salisbury admonished, "Then never put or allow a typist or printer to use a period after that J". Thus began a lifelong battle. "Throughout all my life," Bretz recalled in his unpublished memoirs, "I have fought typists and printers to leave off that damned period and haven't always won." Bretz's biographer, John Soennichsen, (2008, p. 12) quotes Bretz's daughter, Rhoda, on this issue: "He invented the Harlen thing, just as he had invented the J in front of his name—made the whole thing up. Harley Bretz was his given name, but it just didn't ring a bell for him; maybe he didn't think it sounded professional enough."

Upon receiving his Ph.D., Bretz spent a year as an assistant professor on the faculty of the University of Washington. In 1914, Salisbury recruited Bretz to return to the University of Chicago, first as an instructor in geology (1914–1915), then as an assistant professor (1915–1921). Bretz's willingness to return to Chicago seems to have arisen in part because of disagreements with more senior colleagues at the University of Washington over educational philosophy. Perhaps influenced by his own largely self-taught path to geological understanding, and possibly reinforced by his Chicago mentors, Bretz became a lifelong advocate of geological education in the field, as opposed to the classroom. He later wrote in his unpublished memoirs, "My ideal was to teach geology from the field as much as possible." The Washington geology department had emphasized "text book and lecture methods without field work."

In 1916, Bretz initiated an advanced field course during the early summer, in which he took small numbers of University of Chicago students to the northwestern United States. Starting in the summer of 1922, this advanced course moved to the Columbia Plateau region of eastern Washington. Thomas Large,

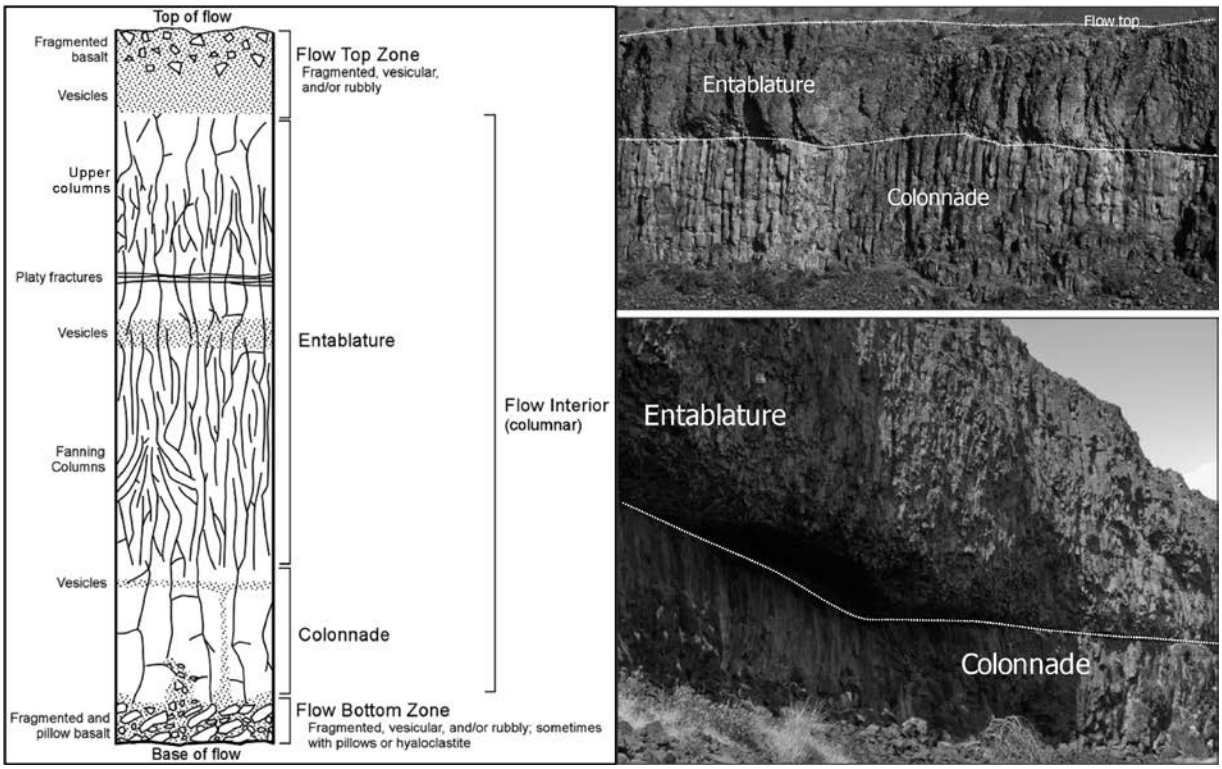

Figure 2. Internal structure and fracture patterns within a Columbia River Basalt flow. These are of particular importance as controls on megaflood erosion processes. See text for further explanation.

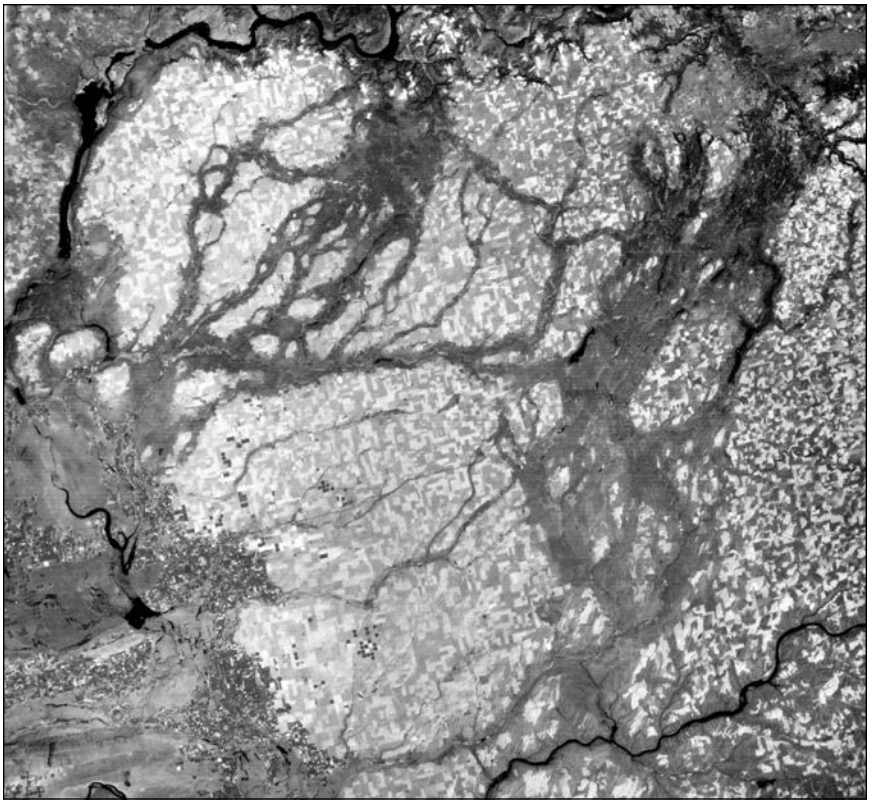

Figure 3. The Channeled Scabland as visible from spacecraft imagery. This scene represents an area of ~160 × 150 km. The scabland channels appear as a darker gray on the image because the overlying cover of loess (bright tones with checkerboard pattern of agricultural fields) was eroded away to expose the underlying basalt bedrock. (Landsat image 1039-18143.)

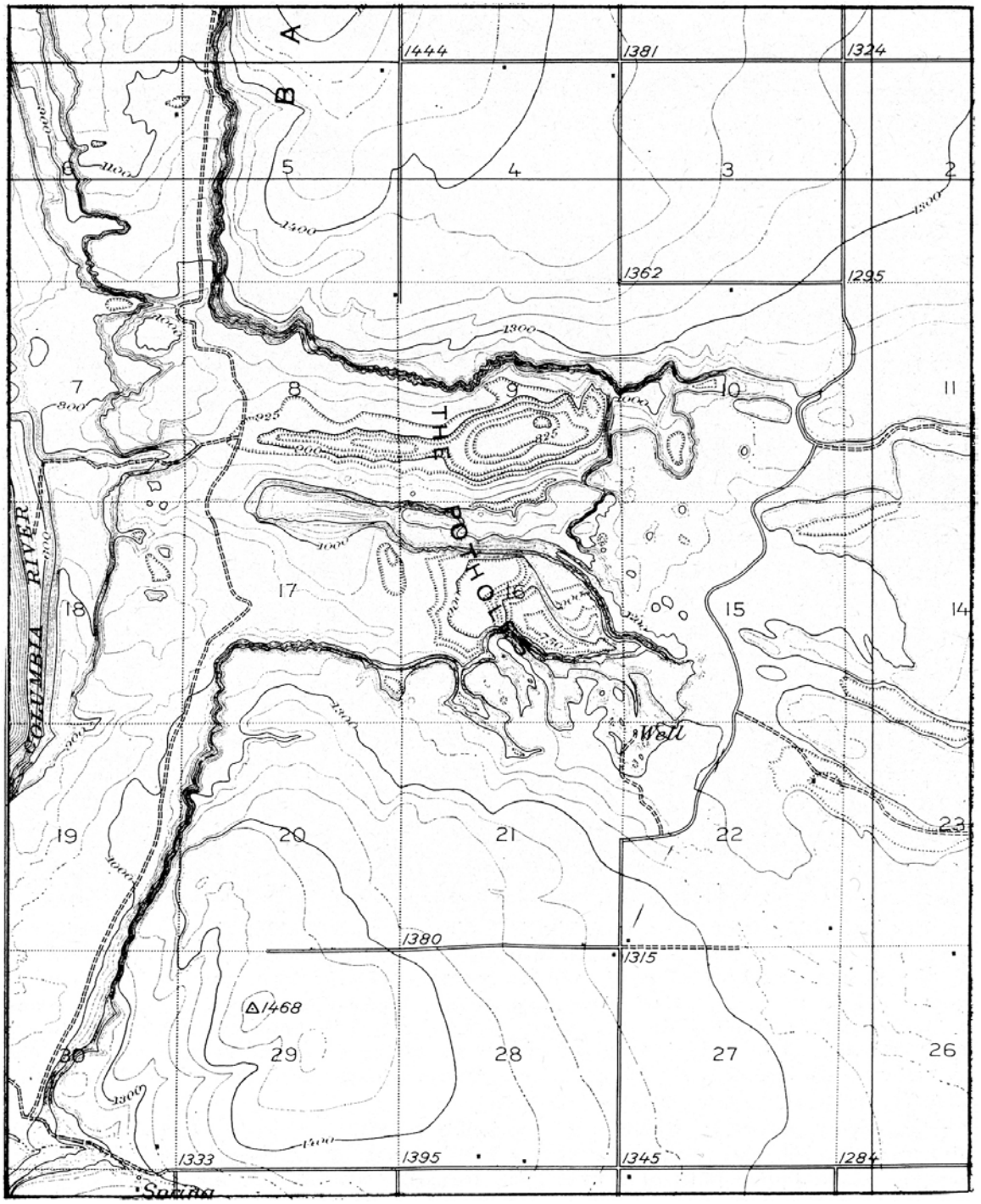

Figure 4. Topographic map of The Potholes, which is one of three cataract spillways that drained late Pleistocene megaflooding flows on the western side of the Quincy Basin. (From the U.S. Geological Survey Quincy topographic quadrangle map, with 25 ft [7.6 m] contour interval and 1 mile [1.6 km] numbered section squares.)

a teacher at Lewis and Clark High School in Spokane, Washington (and one of the founders of the Northwest Scientific Society), aided with local logistical arrangements. In the course of work during the summers of 1922 and 1923, Bretz and his students (Fig. 5) found an amazing assemblage of landforms that included coulees, immense dry cataracts, rock basins, anastomosing channel ways, and gravel bars. Field relations among these features, most notably the multiple levels of divide crossings, led Bretz to propose that an immense cataclysmic flood had swept across the Columbia Plateau in late Pleistocene time, creating the great plexus of channel ways known as the Channeled Scabland.

In a 1923 paper on the Channeled Scabland, Bretz concluded, "It was a debacle which swept the Columbia Plateau" (Bretz, 1923, p. 649). He named this debacle the "Spokane Flood," thereby initiating the famous controversy. As Bretz well knew, the notion of catastrophic flooding directly challenged substantive and epistemological notions of uniformitarianism that were thought (erroneously) to underpin geology as a science (see Baker, 1998). These uniformitarian principles held that cataclysmic processes, like those responsible for the origin of the Channeled Scabland, were unsuitable topics for scientific investigation. To counter this presumption, Bretz conducted extensive field investigations each summer, the results of which he meticulously detailed in more than a dozen major papers from 1923 to 1932.

How was it that this outrageous idea got published? In today's culture of "publish or perish," outrageous hypotheses tend to get soundly squelched within the secret rituals of the anonymous peer-review process. Today's younger scientists, wary of their citation indices, are reluctant to expend effort on topics that deviate from what the community currently holds to be appropriate or fashionable paths of inquiry. But Bretz had some advantages for getting published. He became tenured, promoted to associate professor, and, just prior to the paper submission to the *Journal of Geology*, he was named to the editorial board of that journal. The latter honor meant that Bretz had direct influence on the journal's editorial decisions. More importantly, however, as shown by his earlier conflicts with colleagues over educational philosophy and his own approach to science, Bretz was totally and stubbornly devoted to placing the highest priority on what "Nature" had to tell him, as opposed to what various reputable scientists might have to say about "Nature" through their uniformitarian theories. The ensuing scabland debate would rage on for several decades (see Baker, 1978a, 2008a), and after his decade of intensive work, Bretz largely abandoned the scene for the next 20 years. He trusted that a resolution of the controversy would eventually be found when others finally devoted appropriate field effort to studying the problem.

Resolution of the Channeled Scabland controversy did indeed come gradually, initially with the documentation by Joseph Thomas Pardee (1871–1960) of ice-dammed Pleistocene glacial Lake Missoula in western Montana as the plausible source for the scabland floodwater (Baker, 1995). Eventually the accumulating field evidence became overwhelming, particularly when Bretz and others synthesized new data obtained by the Bureau of Reclamation during the development of the Columbia Basin Irrigation Project in the 1950s. Especially important for convincing the many flood skeptics was the discovery that giant current ripples (subfluvial gravel dunes) cap many of the scabland gravel mounds that Bretz had correctly interpreted in the 1920s to be river bars. As this evidence mounted and as advances occurred in the quantitative understanding of the physical processes of cataclysmic flooding, Bretz's bold hypothesis came to be almost universally accepted by the early 1970s.

Figure 5. J Harlen Bretz (left) with University of Chicago graduate students at a cabin near Spokane, Washington, during fieldwork in the early 1920s. Photograph provided by Brian Macdonald and probably taken by Thomas Large.

At age 97, in recognition for more than 70 years of scientific achievements, J Harlen Bretz was honored with the 1979 Penrose Medal, the highest award of the Geological Society of America. In accepting the award, Bretz (1980, p. 1095) listed his major research accomplishment as follows: "Perhaps I can be credited with reviving and demystifying legendary catastrophism and challenging a too rigorous uniformitarianism." Eccentric to the end, however, he told friends that he did have one major regret about it all. He had outlived all his critics, and he was not able to gloat over them now that he was receiving the long overdue recognition for his work.

MEGAFLOODING

Megaflood Landscapes and Their Significance (Baker)

After centuries of geological controversy, it is now well established that the last major deglaciation of planet Earth involved huge fluxes of freshwater from the wasting continental ice sheets (Baker, 1994, 2002a, 2009a), and that much of this water was delivered as floods of immense magnitude and relatively short duration (Baker, 1997, 2002b). A recent review by Baker (2013) documents 40 examples of late Pleistocene megaflood landscapes in North and South America, Europe, and Asia. The central Asian region is particularly important, with recent studies revealing

many examples with great similarity to those in the northwestern United States (Baker et al., 1993; Komatsu et al., 2009, 2015). Many of the late Quaternary megafloods had short-term peak flows comparable in discharge to the more prolonged fluxes of ocean currents (Baker, 2009a). The discharges for both ocean currents and megafloods generally exceed one million cubic meters per second, hence the prefix "mega." A discharge of 1 million cubic meters per second is also termed a "sverdrup," a unit that has more commonly been applied to ocean currents. Such immense flows likely induced very rapid, short-term effects on Quaternary climates (Baker, 2009b), and the late Quaternary megafloods also greatly altered drainage evolution and the planetary patterns of water and sediment movement to the oceans (Baker, 2007).

The Channeled Scabland region that was classically studied by Bretz is now seen as but a small component in a source-to-sink system extending from ice-marginal lacustrine (glacial Lakes Columbia and Missoula) and possible subglacial sources beneath the Cordilleran Ice Sheet, through the scabland intermediate zone, and on to sink relationships on the abyssal plain of the Pacific Ocean. Other North American glacial megaflood landscapes are now recognized in the Columbia and Snake River drainages of the northwestern United States; in the spillway systems of the upper Mississippi Basin; near the Great Lakes and adjacent St. Lawrence Basin; the Hudson River Basin; the Mackenzie Basin; the Yukon Basin (Porcupine River); the Sustina and Copper River Basins (Alaska); and the Hudson Strait (Fig. 6).

In South America, megafloods of the Santa Cruz River system (Argentina) emanated from the Patagonian Ice Sheet, and other Patagonian megaflooding occurred on the Chilean side. In Eurasia, the megaflooding from the margins of the Fennoscandian Ice Sheet spilled through the English Channel (Gupta et al., 2007). In the mountain areas of central northern Asia, there were megaflood outbursts from the Issyk-Kul area, the Altai Mountains (upper Ob drainage), and the upper Yenesei River system. Less well understood is a much grander scale of possible megaflooding that includes a system of late-glacial flood spillways extending over a distance of ~8000 km from northern and eastern Siberia to the Mediterranean (Grosswald, 1998, 1999; Baker, 2007).

Ice-marginal lakes are the sources of the largest, well-documented glacial megafloods. Perhaps the most famous example is glacial Lake Missoula, which formed south of the Cordilleran Ice Sheet (CIS), in the northwestern United States. The Purcell lobe of the ice sheet extended south from British Columbia to the basin of modern Lake Pend Oreille in northern Idaho. It thereby impounded the Clark Fork River drainage to the east, forming glacial Lake Missoula, which covered ~7500 km^2 of western Montana (Fig. 7). At maximum extent this ice-dammed lake held a water volume of ~2500 km^3 with a depth of 600 m at the dam. Cataclysmic failure of the ice dam impounding this lake resulted in discharges up to ~20 sverdrups near the outlet point (O'Connor and Baker, 1992). On land, these flows produced the distinctive erosional and depositional features of the Channeled Scabland that will be highlighted on this trip. Upon reaching the Pacific Ocean, the Missoula floodwaters continued flowing down the continental slope as hyperpycnally generated turbidity currents. The sediment-charged floodwaters followed the Cascadia submarine channel into and through the Blanco fracture zone and out onto the abyssal plain of the Pacific. As much as 5000 km^3 of sediment may have been carried and distributed as turbidites over a distance of 2000 km west of the Columbia River mouth (Normark and Reid, 2003).

Repeated failures of Lake Missoula are inferred to have occurred between ca. 19 and 15 ka (Waitt, 1985; Atwater, 1986). As recognized by Baker and Bunker (1985), the multiple outburst events were of greatly differing magnitudes. About 15 exceeded 3 sverdrups, and one or more of these exceeded ~10 sverdrups in discharge through the Columbia Gorge (Benito and O'Connor, 2003). The largest failure or failures probably involved a different failure mechanism than the subglacial tunneling envisioned by Waitt (1985), because that mechanism is estimated to yield discharges of only 1–2 sverdrups (Clarke et al., 1984).

Timescale for Cordilleran Ice Sheet Flooding and Glacial Lake Missoula (Baker)

Atwater (1986), from studies of glacial Lake Columbia, infers that the Missoula floods occurred between ca. 15,550 and 13,350 radiocarbon yr B.P. (ca. 19–16 ka in calendar years)–based on varve counts above and below a 14,490 yr B.P. C^{14} date (ca. 17.6 ka) in the middle of the Sanpoil valley's Missoula-backflood sequence (an interpretation disputed by Shaw et al., 1999). Hanson and Clague (2016) studied sections throughout glacial Lake Columbia, and generally concurred with Atwater's conclusions. A section from the Hawk Bay arm of the lake yielded a radiocarbon date from plant detritus that indicates 37 relatively small flood influxes to the lake occurred after ca. 16.3 ka. From this, Hanson and Clague (2016) infer a timescale for which flooding ended at ca. 15 ka. Waitt (1985) and Waitt et al. (2009) follow Atwater (1984, 1986) in contending that a relatively short 2000- to 3000-yr timescale applies to Missoula flooding (and presumably all CIS events, except for some very small late ones).

Waitt (1985) argues that the 2000–3000 yr time interval is traceable bed-for-bed from the basin of glacial Lake Missoula through glacial Lake Columbia, the Channeled Scabland, the Willamette Valley, and presumably all the way to the Pacific Ocean (Fig. 8). A key location for this model is the Burlingame Canyon section of megaflood rhythmites (Touchet Beds) in south-central Washington. Using the Mount St. Helens set S tephra and paleomagnetic secular variation records for this section, Clague et al. (2003) find a longer timescale of accumulation, alternatively interpreted as representing ~5000 yr between either 21 and 16 ka or ~4500 yr between ca. 18 and 13.5 ka. These two age ranges are produced by assuming two different possible ages for the tephra and two different estimates of the timing between flooding events. The younger age range assumes 16.3 ka for the tephra and 60 yr between flow events; the older age range assumes 17.5 ka for the tephra and 130 yr between flow events. Neither interpretation matches the 2000–3000 yr time span inferred by Waitt (1985) from regional correlation to Atwater's (1986)

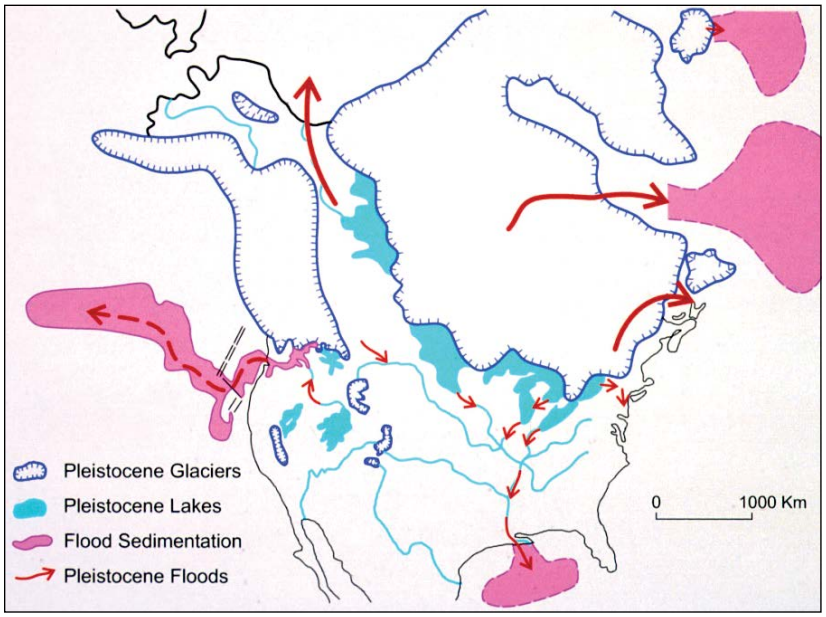

Figure 6. Pattern of late Pleistocene megaflooding areas for North America (Baker, 2013).

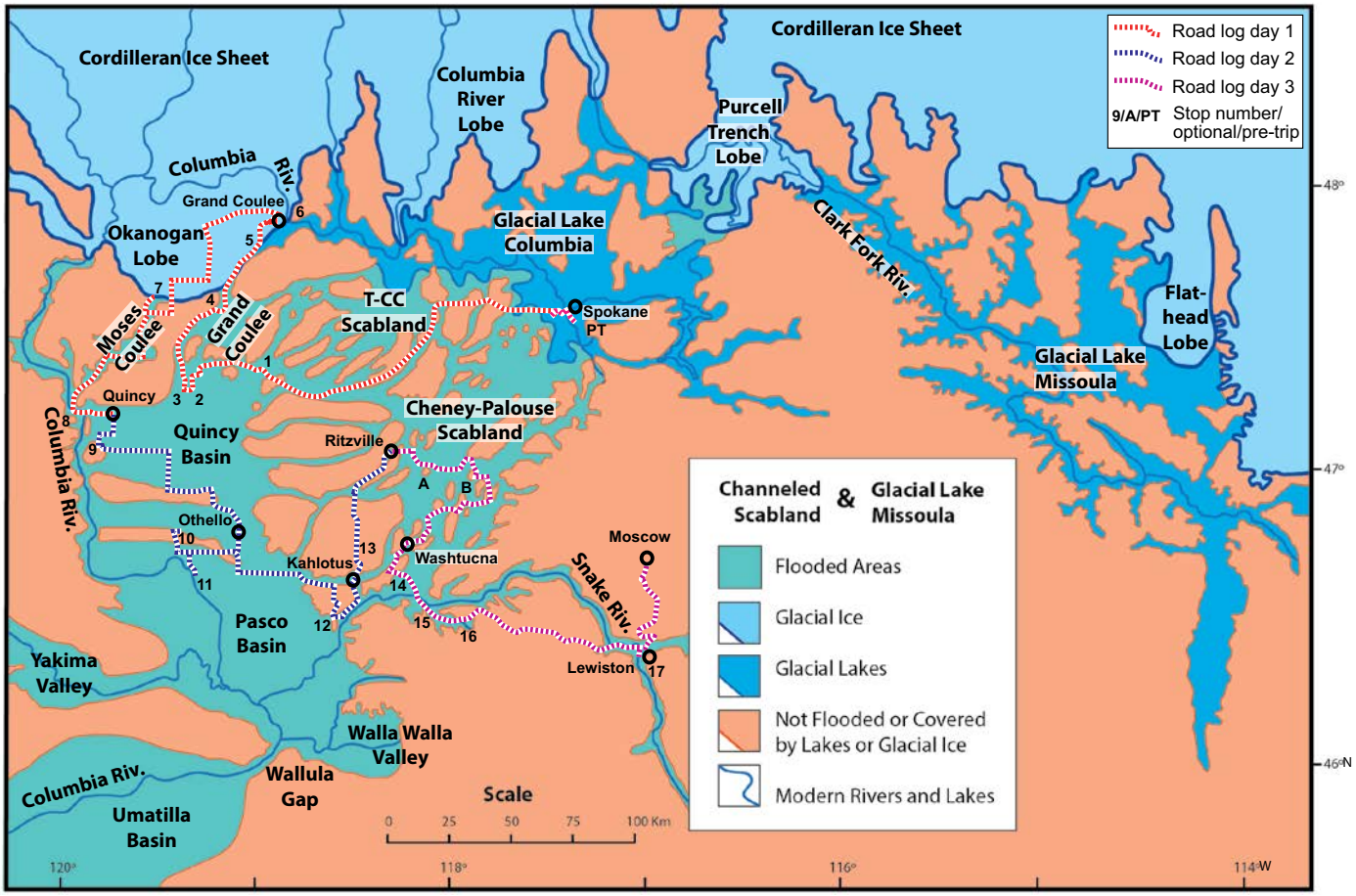

Figure 7. General location of features related to the late Pleistocene megaflooding of the Channeled Scabland. The ice dam for glacial Lake Missoula is at the top center, where the Purcell Trench lobe had its maximum extent. Another glacial lake (Columbia), 600 m lower in elevation than Lake Missoula, formed behind the Okanogan ice lobe to the west (upper left on the map). T-CC refers to the Telford–Crab Creek Scabland. All guide stops (Stops 1–17, Pre-Trip Stop, and Optional Stops A and B) appear on the figure.

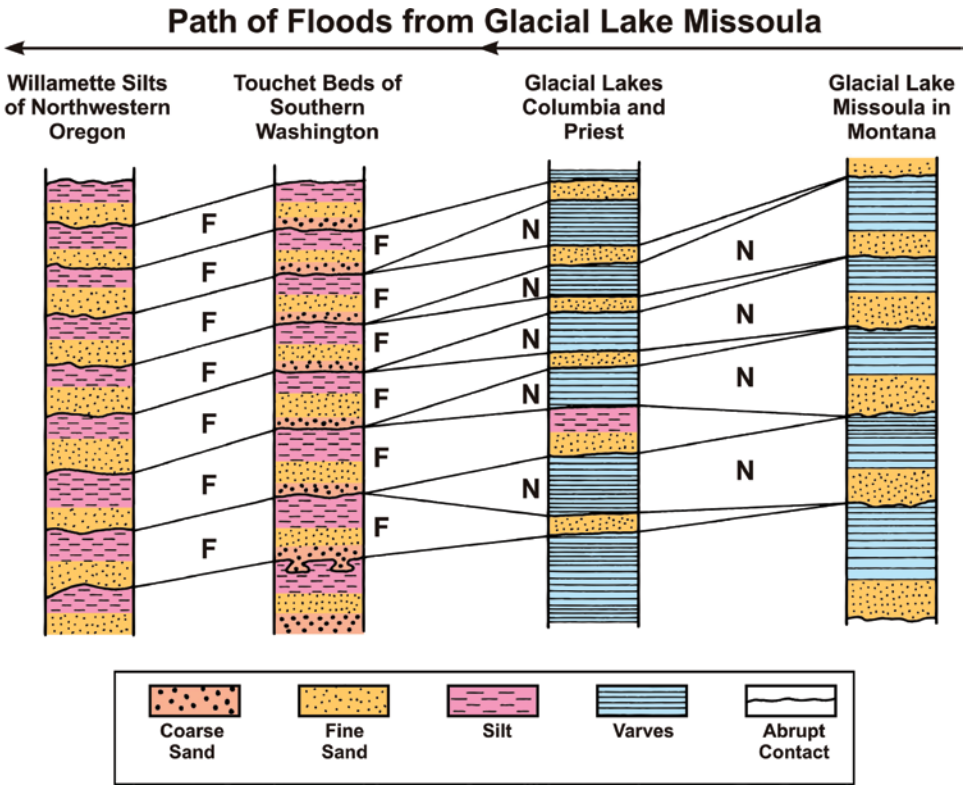

Figure 8. Bed-for-bed correlation of fine-grained flood and flood and/or lacustrine sequences throughout the region impacted by late Pleistocene southern Cordilleran Ice Sheet megaflooding, as inferred by Waitt (1985, 1994). The letters F and N refer, respectively, to layers interpreted to be flood and nonflood in origin.

glacial Lake Columbia sequence of ca. 19 and ca. 16 ka, but both these longer timescales seem better in accord with results from more recent work. Smith and Hanson (2014) cite optically stimulated luminescence (OSL) ages on quartz from three sections of fine-grained glacial Lake Missoula (GLM) glacio-lacustrine sediments (Ninemile, Rail Line, and Garden Gulch) that indicate that the phase of repeated GLM fillings and (low-energy) drainings, originally studied by Chambers (1971, 1984), occurred after 20 ka and before 13.5 ka. The longest apparently continuous varve counts from relatively thick sections of GLM lacustrine sediments indicate ~3000 yr, but the age ranges for the relevant sections are from 19.2 to 16.0 ka (Levish, 1997) and from ca. 15 to perhaps as young as 12.5 ka (Hanson et al., 2012).

Megaflood influxes from the Columbia into the northeast Pacific, inferred from freshwater diatoms (Lopes and Mix, 2009), indicate that the major peaks in freshwater influx occurred at ca. 17.5, 20, 23, 27, and 30.5 ka. Lopes and Mix (2009) estimate that that the epoch of major freshwater inputs began ca. 33 ka and ended ca. 16.5 ka, with a minor pulse at ca. 13 ka. This relatively long timescale for freshwater influxes to the Pacific Ocean from the Columbia River is similar to the time range for influxes of isotopically depleted late Pleistocene groundwater into Columbia River Basalt aquifers in eastern Washington that date from ca. 27 ka to perhaps as young as 13 ka (Brown et al., 2010).

Lopes and Mix (2009) find that the most pronounced peak of freshwater influx occurs at ca. 23 ka, and that this is followed by a rapid decline before more gradually rising freshwater influxes resume ca. 20 ka. These then peak at ca. 17.5 ka and are followed by a decline that reaches low levels by ca. 16.5 ka (Fig. 9). This dual character to the peak freshwater influxes seems to follow a pattern for glacial Lake Missoula that was originally recognized by Pardee (1942), who documented a massive early phase of glacial Lake Missoula draining that emplaced huge gravel bars and eroded constricted areas of the lake basin. Pardee's (1942) work suggests that this was followed by a later, low-energy phase in which rhythmically bedded lacustrine silt units were emplaced in many of the same areas that had earlier been impacted by the high-energy lake-draining phase. Pardee's two-phase late Pleistocene history for glacial Lake Missoula is consistent with both mapping and field relationships (Smith, 2006; Smith and Hanson, 2014) and with hydraulic flow modeling (Alho et al., 2010).

Geochronology of Channeled Scabland Megaflooding (Baker)

Evidence for early Pleistocene megaflooding in the Channeled Scabland region consists of highly weathered flood gravel that is commonly capped with a petrocalcic horizon (Bretz et al., 1956; Richmond et al., 1965; Baker, 1973a; Patton and Baker, 1978a; Baker et al., 1991a; Bjornstad et al., 2001). There is also evidence within the Palouse loess sequence, mainly erosional unconformities, that are inferred to represent early Pleistocene megaflooding phases (McDonald and Busacca, 1988; Busacca, 1989). A recent compilation by Medley (2012) identified 25 field

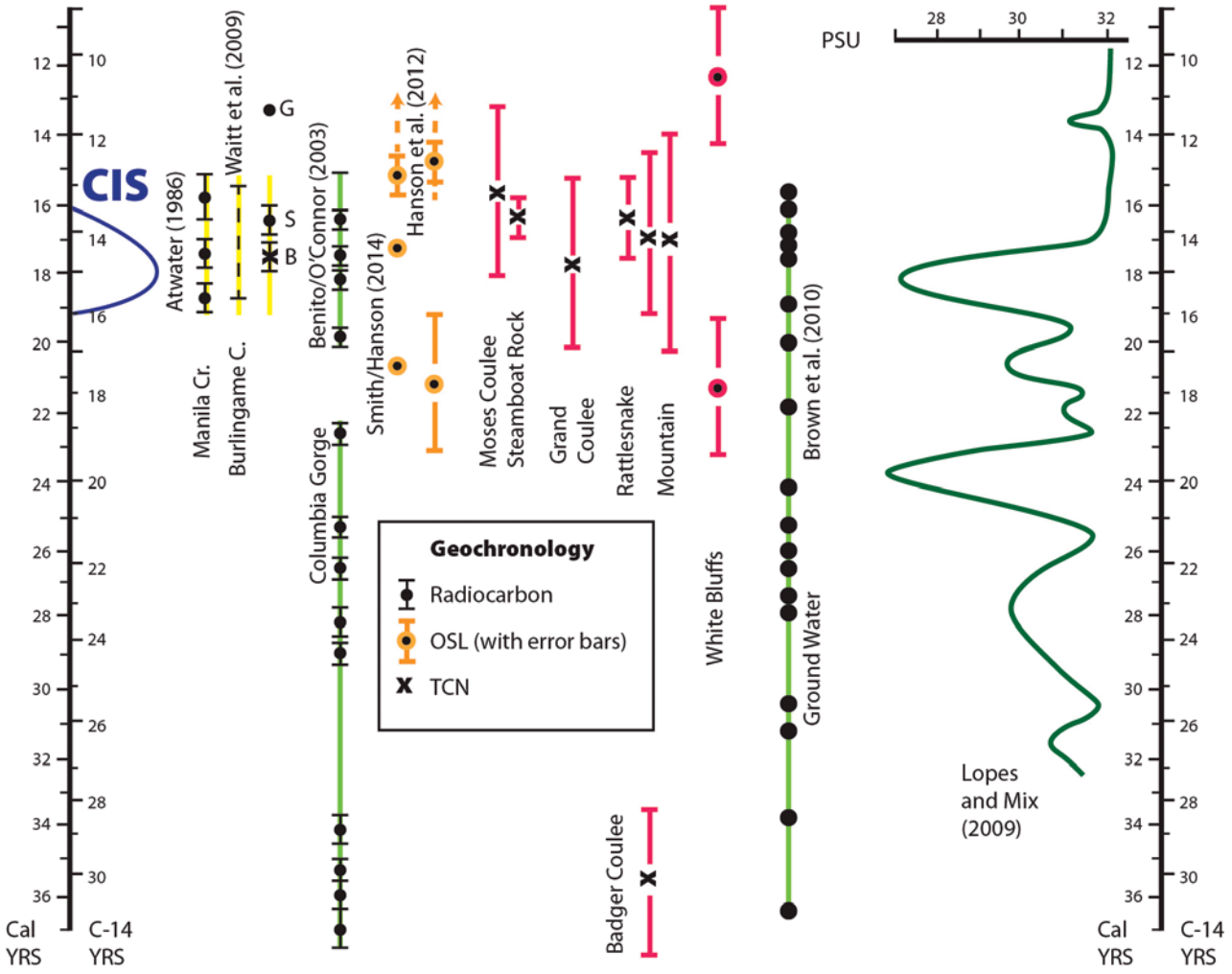

Figure 9. Highly approximate summary diagram (for discussion purposes) illustrating some of the published geochronology data relevant to the timing of northwestern U.S. megaflooding associated with the late Pleistocene Cordilleran Ice Sheet, glacial Lake Missoula, and the Channeled Scabland. The vertical scales are in thousands of yr B.P. (ka) for both radiocarbon (C^{14}) and calendar time scales (approximately calibrated for the radiocarbon dates). From left to right, the plotted data show (1) the approximate southward advance and northward retreat (blue line with left to right, indicating relative ice movement from the Canadian border to maximum southern extent) for lobes of the Cordilleran Ice Sheet (CIS); (2) radiocarbon dates and interpreted duration (yellow line) for the Manila Creek section in glacial Lake Columbia (Atwater, 1986); (3) duration (yellow line) for the 40-flood rhythmite sequence in Burlingame Canyon, as inferred through correlation (Waitt, 1985; Waitt et al., 2009); (4) dates for the Bonneville flood (B) (McGee and Phillips, 2005; Lifton et al., 2015; Oviatt, 2015), for the Mount St. Helens S tephra (S) (Clynne et al., 2008), and for the Glacier Peak G and B tephras (G) (Kuehn et al., 2009); (5) radiocarbon dates from organics recovered from megaflood deposits by Benito and O'Connor (2003) (green line), who provide arguments for rejection of the older dates from the Columbia gorge; (6) OSL dates for the Ninemile and Rail Line sections of GLM rhythmites (Hanson et al., 2012; Smith and Hanson, 2014); (7) TCN dates (^{36}Cl) for a flood-transported boulder on a Moses Coulee megaflood bar, for a glacial boulder on Steamboat Rock, for an exhumed inselberg surface in upper Grand Coulee, and for ice-rafted boulders on Rattlesnake Mountain and in Badger Coulee obtained by M. Zreda, V.R. Baker, and B. Bjornstad (Keszthelyi et al., 2009, their Table 2; Bjornstad, 2014); (8) OSL dates for the White Bluffs site (Keszthelyi et al., 2009, their Fig. 10) obtained by N. Porat, N. Greenbaum, and V.R. Baker (Keszthelyi et al., 2009, their Table 1); (9) radiocarbon ages of glacial-melt derived recharge water in the Columbia Basin (Brown et al., 2010) (green line); and (10) PSU (paleo-salinity units) index for freshwater influxes from Columbia River into Pacific Ocean (Lopes and Mix, 2009) (dark-green line). Note that the TCN dates, with error bars, are indicated in red, and that the White Bluffs dates are actually OSL and not TCN. This diagram is mainly meant to be suggestive for future research.

sites exposing evidence for megaflooding that preceded the late Pleistocene phase, which is the principal focus of this guide. On Day 2, the trip will pass one of these sites at mile 18. Another site, at Marengo, is Optional Stop A, which is on a side trip that can be taken if time permits.

Important chronological markers for the late Pleistocene CIS-related megaflooding events are (Fig. 9): (1) the Glacier Peak G and B tephras (13.7–13.4 ka; Kuehn et al., 2009), which are generally inferred to have been emplaced after scabland flooding (Fryxell, 1965; Waitt et al., 2009); (2) the Mount St. Helens set S tephras (ca. 16 ka; Clynne et al., 2008), which are generally inferred to have been emplaced during flooding from GLM (Mullineaux et al., 1978; Waitt, 1980, 1985; Baker and Bunker, 1985); (3) the Bonneville flood (18.5 ± 0.5 ka; Lifton et al., 2015), which occurred prior to the emplacement of 21 inferred megaflood rhythmite layers (Waitt, 1985) near Lewiston, Idaho; (4) the advance of the CIS into northern Idaho, which constrains the formation of GLM to after 21.4–19.6 ka (Clague, 1980); and (5) the limiting radiocarbon dates for flooding through the Columbia Gorge (ca. 23 ka, according to Benito and O'Connor, 2003).

Recent work on OSL and TCN (terrestrial cosmogenic nuclide) geochronology, plus 2-d hydraulic flow modeling (2dHFM), indicate complex patterns in time and space for late Pleistocene megaflooding along the southern margins of the CIS. Consistent with regional mapping and stratigraphic studies (Smith, 2006) and with 2dHFM (Alho et al., 2010), as well as with the original interpretation by Pardee (1942), the largest outburst(s) from glacial Lake Missoula occurred prior to the emplacement of rhythmically bedded silt sequences on the paleolake floor that were described by Chambers (1971, 1984). OSL dating reveals the latter to be younger than ca. 15 ka (Hanson et al., 2012), and thus not correlated, as previously inferred (Waitt, 1985), to other multi-bedded sequences in the Channeled Scabland region that contain the 16-ka Mount St. Helens set S tephra.

2dHFM results (see discussion below by Alho and Baker) show that blockage of the Columbia River by the CIS Okanogan lobe, ca. 20–15 ka, was critical to megaflood routings for the Channeled Scabland region (Fig. 7). Pre–Okanogan lobe blockage flooding probably emplaced high-level megaflood deposits mapped by Waitt (1982, 1987) in the Columbia Valley north of Wenatchee, as well as coarse-grained rhythmite sequences in the northern Pasco Basin (described and dated by Baker, Greenbaum and Porat, and reported in Keszthelyi et al., 2009). The latter may correlate to the ca. 23 ka meltwater pulse in the eastern Pacific Ocean documented by Lopes and Mix (2009). Post–Okanogan lobe blockage flooding from/through glacial Lake Columbia probably emplaced gravel-dune-mantled bars along the Columbia River valley near Wenatchee and Trinidad, Washington, and younger megaflood deposits, dated to ca. 12 ka, that were confined to the Columbia valley. Flood pathways diverted by the Okanogan lobe over the loess-mantled eastern Channeled Scabland region probably emplaced the much-studied silty rhythmite sequences in the Yakima and Walla Walla valleys, dated between ca. 17 and 15 ka (Waitt, 1980, 1985; Clague et al., 2003).

Retreat of the Upper Grand Coulee cataract around this same time period (dated at ca. 17 ka by Baker and Zreda, as reported in Keszthelyi et al., 2009) resulted in a 250 m drop in the level of glacial Lake Columbia, thereby generating a major megaflooding pulse through the western Channeled Scabland that probably correlates to the ca. 17.5 ka meltwater pulse in the eastern Pacific (Lopes and Mix, 2009) and to ca. 16 ka ice-rafted erratics in the Pasco Basin and above Wallula Gap (^{36}Cl TCN dating by Baker, Bjornstad and Zreda, and reported in Keszthelyi et al., 2009, and Bjornstad, 2014). The whole late Pleistocene history of flooding extended over a prolonged time period, perhaps from as early as 33 ka to 12 ka, as indicated by both marine meltwater pulses (Lopes and Mix, 2009) and groundwater recharge records (Brown et al., 2010). Megaflooding from non-GLM sources may explain some of this newly documented complexity, but the whole story is clearly much more complex than previously believed.

Number and Timing of Floods (Baker)

Based on study of the Willamette silts in northwestern Oregon, Glenn (1965) inferred that there had been 40 late Pleistocene floods emanating from glacial Lake Missoula. From his study of flood slackwater sediments at the Burlingame canyon section in south-central Washington, Waitt (1980, 1985) also inferred a total of 40 late Pleistocene Lake Missoula floods. He correlated these to the Ninemile section of glacial Lake Missoula studied by Chambers (1971), and concluded that all these sections correlated with each other, representing 40 catastrophic glacial Lake Missoula drainings. Similarly, Atwater (1986) inferred that sections of relatively low-energy, fine-grained lake-bottom sediments in glacial Lake Columbia contained coarser sediment beds that resulted from 89 influxes from glacial Lake Missoula. The number of "great floods" (all "gigantic Jokulhlaups") is now claimed to be ~90–100, with peak discharges "diminishing with successive bursts" (Waitt et al., 2009, p. 776).

The timing of the flood events has been estimated by counting what are interpreted to be annual varves, separating what are interpreted to be Missoula flood beds in lacustrine sections inferred to represent 2000–3000 yr of relatively continuous sedimentation in glacial Lake Columbia (Atwater, 1986) and glacial Lake Missoula (Chambers, 1971; Waitt, 1980, 1985). Waitt et al. (2009, p. 783) summarize the conclusions as follows: "Field data reveal periods much less than a century between great Missoula floods. The inferred water budget for glacial Lake Missoula suggests periods of 65 and fewer years. The average period between floods indicated by varves is ~20–35 yr. At the glacial maximum it was much longer; early during glacial advance and during a lingering deglaciation it was much shorter. …" Waitt et al. (2009, p. 783) particularly emphasize the Manila Creek section of Atwater (1986) in glacial Lake Columbia: "From ~20 yr between floods near the beginning of last-glacial Lake Missoula, the period increased to ~50 at the glacial maximum. Then during a long deglaciation, the flood period gradually decreased (with two reversals) to 40, 30, 20, 10, a few, and finally only one or two years."

The timing between megaflood outbursts is interpreted by Waitt (1985) as indicating a "self-dumping" hydraulic instability mechanism for outburst flooding from GLM in which the advancing CIS damming GLM induces gradually longer time intervals between outbursts (and larger floods) until it reaches a maximum, and subsequently induces shorter time intervals between outburst events and smaller peak discharges. However, the pattern of varying intervals between outburst events does not match results from studies of deep-sea core MD02–2496 off Vancouver Island, which indicate cyclic inputs of Columbia sourced flooding with a regular 80-yr periodicity between ca. 19 and 17.3 ka (Hendy, 2009; Hendy et al., 2014). Clearly more work needs to be done in matching the timing of various inferred flooding events for locations along the megaflooding pathways between glacial Lake Missoula and the abyssal plains of the eastern Pacific Ocean.

CIS Megaflooding Sources (Baker)

The phenomenal quantity of water involved in Channeled Scabland flooding led Bretz (1925) to think about possible sources. Only two hypotheses initially seemed reasonable: (1) a very rapid and short-lived climatic amelioration that would have melted the CIS; or (2) a gigantic outburst flood induced by volcanic activity beneath the ice sheet. The latter phenomena were recognized to occur in Iceland, where they are known by the term 'jökulhlaup' (which Bretz initially spelled as 'jokulloup'). Bretz devoted much of the summer field season of 1926 to a search for a subglacial CIS flooding source. In a presentation at the Madison, Wisconsin, meeting of the Geological Society of America, 27 December 1926, Bretz (1927, p. 107) concluded: "Studies in Washington and British Columbia north of the scabland strongly suggest that basaltic flows which were extruded beneath the Cordilleran ice sheet produced the great flood."

After experiencing severe criticism at the 1927 Washington Academy of Sciences meeting, Bretz abandoned the CIS source hypothesis. In that decision he was undoubtedly influenced by one of his critics at the 1927 meeting, Joseph Thomas Pardee. Earlier in the same summer as Bretz's first scabland field season (1922), Pardee had been sent by his U.S. Geological Survey supervisor, W.C. Alden, to study the scabland area southwest of Spokane, Washington. Pardee (1922) reported in print that the area had been glaciated, but he provided few details, and he never published the further results that were anticipated by his preliminary report. Bretz (1978, personal commun.) suspected, from correspondence he had with Pardee in the 1920s, that the latter was considering a flood hypothesis for the origin of the scablands. Pardee (1910) had earlier documented the presence of an immense late Pleistocene lake in the western part of Montana. Named "glacial Lake Missoula," this lake had been impounded by the Cordilleran Ice Sheet, when it cut across the drainage of the modern Clark Fork River, which flows northwestward from western Montana. He inferred that the lake held as much as 2000 km^3 of water, derived from meltwater inputs from surrounding glaciated areas.

Did Pardee suspect that his glacial Lake Missoula had released an immense cataclysmic flood? If he did, Bretz surmised, his superior, Alden, had either dissuaded or prevented him from publishing that idea. Several years after the affair, David White, who was Alden's supervisor, showed Bretz a memorandum of 22 September 1922, in which Alden had written to White concerning Pardee's scabland studies: "…very significant phenomena were discovered in the region southwest of Spokane. … The results so far … require caution in their interpretation. The conditions warn against premature publication. …" Also in 1922, correspondence between local Spokane residents Thomas Large and Barton W. Everman (Baker, 1995) indicates that Pardee informally told Everman that "sub-glacial water erosion" involving water under pressure beneath ice was a possible hypothesis to explain the scabland erosion. Moreover, Pardee wrote to Bretz in 1925, suggesting that Lake Missoula be considered as a possible source for the Spokane flood. In a 1926 letter to J.C. Merriam, Bretz wrote that Pardee proposed Lake Missoula as the Spokane flood source, and that even Alden, "our ultra-conservative in Pleistocene geology," agreed that fluvial processes were involved in the origin of the scablands.

Initially, Bretz seems to have resisted Pardee's suggestion of glacial Lake Missoula as the source of the Channeled Scabland flooding. As noted above, in 1926 he was intrigued by the possibility of subglacial volcanism. Also, along with most other investigators at the time, he believed that Cordilleran ice had covered the area between the Lake Missoula ice dam and the heads of the scabland channels south of Spokane, a distance of 100 km. In 1927, he thought that the Channeled Scabland flooding was older than the latest Pleistocene glaciation that had formed Lake Missoula, and he also thought that Lake Missoula could not have supplied enough water to inundate all the scabland channel ways. In 1928, however, Bretz resolved that the source of the Spokane flood had to be Lake Missoula. Bretz made an extensive presentation of the concept at the Geological Society of America Annual Meeting in Washington, D.C., on 26 December 1929. In the published abstract, Bretz (1930a, p. 92) states, "…[i]t is suggested that bursting of the ice barrier which confined a large glacial lake among the mountains of western Montana suddenly released a very great quantity of water which escaped across the plateau of eastern Washington and eroded the channeled scablands." In subsequent publications (e.g., Bretz 1932), Bretz clearly illustrated the relationship of glacial Lake Missoula to the Channeled Scabland.

There is currently renewed interest in non-Missoula sources for the late Pleistocene megaflooding. Shaw et al. (1999) reintroduced this controversy (appropriately dubbed "back to Bretz" in light of the above history) by hypothesizing (1) that there was only one very great, major late Pleistocene megaflood; (2) that sedimentation of glacial Lake Missoula was independent of the flood events that occurred in the Channeled Scabland (i.e., that Fig. 8 could not be a correct interpretation of the stratigraphic relationships); and (3) that glacial Lake Missoula could not be the only source for those floods. Shaw et al. (1999) also proposed

that the primary source of megaflooding was subglacial, i.e., from beneath the Cordilleran Ice Sheet.

Although the Shaw et al. (1999) proposal for a single megaflood (their hypothesis 1) has been vigorously disputed as inconsistent with the field relationships (Atwater et al., 2000), several lines of evidence are suggestive of a possible role for non-Missoula sources in the late Pleistocene megaflooding history of the Channeled Scabland (their hypothesis 3). There may be a volume problem in regard to the total quantity of water that could be released from glacial Lake Missoula relative to the extent of inundation indicated by high-water marks throughout the megaflooding area (Komatsu et al., 2000; Miyamoto et al., 2006, 2007). However, this conclusion derives from the results for one modeling group, whose results do not match those obtained by another group (Denlinger and O'Connell, 2010; Waitt et al., 2009). Although it has also been suggested that erosion by the numerous floods inferred by Waitt (1980, 1985) might account for the volume problem, the important issue is not the volume of eroded scabland channels but rather that of the various basins and valleys (Pasco, Quincy, Yakima, Snake, etc.) that were filled by the ponded floodwater (an issue that had been noted by Baker, 1973a, p. 21).

Both ice-sheet modeling results (Livingstone et al., 2012, 2013) and field observations (Lesemann and Brennand, 2009) provide some support for non-Missoula sources for late Pleistocene megaflooding related to the Cordilleran Ice Sheet, specifically for subglacial meltwater flooding (hypothesis 3 of Shaw et al., 1999). This flooding would clearly be an addition to the well-documented flooding from Lake Bonneville and glacial Lake Missoula, but one that could enhance the multiple outbursts from the latter and/or provide for flooding that could occur either before or after that lake's existence. In addition to the subglacial lakes that seem likely to have been present beneath the late Pleistocene Cordilleran Ice Sheet, there is also a large region of tuyas in east-central British Columbia that displays extensive evidence for late Pleistocene volcanism and glacial interactions (Hickson and Vigouroux, 2014). This region conceivably might generate the kinds of Icelandic jökulhlaup phenomena that Bretz himself hypothesized in 1926–1927, as noted above. Obviously, this is an issue that needs much more attention in future research.

In their response to criticism of their 1999 paper by Atwater et al. (2000), Shaw et al. (2000) emphasize that both glacial Lake Missoula and subglacially stored water from the Cordilleran Ice Sheet were likely involved in the late Pleistocene megaflooding. They further note that the correlation of varve-bounded beds from glacial Lake Missoula to glacial Lake Columbia, a central point in the bed-to-bed correlation throughout the megaflooded region (Fig. 8), requires that very similar rhythmite beds in one glacial lake (Columbia) be interpreted as megaflood influxes, while those in another (Missoula) be interpreted as lake drainage events. Shaw et al. (1999, 2000) infer that the "flood beds" in both glacial lakes result from jokulhlaup influxes into those lakes, and that these do not necessarily lead to the possibility of bed-to-bed correlation between one lake and the other. Some of the geochronology reviewed above seems to support this interpretation (hypothesis 2), but there clearly is a need for more research into the geochronology and sedimentology.

Megaflood Dynamics (Baker)

Bretz (1925) published the first estimate of the megaflood discharge for what he hypothesized to be the "Spokane Flood" as it passed through Wallula Gap. The calculation was actually performed by Bretz's colleague, D.F. Higgins, who used the Chezy equation to determine a peak discharge of nearly 2×10^6 m^3 s^1 (~160 km^3 d^{-1}) and a mean flow velocity of 10 m s^{-1}. These estimates were subsequently improved upon by systematic slope-area calculations (Baker, 1973a) that relied on the high-water-mark evidence for the megaflooding stages that were exceptionally well preserved throughout the Channeled Scabland and adjacent regions. The slope-area estimates and subsequent one-dimensional step-backwater calculations (O'Connor and Baker, 1992; Benito and O'Connor, 2003) were used to estimate the parameters necessary for understanding the basic hydraulics of the flood flows (Baker, 1973a, 1978b) and their relationships to the scabland erosional and depositional features (Baker, 1973a, 1973b, 1978c; Benito, 1997).

The processes that are conventionally considered to erode channels into rock include abrasion (corrasion), corrosion, cavitation, fluid stressing, physical weathering, and plucking (Tinkler and Wohl, 1998; Whipple et al., 2000; Richardson and Carling, 2005). For the high-energy megaflood flows responsible for the Channeled Scabland, hydraulic plucking of the jointed basalt bedrock (Fig. 2) is considered to be of major importance (Bretz, 1924; Bretz et al., 1956; Baker, 1973b, 1978b, 1979; Baker and Komar, 1987). Benito (1997) correlated the scabland sequence of erosional forms (see Stop 4) to various measures of megaflood flow strength, including mean velocity, flow depth, and power per unit area of bed (Table 1).

Megaflooding of the Channeled Scabland produced phenomenal sediment transport capability, locally entraining immense

TABLE 1. RELATIONSHIP OF FLOW HYDRAULICS TO STAGES OF SCABLAND CHANNEL DEVELOPMENT

Erosional stage	Description	Mean velocity (ms^{-1})	Power per unit area (watts m^{-2})	Flow depth (m)
I–II	Streamlined loess hills	3–5	500–2000	30–100
II–III	Stripped basalt, grooves	3–9	500–3000	35–125
III–IV	Butte-and-basin scabland	7–15	2000–20,000+	100–250
IV–V	Inner Channels	15–25	5000–25,000+	100–250+

Note: Hydraulic data are from calculations by Baker (1973a, 1978b) and Benito (1997).

boulders, as will be seen at Stop 3 on Day 1 of this field trip. While some studies emphasize the competence of flows to initiate the movement of such particles (e.g., Baker, 1973a; Baker and Ritter, 1975), a more productive approach may be to estimate the paleohydraulic conditions of boulder deposition by high-energy megaflooding (O'Connor, 1993). Another interesting aspect of high-energy megaflooding is the range of particle sizes transported as bedload, suspended load, and washload (autosuspension load). Komar (1980, 1988) and O'Connor (1993) found that at sustained bed shear stresses of 1000 N m^{-2}, particles as large as 10–20 cm can move in suspension, while coarse sand will move as washload. Extrapolation of Komar's (1980, 1988) results by Komatsu and Baker (1997) suggests that at the phenomenally high bed shear stresses of 10^4 to 10^5 Nm^{-2} that can be achieved in the most energetic megaflooding (Baker and Costa, 1987; Baker and Komar, 1987; Baker, 2002b), the flows will suspend boulders up to several meters in diameter (Fig. 10).

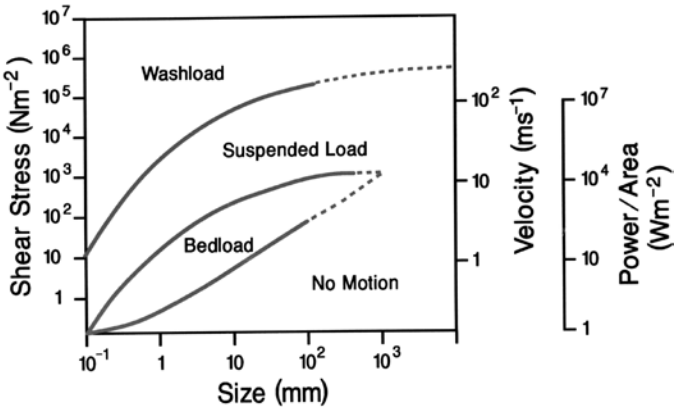

Figure 10. Modes of sediment transport for different particle sizes achieved over very broad ranges of bed shear stress, mean flow velocity, and power per unit area of bed.

Paleohydraulic Modeling of the Missoula Floods (Alho and Baker)

Baker (1973a) used paleohydaulic calculations to quantify the late Pleistocene Channeled Scabland megaflooding, and these estimates were subsequently improved upon by employing 1-d computerized hydraulic modeling procedures (O'Connor and Baker, 1992; Benito and O'Connor, 2003), which had earlier been introduced as a part of the new science of paleoflood hydrology (Baker, 1987a, 2008b; Baker and Pickup, 1987; Ely and Baker, 1985). Computational advances subsequently allowed for the application of 2-d modeling (Craig, 1987), which was followed by the application of more advanced codes by Komatsu et al. (2000) and Miyamoto et al. (2006, 2007). Using a high-resolution (250-m) 2-d model for the Missoula flooding pathways, Denlinger and O'Connell (2010) showed that a less-than-maximum discharge output from glacial Lake Missoula generally matched high-water-mark indicators identified along the flood path (Baker, 1973a; O'Connor and Baker, 1992; Benito and O'Connor, 2003), although it failed to fill the Pasco Basin to the maximum level indicated by the field evidence. However, this simulation required 250 d of computation time for a single full-model run, thereby limiting the ability to explore multiple scenarios for various Missoula flooding outburst levels (Clarke et al., 1984) and alternative flood pathways produced by the varying configurations of boundary conditions. To alleviate these problems, we employ a code that can run a simulation in a couple of days (on a 1000-m grid), thus allowing us to produce multiple scenarios for glacial Lake Missoula outburst flooding. The paleohydraulic modeling scheme uses a modified version of the TUFLOW 2-d hydraulic model, which solves the full 2-d, depth-averaged momentum and continuity equations for free-surface flow, using a finite-difference procedure (TUFLOW, 2016) and the altering direction implicit (ADI) scheme on a square mesh.

Model outputs for two preliminary TUFLOW paleohydraulic modeling runs are fit to the boundary conditions shown in Figure 11. Each model run simulates 80 h into a maximum glacial Lake Missoula outburst of 17×10^6 m^3s^{-1}. These model runs use a 1000-m DEM, but we can readily increase the resolution where needed. The scene extends ~600 km from the east (right), near the present-day Idaho/Montana border, to the west (left) at the mouth of the present Columbia River (Fig. 11). The Figure 12A model run is for conditions that existed just prior to the late glacial recession of the upper Grand Coulee cataract (Bretz, 1932), but it incorporates diversion of floodwater by the Okanogan lobe of the Cordilleran Ice Sheet. The Figure 12B run depicts the flooding after recession of this 250-m-high cataract into the basin of glacial Lake Columbia and before recession of the Okanogan lobe. Note the major differences in water depths (and inundation levels) indicated by the color scale, and in the regional pattern of flooding, especially in the central Channeled Scabland region (Telford–Crab Creek and Cheney-Palouse scabland tracts) and in the upper Snake River valley/canyons. Variations in pathways occupied by different outburst flood routings result in different ages for the bedrock scouring and boulder transporting that can be dated by cosmogenic nuclide methods. Moreover, the different flooding depths indicated by modeling (Fig. 12) are relevant to emplacement of the highest-level, ice-rafted erratic boulders that will have been dated by cosmogenic nuclide methods. Parameters important to understanding the patterns of bedrock scour and boulder transport include both bed shear stress and mean flow velocity, both of which are easily generated as outputs from the modeling (e.g., Alho et al., 2010).

The limited existing dating constraints on the floods (Benito and O'Connor, 2003) and modeling (Alho et al., 2010; Denlinger and O'Connell, 2010) clearly indicate that there have been a variety of different flow pathways for the late Pleistocene megaflooding (Fig. 12) involving different inundation levels for various flow events, and possibly even different source regions for generating the flows. Future research should explore these issues by employing an iterative approach involving geochronology results and results generated from the modeling, with each

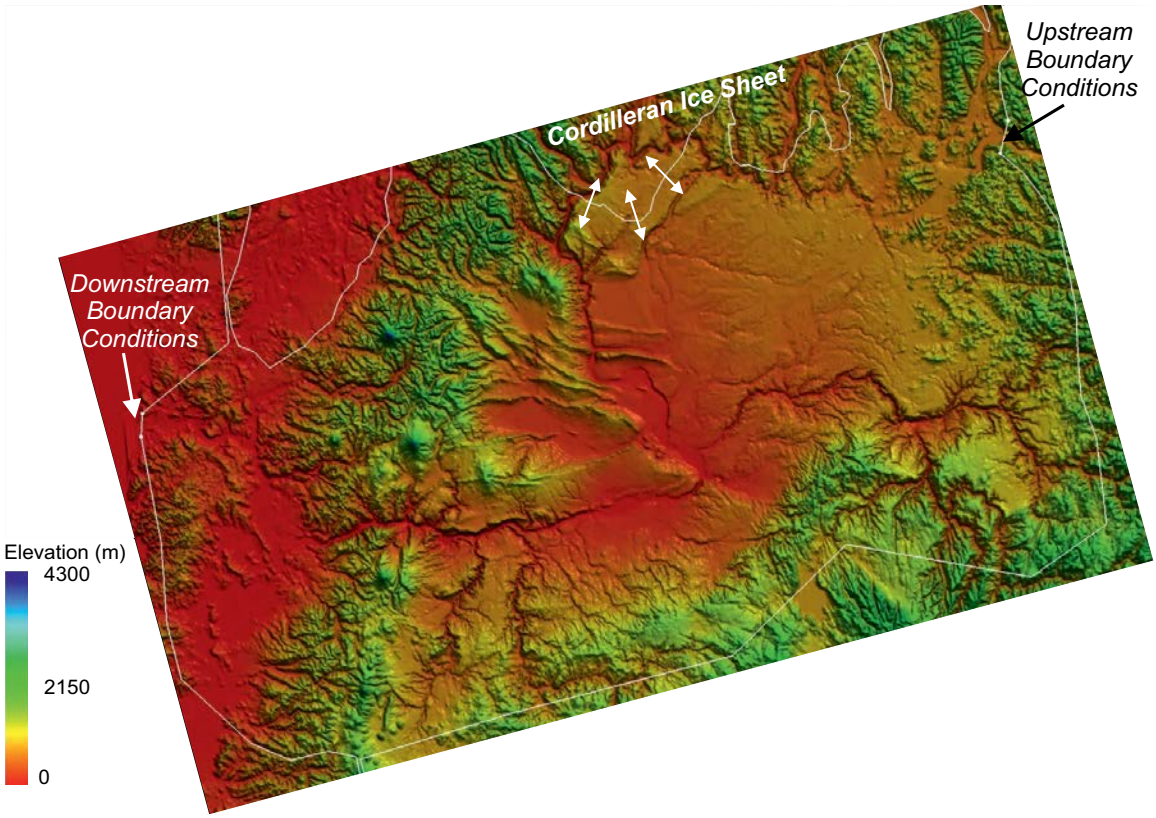

Figure 11. Boundary conditions for 2-d hydraulic modeling runs shown on a digital topographic map of the Columbia Basin. Note especially the position of the late Pleistocene maximum extent of the Okanogan lobe of the Cordilleran Ice Sheet.

informing inferences to be made for subsequent employment of the other (i.e., identify model runs based on the dating results, and identify new sites for dating related to modeling results). This iterative approach will enhance understanding of late Pleistocene megaflooding in the Pacific Northwest, and it will afford opportunities to make major advances in understanding the temporal and spatial patterns related to that flooding.

Earliest Human Migration to the Americas (Baker)

The best-documented early human migration pathway from Beringia southward began ca. 13 ka and proceeded through the ice-free corridor that had recently opened up between the Cordilleran and Laurentide Ice Sheets. Less well documented, but implied by a number of confirmed, older human occupation sites, combined with recent genetic studies (Curry, 2012), is a possible eastern Pacific coastal route that may have been active as early as 16 ka. This earlier migration path would have been greatly impacted by the megafloods from glacial Lake Missoula. Even the later migrations would have encountered the late phases of megaflooding that were confined to the Columbia valley as early people of the Clovis culture moved southwestward from the ice-sheet margins.

Planetary Significance of Megaflooding (Baker)

The recognition of cataclysmic flooding landscapes on Mars (Baker and Milton, 1974; Baker, 1982, 2001; Burr et al., 2009) and its probable relation to climatic change on that planet (Baker, 2001; Baker et al., 2015) has further emphasized the importance of understanding megaflooding processes. The Martian megafloods are hypothesized to have induced the episodic formation of a northern plains "ocean," which, with contemporaneous volcanism, led to relatively brief periods of enhanced hydrological cycling on the land surface (Baker et al., 1991b; Baker, 2001). Megafloods on both Mars and Earth are hypothesized to involve abrupt and spectacular planet-wide climate oscillations, and associated feedbacks with ocean circulation, land-surface weathering, glaciation, and atmospheric carbon dioxide (Baker, 2009b).

Eolian Deposits of the Columbia River Basin (Gaylord)

Eolian features are an important geomorphic component in the northern and southern portions of the Columbia River basin in Washington (McDonald and Busacca, 1988, 1992; Busacca, 1989; Gaylord and Stetler, 1994; Stetler and Gaylord, 1996; Gaylord et al., 2001, 2003). Erosional eolian features include

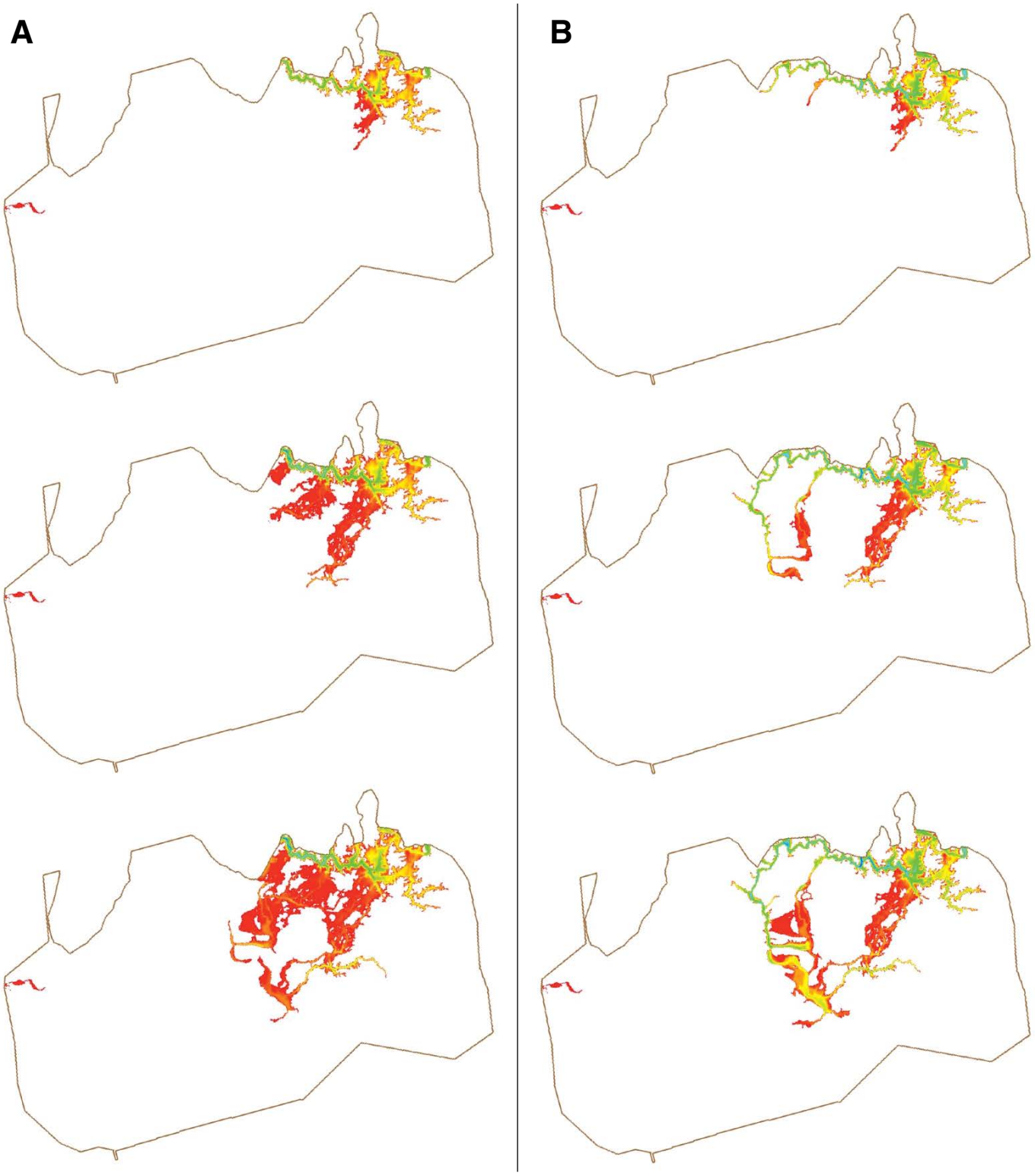

Figure 12. (A) Flow depths calculated for three successive time steps by a 2-d hydraulic modeling run with blockage of the Columbia River by the Okanogan lobe and prior to the retreat of the great 250-m-high cataract of the upper Grand Coulee to the region of glacial Lake Columbia. (B) The modeled flow depths of megaflood inundation for three successive time steps following completion of the upper Grand Coulee pathway to the megaflooding and without an Okanogan lobe blockage of the Columbia River. Red indicates lower flow depths, green indicates moderate flow depths, dark blue indicates higher flow depths. (In the lefthand diagram, the scale goes from 0–480 m; in the righthand diagram, the scale goes from 0–~320 m.)

yardangs sculpted from moderately indurated megaflood and eolian sedimentary deposits, sand blasted, megaflood-transported gravel ventifacts, dispersed pebble lags, sand dune blowouts, and deflationary hollows including playas. Variously weathered sand dunes, sand sheets, and loess deposits mantle the basin to depths of decimeters to meters. These deposits largely overlie basalt and sedimentary bedrock as well as megaflood and alluvial gravel, sand, and silt-clay sedimentary deposits.

The nature and distribution of sand-rich eolian deposits are primarily a function of the availability of loose sediment, the direction and frequency of sand-moving winds, soil moisture, and surface roughness. Silt- and clay-rich eolian deposits depend upon these factors, but also upon the relative percentage of sand-sized particles in source sediment, whose saltating transport mode is the most important single mechanism by which the smaller particles become entrained by the wind (Bagnold, 1941; Chepil, 1945a, 1945b; Gillette, et al., 1974; Pye and Tsoar, 1990; Pye, 1995).

In general, the textural characteristics of flood-sand-associated eolian deposits change from north to south across the Columbia River Basin with coarser-grained, sand- and gravel-enriched flood deposits most common in the north, and finer-grained, sand-, silt-, and clay-enriched deposits favored in the south. Many of the sand- and gravel-enriched deposits in the Quincy Basin accumulated in areas of flood flow expansion, such as below the outlet of the Grand Coulee (Ephrata fan) and along the western margin of the basin where constrictions in the Columbia River valley (e.g., Sentinel Gap cutting through the Saddle Mountains anticline) temporarily impounded megaflood flows (Baker, 1973a, 1978c, 1989). These topographically induced flow perturbations decreased flow competence and encouraged sediment deposition. An abundant volume of finer-grained flood sediment remained in temporary suspension, bypassed the northern scabland, and accumulated in stratigraphically thick successions of fine sand-, silt- and clay-rich slackwater rhythmites in the Pasco and Umatilla Basins in south-central Washington and northern Oregon, respectively. There are also local deposits of fine-grained sediments in the northern Columbia River Basin, along the Columbia River valley, and associated with the deposits of glacial Lake Columbia.

The segregation of megaflood sedimentary deposits into generally coarser-grained northern Columbia River Basin and finer-grained southern basin deposits is reflected in the nature of the eolian deposits. Moderately thick and extensive sand dune and more localized sand sheet accumulations, and thinner, less extensive loess deposits characterize the northern basin eolian deposits (McDonald and Busacca, 1988; Busacca, 1989; Gaylord et al., 2002, 2003; Dalman, 2007). More widespread sand dune and sand sheet deposits and thicker, more extensive loess deposits characterize the southern parts of the basin (e.g., McDonald and Busacca, 1988; Busacca, 1989; Gaylord and Stetler, 1994; Stetler and Gaylord, 1996; Gaylord et al., 2001; Sweeney et al., 2000, 2005, 2007). The sources for these eolian deposits were primarily mixed sand, silt and clay that was concentrated in the south-central part of the basin and especially in the vicinity of Wallula Gap.

■ OPTIONAL PRE-TRIP DAY—SPOKANE AREA

This optional pre-day field trip will start from Spokane International Airport, Washington. It will focus on sections along Latah Creek, exposing glacial Lake Columbia sedimentation that was influenced by megaflooding inputs. Because the optional pre-day trip will be very useful for providing participants with a perspective on the issues that will be discussed on the regular three-day program, it is highly recommended.

Simplified driving directions: From the Spokane airport parking area, follow W. Airport Drive toward Spokane. Merge on to U.S. 2 toward I-90. Merge on to I-90 toward Spokane. Take exit 279–U.S. 195 South. Continue 4.8 miles on U.S. 195, and turn left at S. Hatch Road in order to get back on U.S. 195 heading north. From the junction with S. Hatch Road proceed north on U.S. 195 0.5 miles to where an unnamed dirt road enters from the right. Turn right on the dirt road and continue 0.25 miles to park near a view of a steep cut bank along Latah Creek. This is site LaCk 1, described below. (The LaCk 2 site will not be visited.)

OPTIONAL PRE-TRIP STOP. Latah Creek Site—Glacial Lake Columbia Sedimentation: Sedimentology and Stratigraphy of Late Quaternary Megaflood-Influenced Sedimentary Deposits in the Latah Creek Valley near Spokane, Washington (Gaylord, Meyer, and Breckenridge)

Introduction

The Latah Creek valley, south of Spokane, Washington, has been at the center of glacial megaflood and proglacial lacustrine activity throughout the Pleistocene. The record of sand-, silt-, and clay-rich megaflood-influenced deposition in this valley contrasts with the fines-depleted, gravel-dominated record of megaflood deposits on the Rathdrum Prairie to the north and east (Breckenridge and Othberg, 1998) (Figs. 13, 14). Scour-and-fill features in the gravel-rich Rathdrum Prairie deposits speak to the intensity of erosion and flooding following partial or complete failure of the ice dams that held glacial Lake Missoula (Breckenridge and Othberg, 1998). These gravel-rich deposits, while telling about proximal megaflood processes, are less informative about the timing and nature of megaflooding in more marginal and distal areas of the Channeled Scabland, where a more texturally diverse assortment of deposits attests to a wider range of megaflood processes (e.g., Waitt, 1980, 1985; Atwater, 1986, 1987; Smith, 1993; Baker, 2009c). Latah Creek, though proximal to the failed ice dam, was largely separated from the most erosive of the floodwaters by a bedrock-cored upland known locally as the South Hill (Fig. 14). The Latah Creek valley also was repeatedly submerged beneath proglacial lake waters that were impounded behind the Okanogan lobe of the Cordilleran Ice Sheet, making it a preferred depocenter for proglacial lacustrine and megaflood sedimentary deposits.

Prompted by questions about the sedimentary history of the Latah Creek flood and proglacial lacustrine deposits, Meyer (1999) undertook a sedimentary and stratigraphic study that complements previous investigations (Kiver and Stradling, 1982;

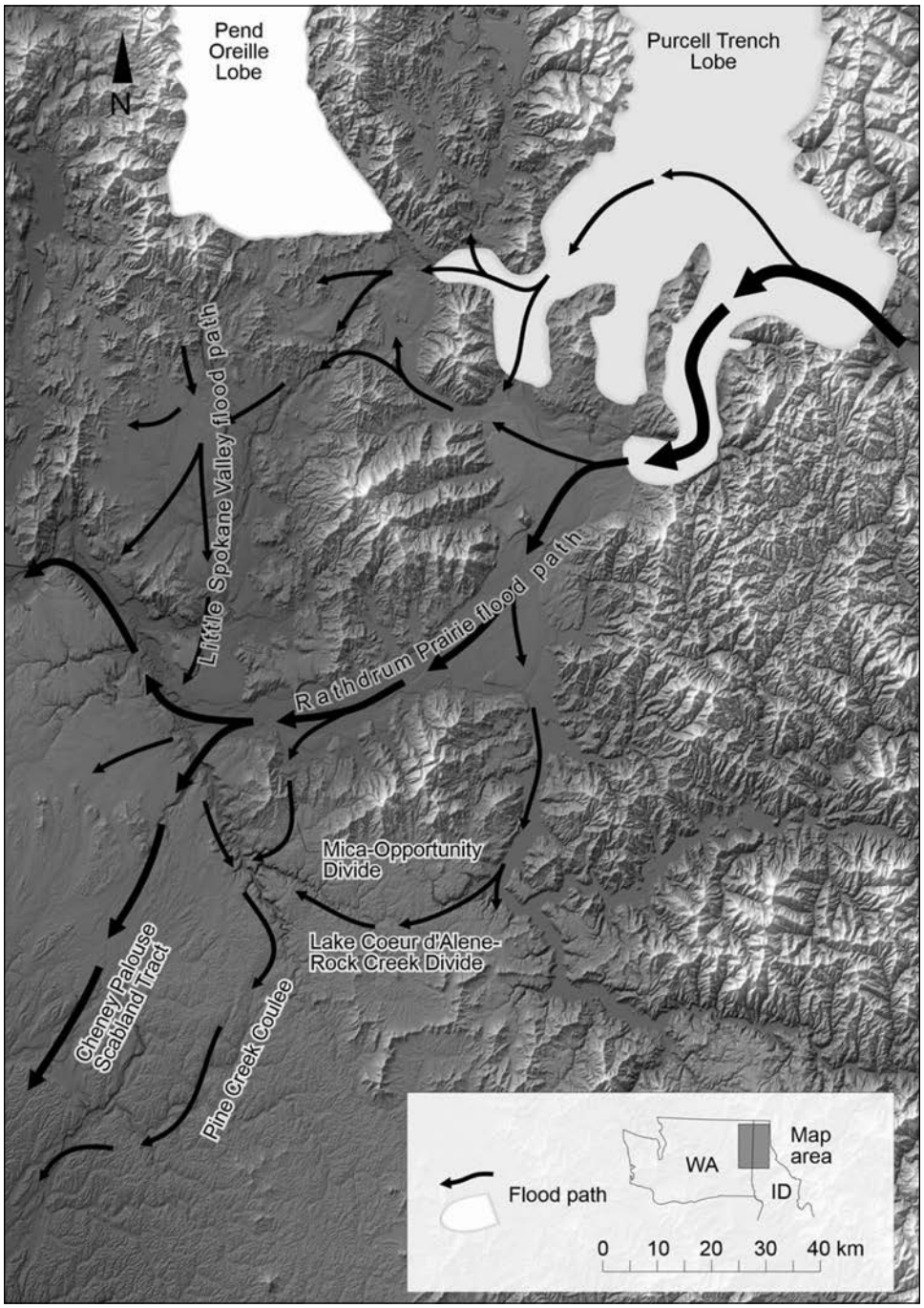

Figure 13. Digital elevation model (DEM) map of northeastern Washington, highlighting major physiographic features including Latah Creek, Rathdrum Prairie, and Cheney-Palouse scabland tract. Note that the primary glacial megaflood pathway from Lake Missoula to the Latah Creek valley was across the Rathdrum Prairie. Possible pathways for the exceptionally large floods to reach Latah Creek were via the Mica-Opportunity Divide and via the Setters divide. Once these waters reached the mid- and upper reaches of Latah Creek, geomorphic evidence suggests that the floodwaters were directed down the Cheney-Palouse scabland tract by way of Marshall Creek or Pine Creek Coulee, tributary valleys near the confluence of Latah Creek with the Spokane River. Rectangle in lower right outlines area shown in this figure.

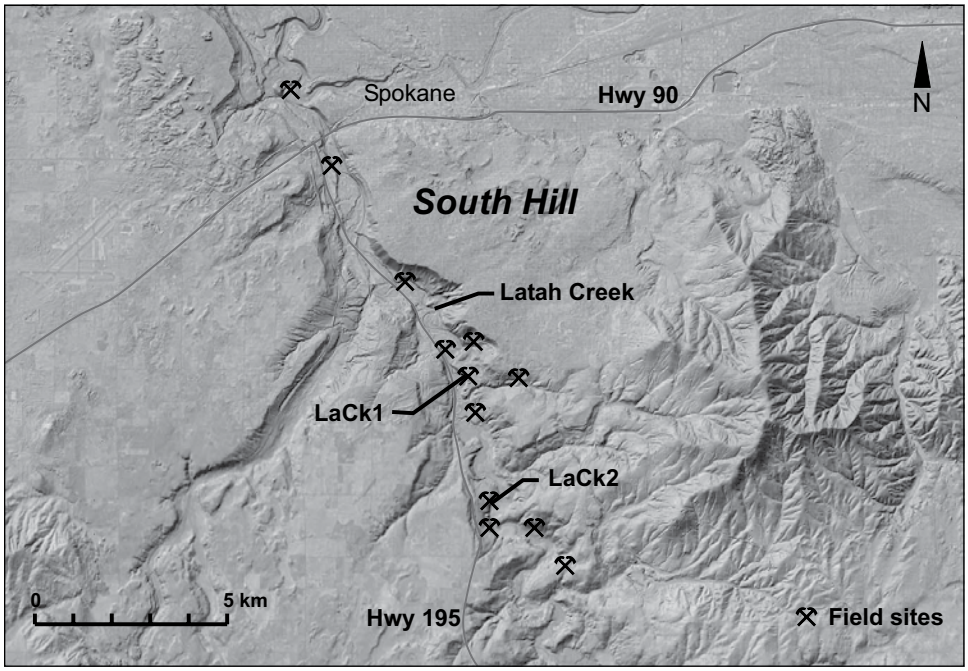

Figure 14. Digital elevation map showing Latah Creek valley and its relation to Spokane and South Hill. Cross-hammer symbols with letter identifications show locations and sites discussed in text; symbols without letter identification were examined in detail by Meyer (1999).

Kiver et al., 1991; Rigby, 1982; Waitt, 1984, 1985; Waitt and Thorson, 1983) of Latah Creek valley Quaternary deposits and their relation to the megafloods. Meyer (1999) based his study on 25 exposures that ranged from a few meters to 10s of m high and 10s to >100 m wide; these exposures permitted him to identify and correlate facies and stratigraphic trends, investigate provenance, and reevaluate the previously determined sedimentary depositional history. Meyer (1999) also collected and analyzed a limited number of paleomagnetic samples to preliminarily assess the timing of a large and prominently exposed paleo-landslide.

The Quaternary sedimentary deposits exposed along Latah Creek provide an excellent opportunity to view proximal-to-source megaflood-related deposits on the northeastern limits of the Channeled Scabland. In this section, the sedimentary and stratigraphic history of the Quaternary sedimentary deposits, as well as the provenance of the Latah Creek valley are described, interpreted, and placed in the broader context of Channeled Scabland evolution.

Regional Geology

Latah Creek has incised an ~25-km-long, NW-trending valley (Figs. 13 and 14) into lithologically diverse bedrock and Quaternary sedimentary deposits. The basement rocks that underlie the glacial megaflood deposits include low- to high-grade metasedimentary strata of the Precambrian Belt Supergroup, high-grade metamorphic rocks of the Cenozoic Priest River metamorphic core complex, and Mesozoic and Cenozoic plutonic crystalline rocks (Joseph, 1990; Stoffel et al., 1991). The geology of the Latah Creek drainage is dominated by basaltic strata of the middle Miocene Columbia River Basalt Group (Reidel and Hooper, 1989), Pleistocene glacial megaflood and proglacial lacustrine deposits, and younger Pleistocene and Holocene alluvium and colluvium.

The Cordilleran Ice Sheet did not reach the Latah Creek drainage during the last (late Wisconsin) glaciation (Richmond et al., 1965; Kiver and Stradling, 1982; Waitt and Thorson, 1983; Carrara et al., 1996). However, asynchronously advancing lobes of the ice sheet (Atwater, 1986, 1987) blocked stream channels and impounded primarily west-directed stream and floodwaters (Fig. 7) creating proglacial lakes that submerged lowland areas adjacent to the ice sheet, including the Latah Creek valley. The timing of these advances of ice sheet lobes across the Columbia, Colville, Little Spokane, Priest, and Clark Fork Rivers is not known with confidence, largely because of a scarcity of directly dated materials. Still, the thick succession of proglacial deposits preserved along Manila Creek (in the Sanpoil valley located between the Okanogan and Columbia River ice lobes; Fig. 7) provided the basis for a broadly constrained chronology of the late Pleistocene megaflood and inter-megaflood activity in the region (Atwater, 1986, 1987). Interpretation of the Manila Creek depositional history suggests that the maximal advance of the Columbia River lobe produced glacial Lake Spokane just prior to creation of glacial Lake Missoula (when the Clark Fork River was blocked by the advancing Purcell Trench lobe). About the same time as glacial Lake Missoula formed, the Okanogan lobe advanced across the Columbia River to create glacial Lake Columbia (Atwater, 1986, 1987). Glacial Lakes Columbia and Spokane were parts of a largely contiguous body of water that flooded the Latah Creek valley (Richmond et al., 1965; Waitt and Thorson, 1983). Ancient strandline elevations indicate that Lake Columbia/Spokane levels fluctuated between 610 and 732 m a.s.l.

(above sea level) (Kiver et al., 1991). The magnitude of these lake-level fluctuations is attributed to variability in the sizes and frequencies of megaflood events, varying geometries of glacial ice lobes, and to the differing degrees of floodwater spillover from proglacial lakes during megaflood events.

Understanding whether megaflood incursions into the Latah Creek valley were pre-Late- or Late-Wisconsin (or both) has been hindered by the scarcity of reliable marker beds or datable materials. The absence of weathering or pedogenic features in gravel deposits near the base of the Latah Creek stratigraphic section has been cited as evidence that the entire succession accumulated during the late Wisconsin (Waitt, 1984). In contrast, ca. 30–40-ka radiocarbon ages from charcoal preserved in nearby megaflood deposits, have also been cited as evidence for pre–late Wisconsin flooding in Latah Creek (Rigby, 1982; Kiver et al., 1991), leaving the question unresolved. Pre–late Wisconsin megafloods have also been suggested for weathered flood gravel deposits near Malden and Willow Creek Bar (20 and 80 km SE, respectively from Latah Creek; Kiver et al., 1991). In addition, scours into loess >150 km downstream from Latah Creek have been suggested as evidence, on the basis of associated tephra layers, to indicate a ca. 36-ka glacial megaflood event (McDonald and Busacca, 1988; Busacca, 1989).

Provenance of the Latah Creek Quaternary Sedimentary Deposits

As discerned from thin section petrographic analysis of sand-sized minerals and lithic particles, Latah Creek sediment consists of (in decreasing order of abundance): volcanic (basalt), plutonic (granitoid), and metamorphic (metasedimentary) particles (Meyer, 1999). Dense (heavy mineral), grains are dominated by amphibole and pyroxene and contain lesser percentages of zircon, epidote, garnet, and sphene. Except for differences in percentages of lithic clasts, and especially basalt, the compositions of the Latah Creek and Rathdrum Prairie samples are closely comparable. It is largely on the basis of these data that the Latah Creek sedimentary deposits are interpreted to have been transported to their depositional sites primarily via the Rathdrum Prairie (Meyer, 1999).

Sedimentology, Sedimentary, and Stratigraphic History

The Latah Creek valley exposes beds and lenses of complexly interstratified sand, gravel, and mud that are grouped into three informal lithostratigraphic units: (1) lower unit (sand- and gravel-rich facies), (2) middle unit (mud-, silt-, and clay-rich facies), and (3) upper unit (sand- and gravel-rich facies) (Meyer, 1999). The gravel to very fine sand facies of the lower and upper units are lithic rich, and consist of ~50% metamorphic (dominantly quartzite and metasiltite), ~15% granitic, ~10% basaltic clasts, ~15% detrital quartz, and ~10% feldspar and accessory (dense) minerals. Fine-grained clastic particles from the middle unit facies consist primarily of quartz, feldspar, and accessory (dense) minerals.

Lower unit. This unit (Figs. 15, 16) is up to 35 m thick and overlies Miocene basalt. To facilitate its description and interpretation, this unit is divided into: (1) a thicker, lower subunit of sand with some gravel, and (2) a thinner, sand-rich upper subunit. The lower subunit consists of 1.5–2.5-m-thick tabular beds of normally graded, horizontally stratified, and cross-stratified gravel and sand that grade upward into beds of laminated fine sand and silt capped by couplets of thinly laminated, silt clay. Angular to subangular pebble- to boulder-clasts are concentrated in crudely to distinctly horizontally stratified beds in the lower half of the subunit. Gravel clasts also occur as isolated (outsized) cobble-boulder clasts and boulder- to cobble-clast clusters. Lower subunit sand beds grade upward from planar-horizontal strata to planar and trough cross-strata that dip primarily to the south; however, at one exposure, cross-stratal dips are nearly bimodal. Thinly laminated 0.1–0.5-cm-thick silt-clay couplets occur in 20–40-cm-thick beds that are laterally traceable for 10s of meters.

Sixteen of the normally graded lower subunit beds are preserved in an ~32-m-thick stratal succession located ~5 km from the confluence of Latah Creek and the Spokane River (Rigby, 1982; Waitt, 1984; Kiver et al., 1991). The total thickness of these beds is <10 m and thins to less than 10 km upstream from this site. Samples of detrital wood and peat are preserved in sand-rich beds in this subunit, and these yielded radiocarbon ages of >40,000 (WSU-5037) and 32,450 ± 830 yr B.P. (WSU-5038) [ca. 36,560 ± 1860 yr B.P.], respectively.

Flow shear and load-induced deformation features are common in the lower subunit deposits. Normally graded beds commonly contain 5–70-cm-long, laminated silt/clay rip-up clasts near their bases. The most conspicuous deformation feature in the lower subunit, however, is a displaced sedimentary block consisting of a stacked, succession of normally graded beds (left side of gully in Fig. 15) that sharply overlie horizontally stratified, sand-dominated, normally graded lower-unit deposits. The sharp detachment surface on which this block was displaced is at least 40 m long and dips 25–30° to the NW. The tilted strata on the left (NW) side of this exposure are generally undeformed internally except for a 2-m-wide anticlinal fold in lower strata at the southern limit of the block. A separate set of broadly folded strata on the right (south) side of the gully is located at the same elevation as this anticlinal fold.

Strata from the upper subunit (of the lower unit) consist of 30–60 cm-thick, normally graded beds of very coarse to fine sand. These normally graded beds are characterized by planar horizontal strata in their lower halves and south-dipping 10s of cm-thick sets of planar cross-strata and ripple cross-laminations in their upper halves. No beds with laminated silt-clay couplets occur in the upper subunit.

Interpretation. The grain sizes, fabrics, sedimentary structures, tabular shapes, and normal grading of beds in the lower subunit suggest they resulted from a succession of turbulent, sediment-laden glacial megafloods that flowed into the standing waters of a lake as turbidity and/or density currents. Silt-clay couplets that cap these normally graded deposits are interpreted as annual lake varves. Similar, normally graded megaflood rhythmites, also capped by lake varves, are exposed along Manila

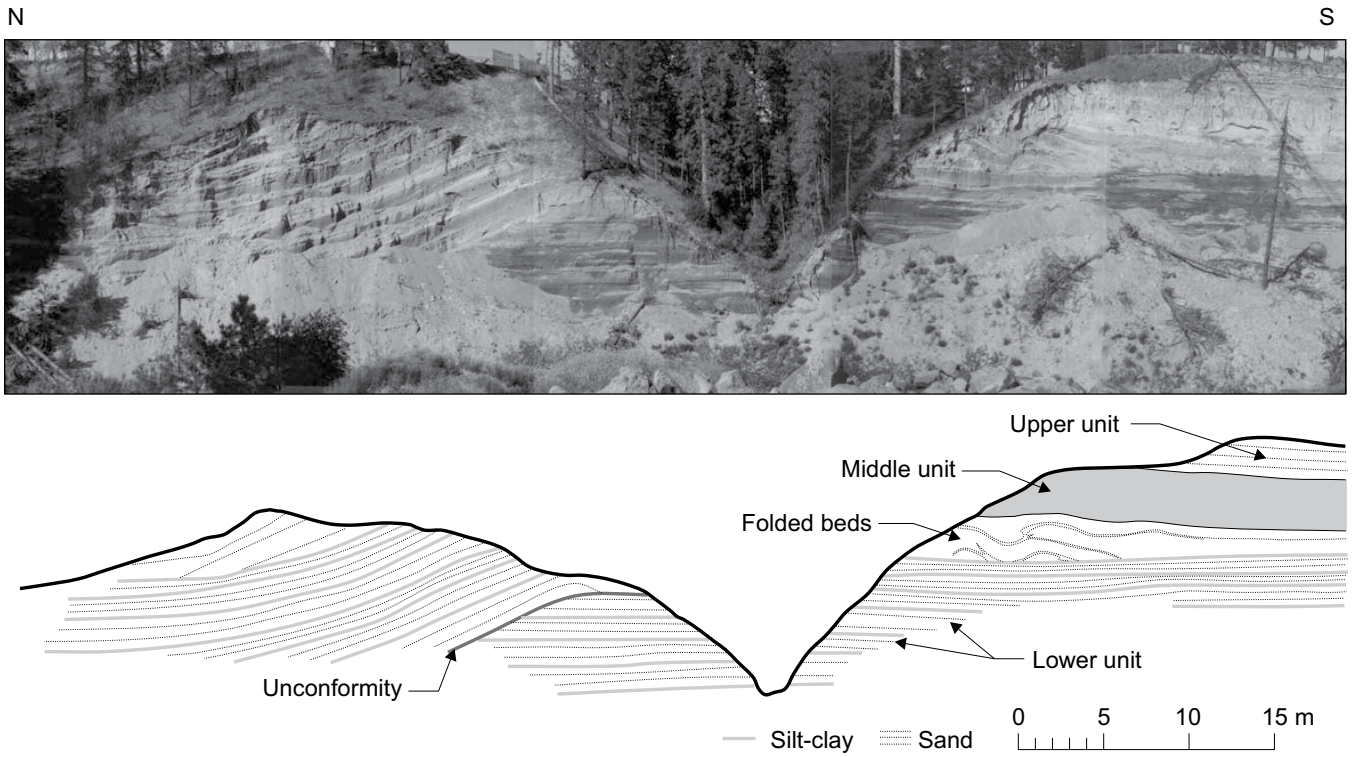

Figure 15. Field Site LaCk1 (see also Fig. 14). View is to east. Note that horizontal rhythmites of the lower unit to the left (north) of the gully near the center of the figure are cut by a displacement surface that is overlain with a displaced landslide block. Middle unit exposed to right (south) of the gully is capped by upper-unit deposits as described in the text.

Creek ~90 km northwest of Latah Creek (Atwater, 1986, 1987). Those Manila Creek rhythmite deposits were attributed by Atwater (1986, 1987) to megaflood-induced turbidity currents that flowed into proglacial Lake Columbia.

High rates of sediment fallout from suspension within turbidity current flows often generate upper-stage planar-horizontal strata at the expense of lower-stage ripple and dune bedforms (Simons et al., 1965; Allen and Leeder, 1980; Lowe, 1988; Kneller and McCaffrey, 1999). Such turbulent flows as well as associated hyper-concentrated megaflood flows were favored for generation of the lower-unit deposits along Latah Creek (Meyer, 1999). As flow velocities waned and the concentrations of suspended sediment diminished, tractional transport contributed to the generation of the 2- and 3-dimensional subaqueous dunes that produced planar and trough cross-strata.

The abundance of isolated (outsized) gravel clasts and clusters of gravel clasts in the lower subunit is attributed to hindered settling and differential tractional transport of large gravel clasts; these grain-support mechanisms are common within turbidity currents and cohesionless hyper-concentrated flows (Lowe, 1982; Smith and Lowe, 1991). Outsized cobble- to- boulder-sized clasts and clast clusters also have developed during modern Icelandic jökulhlaups (Russell and Knudsen, 1999a, 1999b), when both turbidity current and hyper-concentrated flow conditions developed. The deformation structures in the lower unit, including flame and ball-and-pillow features, folds, rip-up clasts, and overthrusts are consistent with the loading and flow-induced shearing that accompanied the powerful, sediment-laden glacial megafloods. The predominance of south-directed flows is evidence that the megafloods repeatedly entered the valley from the north. The relative rarity of opposing, north-directed paleocurrent indicators suggests that few megafloods entered the Latah Creek valley via the Mica-Opportunity divide (Fig. 13).

The upper, sand-rich subunit of the lower unit was deposited by flows that were not competent to transport gravel clasts. The absence of varved couplets or weathered surfaces separating the tabular, normally graded beds suggests that deposition may have resulted either from frequent, temporally distinct floods, or from pulsating flows during a few, or even a single, large megaflood. Successive, normally graded flood rhythmites deposited during a single modern Icelandic jökuhlaup have been observed to dominate m thick depositional successions (Russell and Knudsen, 1999a, 1999b). We suspect that the overall thinning of the rhythmites in the upper subunit signals the progressive retreat of proglacial lakes from the Latah Creek drainage. Ultimately, deposition of the upper subunit of the lower unit was followed by an episode or episodes of significant stream incision.

The incorporation of peat and charcoal with ca. 32.4 ka (ca. 36 ka cal yr) and >40 ka radiocarbon ages in lower unit strata (Fig. 16) is consistent with radiocarbon ages reported from

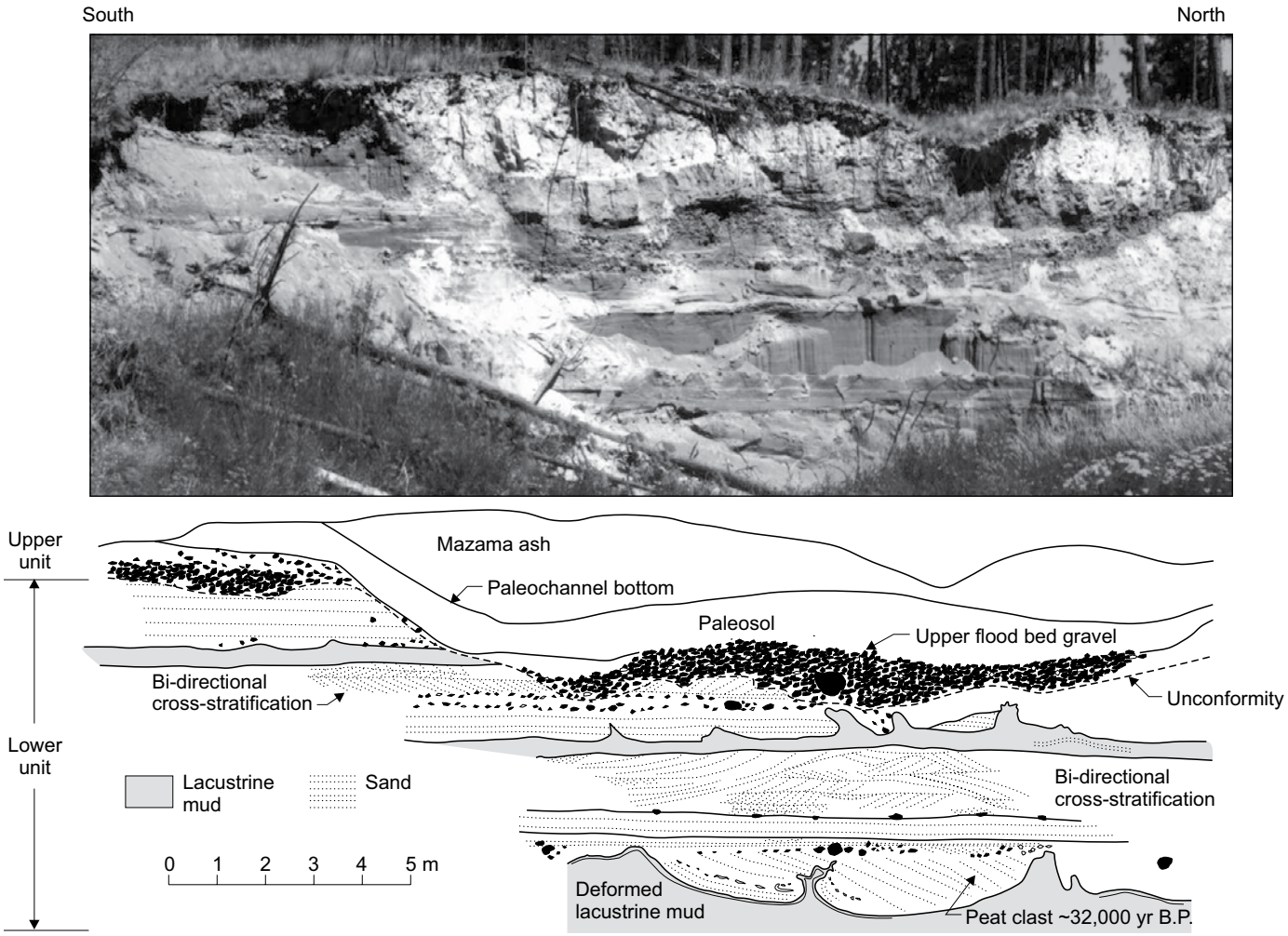

Figure 16. Field Site LaCk2 (see also Fig. 14). View is to west. This exposure reveals sand- and mud-rich lower- and gravel-rich upper-unit deposits separated by an unconformity. Note also the large-scale deformation features, radiocarbon-dated peat clast, and bidirectional paleocurrent indicators. Holocene scour surface and sediment containing Mount Mazama tephra (ca. 7.7 cal ka) cap the succession.

postulated pre–late Wisconsin megaflood deposits in the nearby Pend Oreille River and Little Spokane River valleys (Kiver and Stradling, 1982; Kiver et al., 1991). It is possible, however, that younger, late Wisconsin megafloods simply reworked organic-bearing pre–late Wisconsin deposits.

The orientations of convolute laminations and the geometries of the folded strata above the displacement surface indicate that the slide block was displaced in a roughly north-to-south direction. Only the distal portion of the ancient slide toe, however, is visible, with the remainder obscured beneath colluvial and alluvial cover. The causes of the slide failure are uncertain but may have been facilitated by undercutting of an over-steepened valley wall, high-pore fluid pressures, or perhaps even local seismic activity.

Paleomagnetic data described in Meyer (1999) indicate that the beds in the displaced block were originally horizontal. The convolutely deformed mud that drapes the unconformity is interpreted as a proglacial lake deposit that accumulated just prior to landslide movement. The draped muds, largely conformable nature of the strata in the slide mass, and the subsequent deposition of the overlying middle (lacustrine) unit on top of the slide block strongly suggest some of the slide displacement occurred underwater.

Middle unit. Thick beds of silt and clay with occasional lenses and stringers of very fine to fine sand characteristic of the middle unit are recognized from a limited number of exposures along Latah Creek (Figs. 14, 15). Middle unit beds are up to 3 m thick and consist of massive to crudely horizontally stratified medium to coarse silt that accumulated on top of lower-unit deposits. At a few locations, the upper half of the middle unit is cut by 2-m-high, vertically aligned columnar joints spaced 20–30 cm apart (Meyer, 1999). Irregular, vertically oriented sediment-filled fractures resembling igneous dikes also cut the middle unit locally. These fractures widen upward to >1.5 m, and

contain angular gravel-sized clasts of clay-cemented sediment that are identical to the sediment in the fracture walls.

Interpretation. The uniformly fine grain sizes and massive to horizontally stratified nature of the middle unit, as well as its stratigraphic context suggests it accumulated primarily from suspension settling in a proglacial lake. The north-sloping basal surface of the middle unit is interpreted to be a relic from prior fluvial incision. The massive to crudely horizontal planar character of strata is consistent with deposition from suspension settling. The finer-grained character of silt beds in this unit suggests deposition was either relatively distal from, or otherwise sheltered from, stronger currents. The prismatic jointing and lighter colors of the upper-unit deposits suggest that a portion of the middle unit may have been exposed at the surface and thus was subject to pedogenically related shrinking and swelling; however, the absence of more obvious weathering features makes this interpretation speculative. The irregular, vertical sand- and gravel-filled fractures that cut the middle unit are interpreted as forcefully injected clastic dikes, perhaps triggered by either seismic- or flood-induced vibrations, as suggested for clastic dikes recognized elsewhere in the Channeled Scabland (Pogue, 1998).

Upper unit. Deposits of the upper unit are up to 45 m thick and consist of crudely to well-defined beds of planar-horizontal and cross-stratified sandy gravel and sand that display a similar textural range to that of the lower-unit deposits (Figs. 15, 16). Contacts between beds in the upper unit are generally sharp and horizontal to broadly concave up. Upper-unit deposits also contain higher concentrations of cobble and boulder clasts; only a single bed (isolated and laterally discontinuous) of laminated silt-clay couplets was recognized in this unit.

The lower ~40 m of the upper unit is dominated by relatively fines-depleted, crudely to distinctly horizontally stratified, and locally cross-stratified, matrix- and clast-supported granule-boulder gravel and granule-pebble-rich sand. Planar cross-strata dip uniformly to the south within < 0.5-m-thick, generally tabular beds. Up to 1-m-long, angular to subangular outsized clasts of basalt and 1–20-cm-diameter clay and silt intraclasts are common. A 6-m-thick deposit of monoclinally shaped beds developed in upwardly fining, gravelly sand at one site (Meyer, 1999). The upper ~5 m of the upper unit consists of stacked, normally graded, 20–40-cm-thick beds of very coarse to fine sand. These beds thin and grade upward from horizontal and planar cross-strata to climbing ripple cross-laminations. A total of 12 normally graded beds were counted in this unit.

The uppermost strata of the upper unit are truncated by a series of sharp, 1–3-m-deep concave-up scours that were filled with loosely consolidated sand and gravelly sand that contains remobilized Mt. Mazama tephra (ca. 7700 cal ka). These uppermost deposits are capped by mixed loess and colluvium upon which the modern soil has developed.

Interpretation. The textural sedimentary structural and stratigraphic character of upper-unit deposits suggest they resulted primarily from glacial megafloods. The preservation of a single discontinuous bed of laminated silt-clay and the scarcity of silt-clay rip-up clasts suggest that deposition was relatively passive and that there was at least one interval of lake development during its accumulation. The crudely to occasionally well-defined nature of the stratification, abundance of outsized clasts, and fines-depleted nature of the lower ~40 m of the upper unit deposits suggest that hyperconcentrated flows (Culbertson and Beverage, 1964; Smith, 1986; Pierson and Costa, 1987; Costa, 1988; Lord and Kehew, 1987; Smith and Lowe, 1991) played an important role in their accumulation. Deposits similar to these have been observed in modern jökulhlaups in Iceland (Maizels, 1989; Russell and Knudsen, 1999a, 1999b) and Siberia (Carling et al., 2002), and from Pleistocene megaflood deposits described in Saskatchewan and North Dakota (Lord and Kehew, 1987). The upwardly aggrading monoclinally draped foresets in this unit are attributed to the southward progradation of large subaqueous bedforms during megaflooding. Lateral translation and aggradation of these tractionally transported bedforms is common when the rates of suspended-load fallout are high; similar climbing bedform features have also been observed in Siberian jökulhlaup deposits (Carling et al., 2002). The overall upward-fining of the lower portions of the upper unit indicates there was a corresponding decrease in coarse-sediment transport competence as the megafloods waned.

The progressively finer-grained and thinner character of the normally graded beds in the upper ~5 m of the upper unit are attributed to megaflood-induced turbidity currents in a proglacial lake. The stacked nature of these rhythmites suggests that they may have accumulated following flow pulses similar to those documented from modern Icelandic and Siberian jökulhlaups (Maizels, 1989; Russell and Knudsen, 1999a, 1999b; Carling et al., 2002). Because of the potential for removal of these deposits by subsequent megafloods, the number of rhythmites (12) recorded for these uppermost deposits is regarded as a minimum. The scours, loose sediment, and ca. 7.7 ka Mazama tephra in the uppermost deposits of the upper unit are attributed to post-megaflood reworking.

Summary of Depositional History

The stratigraphic and sedimentary record of Quaternary deposits preserved in the Latah Creek valley reveal at least two episodes of Pleistocene glacial megaflooding that was largely coincident with prolonged proglacial lake development. Reconstruction of megaflood pathways into the Latah Creek valley largely agrees with findings from previous studies (Bretz et al., 1956; Bretz, 1969; Waitt, 1985; Atwater, 1986) that suggested the megafloods originated primarily from glacial Lake Missoula following failures of the Clark Fork, Idaho, ice dam.

A six-stage Latah Creek depositional history is outlined in Figure 17 and summarized here: (1) Latah Creek excavated its channel into Miocene basalt during pre-last glacial times. (2) Ice sheet advances into northern Washington and Idaho during the late Pleistocene blocked largely west- and southwest-flowing drainages, creating proglacial lakes that were impacted by flood influxes when temporary ice lobe dams failed or were partially

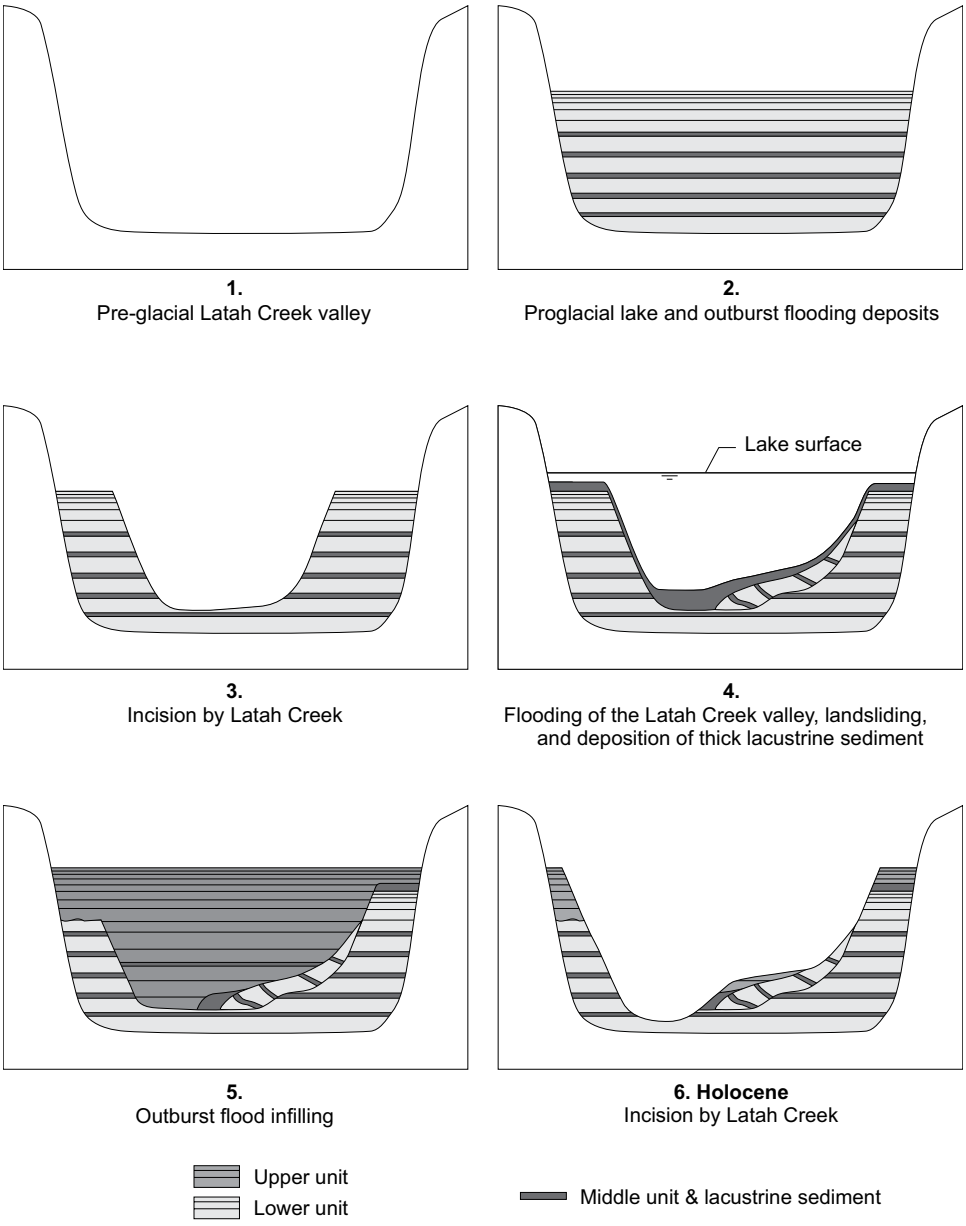

Figure 17. Six-stage summary of erosion and deposition at Latah Creek as described in the text.

breached. A series of variably high-magnitude, sand- and gravel-laden megafloods produced the normally graded rhythmites near the base of the lower unit; this lacustrine deposition was dominantly from turbidity/density current and hyper-concentrated flows. Glacial Lakes Columbia and Spokane, into which megaflood waters flowed, likely persisted for decades as discerned from detailed varve counts from the Manila Creek strata (Atwater, 1986) and observed in Latah Creek. The upper subunit of the lower unit resulted from small magnitude, temporally distinct glacial megafloods. Coincident with upper subunit deposition, the lake-impounding ice sheet retreated and lake levels fell. (3) Continued retreat of the ice sheet prompted fluvial incision that ultimately removed at least 30 m of lower-unit megaflood and lake deposits. (4) Readvance of ice sheet lobes north and northwest of Spokane again blocked drainages and promoted expansion and rise of proglacial Lakes Columbia and Spokane. At least one over-steepened valley wall failed and slid into the lake prior to the accumulation of the middle unit. (5) Short-lived readvances and subsequent deterioration of nearby ice sheet lobes led to renewed megaflooding, falling proglacial lake levels, and diminished lake surface areas. The lowest units in the upper unit signaled the return of a few high-magnitude floods that flowed

either into shallow lake waters or into the stream valley; megaflood deposition was largely via hyperconcentrated flows. Upper-unit deposits resulted from more frequent, though low-magnitude megafloods that produced turbidity current deposits in slackwater areas. (6) Continued disintegration of the Cordilleran Ice Sheet promoted falling proglacial lake levels, lake bed exposure, and renewed Latah Creek incision. The final episode of incision in the Latah Creek valley was accompanied by episodic Holocene alluvial, colluvial, and loess deposition, Mazama tephra airfall accumulation, fluvial reworking, and pedogenesis.

Radiometric ages of Latah Creek wood suggest the bulk of the Quaternary sedimentary deposits in this valley accumulated after ca. 32 ka radiocarbon yr B.P. (ca. 36 ka cal yr B.P.), a time frame that leaves open the possibility that both pre-late and late Wisconsin megaflood episodes are preserved in the valley. However, until the depositional history of the Latah Creek sediment can be correlated with more tightly constrained depositional histories elsewhere in the scabland, or direct depositional ages can be determined from the Latah Creek deposits, a pre–late Wisconsin sedimentary history is an intriguing, but still unproven possibility.

ROAD LOGS—DAYS 1–3

Distances for each day are given in miles from the starting point, and distance to the next mileage point is indicated within brackets after the descriptions.

■ DAY 1—SPOKANE TO QUINCY

Mileage	*Directions*
0.0	Depart from Spokane International Airport parking lot toward Spokane on W. Airport Drive. Follow sign to exit left from W. Airport Drive and merge on to U.S. 2 West toward Wenatchee. Set odometer to 0.0. [1.0]
1.0	Route proceeds westward over the Sunset Prairie (part of the Spokane Plains), which is thinly mantled by eolian silts that overlie flood-emplaced sand and gravel. [3.2]
4.2	Entering Airway Heights, a suburb that mainly serves Fairchild Air Force Base. [1.8]
6.0	Rambo Road enters from the right. A short side trip up this road will cross a field of subfluvial dunes (“giant current ripples”). These examples are unlike others that will be seen on the field trip because they are composed mainly of coarse sand, not gravel. The main road passes through a general area that is mantled by such dunes, which locally reach heights of 4 m and spacing of 100 m. To the southwest of this area, Stradling and Kiver (1986) found the Mount St. Helens S tephra in a trough between dunes that was overlain by deposits they interpreted to be later flood sediments. Check that odometer reads 6.0 at this point. [3.4]
9.4	Road descends into the valley of Deep Creek down a slope that is underlain by megaflood sand and gravel that comprises a large delta-like emplacement by the last major late Pleistocene floods that crossed the Sunset Plains and flowed southwest into the Channeled Scabland. [1.5]
10.9	Hills to the south (left) are steptoes near Medical Lake, those to the southwest are near Reardan. [1.4]
12.3	The road ascends onto an upland that had been mapped as loess. More recent mapping (M. McCollum, 2015, personal commun.) has shown that only a very thin cover of eolian silt overlies a thick residual weathering profile developed on the Miocene basalt bedrock. This is locally overlain by a highly weathered, polymictic pediment gravel. [2.3]
14.6	Two steptoes, Magnison and Hanning buttes, are visible to the south (left). [3.5]
18.1	Reardan, Washington. SR-231 joins from right. The Audubon lakes visible to the right, just north of Reardan, are at the headwaters for Crab, Deep, and Spring Creeks. The lakes are developed on a small area of basement rocks that form a triple drainage divide, where the Pleistocene megafloods crossed an ancient mountain range that had been surrounded by the Miocene Columbia River Basalt Group lava flows. Also occurring in this area are some of the silt mounds that are widespread throughout the Channeled Scabland region. Numerous hypotheses have been proposed for their origin. What do you think? [3.3]
21.4	The road ascends onto an upland underlain by the residual weathering profile on the basalt. Locally, this weathering horizon is overlain by the lag gravel and thin loess cover. This upland separates the heads of megaflood overflow areas to the Cheney-Palouse Scabland tract to the east from the Telford–Crab Creek Scabland to the west. [9.6]
31.0	Junction with SR-25, which trends north toward Fort Spokane. Continue west on U.S. 2 into Davenport. [0.9]
31.9	Junction with SR-28 (12th Street). Turn left (south) on SR-28 toward Harrington and Odessa. [13.7]
45.6	Junction with SR-23 in Harrington. Continue southwest on SR-28. [10.7]
56.3	Road intersections, continue on SR-28. Descending to Coal Creek Coulee. [4.7]
61.0	Pass junction with Lamora Road. [9.2]
70.2	Intersection with SR-21 near Odessa. Continue on SR-28. [0.4]
70.6	Cross Crab Creek. [1.5]
72.1	View of basalt ring structure on right. Possible brief photo stop. [0.9]

The Odessa Craters (Baker)

The Odessa craters are enigmatic circular features in the Channeled Scabland. Where their internal structure is exposed because of flood erosion, detailed examination shows that they

are features inherent within the lava. Several competing hypotheses were suggested for their formation in the 1970s, with the "sag-flowout" model (McKee and Stradling, 1970) being the most widely accepted at the time. In this model, material from the interior of the lava flow wells up through a crack and the crust sags downward into the flow. However, this model does not explain the association with palagonite and phreato-volcanism described by Hodges (1978). She suggested a modification of the sag-flowout model in which phreato-volcanism removes material from the interior of a cooling lava flow, builds cones atop the flow, and thereby causes the solidifying flow crust to sag. The shortcoming of this model is that it predicts phreato-volcanic products on the surface of a thick lava flow, deposits that are not observed (Keszthelyi and Jaeger, 2015).

More recent work has suggested an alternative model involving inflation (rather than sagging) around a zone of steam escape (Jaeger et al., 2003; Keszthelyi and Jaeger, 2015). Basically, where steam venting quenched molten lava in a flow interior, the lava was unable to inflate, and the flow remained locally thin. This produced conical depressions with tilted joints, and in the best developed structures, radially symmetric auto-intrusive dikes that propagated along the tilted joints. This hypothesis is supported by the observations of lava flows seen in cross section at Banks Lake and Frenchman Springs Coulee, and it unites the disparate field observations of McKee and Stradling (1970) and Hodges (1978) under a single, self-consistent model. The current topographic expression of the Odessa craters has little to do with their volcanic origin; instead, the craters are mainly the result of the flood erosion preferentially plucking the looser material (including phreato-volcanic deposits) from inside the cones.

73.0 View of scabland. [1.5]

74.5 View of gravel dunes (giant current ripples) (Fig. 18). [4.4]

Fluvial Gravel Dunes (Giant Current Ripples) (Baker)

Megaflood gravel surfaces in the Channeled Scabland are commonly mantled with "giant current ripples," also known as "subaqueous gravel dunes" (Carling, 1999), composed of coarse gravel and boulders (up to 1.5 m in diameter). The dunes on the Odessa gravel bar (Fig. 18) average ~2.5 m in height and ~65 m in spacing (Baker, 1973a). Although Bretz (1930b, p. 400) made a brief reference to these particular features, it was not until later work (Bretz et al., 1956) that the name "giant current ripples" (GCRs) was applied to such transverse gravel depositional forms in the Channeled Scabland. Following Pardee's (1942) discovery of similar features in the basin of glacial Lake Missoula, Bretz et al. (1956) identified about a dozen examples in eastern Washington. Subsequently, Baker (1973a) documented 60 of the most prominent sets of GCRs. The striking appearance of the scabland GCRs on air photos arises from local post-depositional factors. Eolian silt deposits in the swales between the bedform crests locally produces differences in vegetation cover. In drier regions, the gravelly summits are covered by sagebrush (*Artemisia tridentata*), and the adjacent swales are covered by cheat grass (*Bromus tectorum*).

78.9 Road descends to scabland. [3.9]

82.8 County line. [0.4]

83.2 Road to Marlin (W NE) on right. Stay on SR-28. [6.1]

89.3 Road intersection. Continue on SR-28. [2.8]

92.1 Intersection with Kappel Road. Turn right toward town of Wilson Creek. [0.1]

92.2 Park on right shoulder. View of bars 2 and 3 (Stop 1).

Figure 18. Giant current ripples along Crab Creek Coulee west of Odessa.

STOP 1—Wilson Creek Bars (N47.4194°, W119.1314°) (Baker)

Prior to invasion by Pleistocene cataclysmic flooding, Crab Creek was a meandering valley cut into the Columbia River Basalt Group lava flows (Bretz et al., 1956). The valley sides and interfluves were thickly mantled with the Palouse loess. Just upvalley from this stop, one can clearly see the form of the pre-flooding bedrock valley meanders. One theory of bedrock meandering (Dury, 1965) would suggest that the wavelength of the bedrock meanders (~2 km) would be associated with a bankfull discharge of ~850 m^3s^{-1}. The peak discharges for Pleistocene megaflooding in this area were estimated by Baker (1973a) at 2.8×10^6 m^3s^{-1}. It is the imposition of such immense discharges on a relatively small valley, a condition that can be termed "overfitness," that led to so much skepticism when Bretz (1923, 1928) presented his observations to his fellow geomorphologists. Bretz argued that the pre-flood valleys simply did not have the capacity to convey the immense discharges that were imposed upon them. This induced the flows to spill out of the valleys and cross preflood divides, ultimately leading to the large-scale anastomosing pattern of scabland channel ways.

Bretz et al. (1956, p. 977–980) and Bretz (1959, p. 38–39) highlight this area for its association of gravel bars with giant current ripples, as well as trenched spur buttes that developed when the insides of bedrock meander bends were scoured by the high-velocity megaflood waters (Fig. 19). The bars are composed of coarse gravel and boulders that are organized into foreset bedding that dips in a down-flow direction. Giant current ripples (subfluvial dunes) occur on 16 bar surfaces in this area (Baker, 1973a). Most of these are pendant bars: flow-streamlined mounds of gravel that accumulate downstream from bedrock projections on the scabland channel floors. The projections can be knobs or buttes of basalt, or they may involve the inside bends of preflood meandering bedrock valley. In this area, the bar surfaces are generally ~30 m above the floors of the pre-flood valleys and ~30–60 m below the local high-water marks for the megaflooding (Baker, 1973a). The bars are ~1–2 km in length.

Turn around and return to SR-28. [0.1]

92.3 Intersection with SR-28, turn right and continue west on SR-28. [0.8]

93.1 Bar 3 gravel pit on right. [1.4]

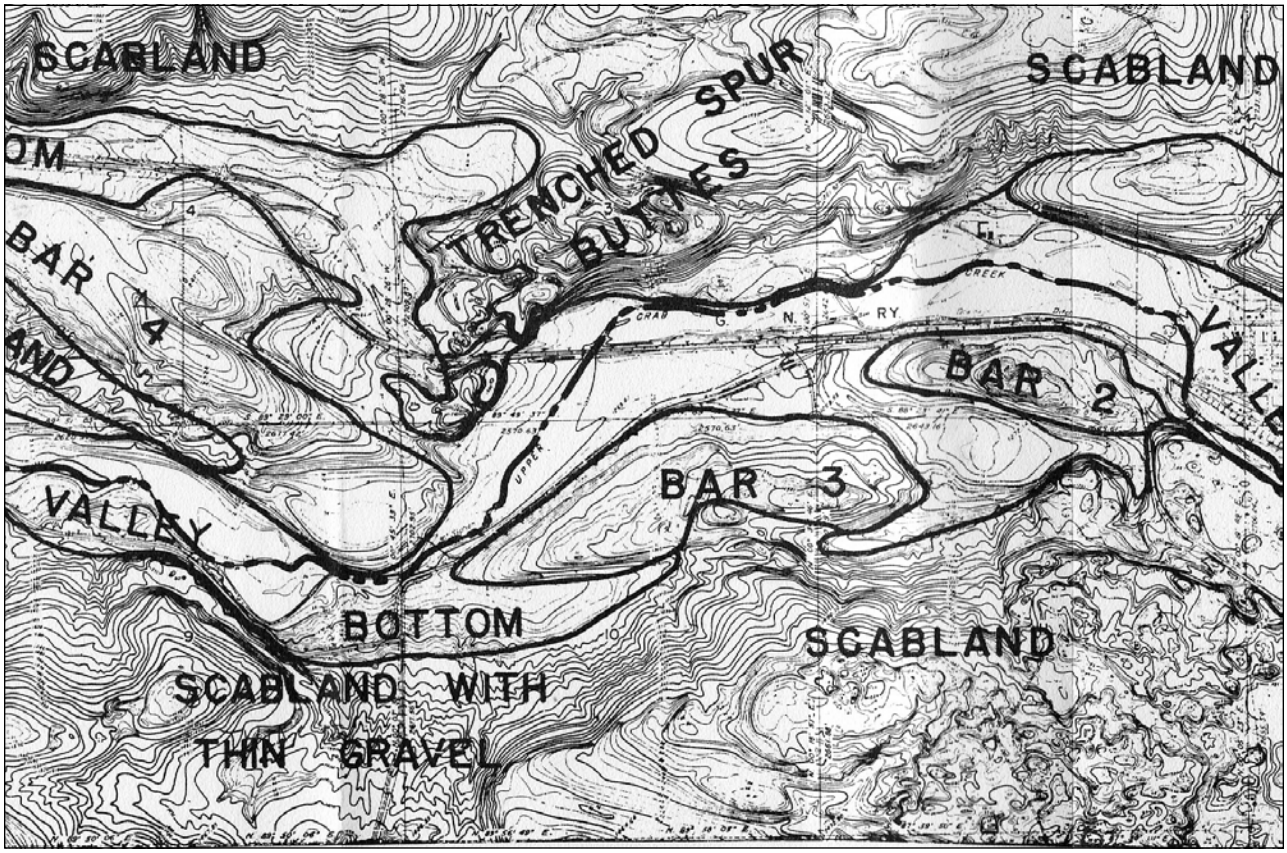

Figure 19. Portion of a topographic map for the Wilson Creek area showing gravel bars and trenched spur buttes (from Bretz et al., 1956, and Bretz, 1959). The area shown is 28 km × 12 km and north is to the top of the figure.

94.5 View of bar 3 gravel dunes (giant current ripples). [3.7]
98.2 View of Long Lake. [0.6]
98.8 Post-flood lake silts. [1.1]
99.9 Cross Crab Creek. [1.5]
101.4 Junction with Pinto Ridge Road—possible side trip to Pinto Ridge and Dry Coulee.

▸ OPTIONAL SIDE TRIP—Pinto Ridge–Dry Coulee

Reset odometer.

0.0 Junction SR-28 with Pinto Ridge Road. Turn right onto Pinto Ridge Road and continue north. [0.6]
0.6 Cross Main Canal, Columbia Basin Irrigation Project. [0.1]
0.7 Bar of flood gravel (flood level 1360 ft elevation). [1.9]
2.6 Palouse loess exposed in roadcut on left. [1.0]
3.6 Junction with Road 26 NE. Continue north on Pinto Ridge Road. [1.1]
4.7 **Photo stop.** View to north of Lenore Canyon, upper Grand Coulee, Hudson Coulee, and early flood bars of the Hartline Basin. [0.7]
5.4 Road passes through flood gravel bar at elevation of 1720 ft. [0.7]
6.1 Summer Falls Road on right, Dry Coulee Road on left. [0.0]
6.1 Turn left on Dry Coulee Road (gravel). [0.4]
6.5 View of Dry Coulee and High Hill. [1.3]
7.8 Gravel bar on right. [0.5]
8.3 Scabland buttes and gravel bar. [0.8]
9.1 Irrigated farmland on silts (probably emplaced in a post-flood lake). [0.7]
9.8 Road is on gravel bar. Note boulders on the right. [0.7]
10.5 Descend from gravel bar. [1.4]
11.9 Pavement resumes. [1.0]
12.9 Junction with Road 25 NE. Continue southeast on Dry Coulee Road. [0.3]
13.2 Leaving Dry Coulee. [0.9]
14.1 Old railroad grade on left. [0.3]
14.4 End of Dry Coulee. [0.6]
15.0 Old railroad cut on left. [0.8]
15.8 Junction with SR-28. Cross highway and continue south on Adrian Road (see below).

▸ Add 13.1 to mileage *if* you took the OPTIONAL SIDE TRIP, *then continue on with the regular Road Log below.* ◂

REGULAR ROAD LOG (*continued*)

101.4 Junction of SR-28 and Pinto Ridge Road. Continue west on SR-28. [2.7]
104.1 Junction of SR-28 with Dry Coulee Road (north) and Adrian Road (south). Turn left on Adrian Road. [1.0]
105.1 Gravel bar exposure on right. [0.5]
105.6 Road to right. Exposures of rounded gravels. [0.1]
105.7 Cross railroad track, road bends to right in Adrian. [0.6]
106.3 Junction with 20 NE Road. Turn right onto 20 NE Road. [2.7]
109.0 Junction with B NE Road just before railroad crossing. Turn left onto B NE Road. [0.2]
109.2 Boulders on right are from the proximal Ephrata fan. [1.0]
110.2 Junction with 19 NE Road (Grant Orchards Road) at stop sign. Turn left onto 19 NE Road. [0.4]
110.6 Road bends to right and becomes B NE. [0.1]
110.7 Boulders on right. [0.7]
111.4 More Ephrata fan boulders. [0.3]
111.7 Pass junction with 18 NE on right. Continue on B5 Road. [2.0]
113.7 Pass junction with 16 NE on left. Continue on B5 Road. [0.1]
113.8 Road bends right. Stop, pull off, and park on the left side of the road above fish hatchery on left (Stop 2).

STOP 2—Rocky Ford Creek (N47.3239°, W119.4361°) (Baker)

The Ephrata fan (Fig. 20) is an immense accumulation of gravel and sand that resulted when megaflood waters from Crab Creek, Dry Coulee, the lower Grand Coulee (ending at Soap Lake), and smaller scabland channels entered the Quincy Basin. The deposit probably formed more in the manner of an immense expansion bar (Baker, 1973a), rather than a fluvial fan in which relatively small alluvial channels shift across the fan surface without ever inundating the entire surface at once. Local areas of surface scour occurred on the fan, the most prominent of which is Rocky Ford Creek. The spring-fed headwaters of Rocky Ford Creek can be seen at this stop. The scour probably developed during waning flood stages, when draining of the inundated Quincy Basin caused relatively steep water-surface gradients to occur over the depositional surfaces that had been constructional during the high stages of megaflooding (Baker, 1973a). The scour processes produced the lag concentration of boulders on the fan surface, many of which can be seen from this viewpoint. An alternative explanation for the morphology of the Ephrata fan is that it was progressively incised by a sequence of multiple floods of successively decreasing magnitudes (Waitt, 1994; Waitt et al., 2009). It may also be that a more complex combination of these mechanisms occurred.

The proximal portions of the Ephrata fan, as seen at this stop, are composed of gravel and coarse boulders. Where exposed, as along the road beyond the stop, the gravel is organized into foreset beds that dip away from the megaflood source inputs to Quincy Basin. More distal portions of the fan, which will be seen on Day 2 of the field trip, are composed of sand, the surface layers of which have been locally modified into fields of eolian dunes.

In its proximal portions, the fan sedimentary thickness is up to ~40 m. Local scour to bedrock through the coarse-grained

fan sediments, as here in the headwaters of Rocky Ford Creek, allows cool groundwater to emerge from the gravel, thus providing an ideal location for the fish hatchery that is seen below the viewpoint.

Continue on 19 NE Road. [0.1]

113.9 Planar foreset beds exposed in flood gravel on right. [0.2]
114.1 Fish hatchery. Begin gravel road. [0.3]
114.4 Three-way junction. Turn right onto Hatchery Road NE. [0.3]
114.7 Flood boulders, both basalt and granite. [1.0]
115.7 Pull off on right (Stop 3).

STOP 3—Immense Boulder on Ephrata Fan (N47.3275°, W119.4680°) (Baker)

This immense boulder (Fig. 21) measures ~18 × 11 × 8 m. It has a prominent crescent-shaped scour mark (now mostly filled with talus) cut into the sediment on the northwest (upstream) side of the boulder, and an elongate elliptical scour hole on the southeast (downstream) side. This scour pattern can be explained by a dual vortex system generated by the blunt obstacle posed by the boulder to the megaflood flow field during the waning stages of a flood (Baker, 1973a, 1978c; Baker and Komar, 1987). The size of this boulder attests to the transport capability of the megaflood waters (Fig. 10) as they poured through the Soap Lake constriction point. The boulder consists of basalt entablature, the interlocking jointing of which likely led to its remaining intact during transport from outcrops that lie ~8 km to the north. The many other large boulders in this area are smaller, which may be the result of their inability to remain intact during transport. An alternative hypothesis is that this boulder was ice-rafted into the present location. However, there are many problems with that hypothesis that will be further discussed on the trip.

Continue on Hatchery Road NE. [0.7]

116.4 Junction with Route 17. Turn right onto Route 17. [0.8]
117.2 High divide at proximal end of Ephrata fan. [0.9]
118.1 Small lake on right formed by filling scour into Ephrata fan. [0.5]
118.6 Railroad underpass. [1.5]
120.1 Junction with SR-28. Cross SR-28 and continue straight into town of Soap Lake on SR-17. [0.6]
120.7 Junction with Main Avenue in town of Soap Lake. Continue on SR-17. [0.1]
120.8 Soap Lake on left. The lake occurs at a constriction point for the megaflood waters coming down the Grand Coulee. From here, the flooding poured out onto the Ephrata fan. The scour at Soap Lake extends to 62.5 m below the current lake surface, and is overlain by 33.5 m of flood gravel. The nozzle-like flow from the Soap Lake constriction into the Quincy Basin likely generated a hydraulic jump at the time of maximum megaflooding (Baker, 1973a). As the lowermost lake in a chain extending through the lower Grand Coulee, Soap Lake has a high alkalinity, mainly from Na_2CO_3, and harbors an interesting biota. [0.3]
121.1 Basalt roadcut on right. [0.8]
121.9 Silt deposits of Pleistocene Lake Bretz (Landye, 1973) exposed on right. [1.3]
123.2 Junction with 23 NW. Continue on SR-17. Exposure of colluvium over lake silts on right. Basalt scabland to right contains Horsethief Cave. [0.3]
123.5 Entering Lenore Canyon (Lower Grand Coulee). Silts are from Pleistocene Lake Bretz. [1.1]
124.6 Note hanging valleys on wall of Lenore Canyon to left. [1.1]

Grand Coulee (Baker)

Hanging valleys and stacks of columnar-jointed lava are visible on the western side of Lenore Canyon. In the northwestern United States, the term "coulee" is applied to very large steep-walled, trench-like troughs that typically do not contain streams along their valley floors. Coulees are commonly the spillways and flood channels of the overall scabland plexus, and many were parts of pre-flood fluvial valleys that formerly were shallowly incised into the basalt plateau. Hanging valleys occur where the tributaries to these valleys are no longer graded to a main valley floor—because of deepening and widening by the cataclysmic flood scour. Examples occur in Lenore Canyon and Moses Coulee (the latter will be seen near the end of the day), where the pre-flood tributaries enter cliff faces on the coulee margins at elevations of ≥100 m above the coulee floor.

The Grand Coulee is the most spectacular of the structurally controlled elements of the western portion of the Channeled Scabland (Fig. 22). The basalt layers of the moderately (45–60°) eastward-dipping limb of the coulee monocline were weakened by extension, thereby becoming more easily eroded by the plucking action of the megaflood waters than was the flat-lying basalt to the east.

125.7 Lake Lenore on left. [4.0]
129.7 Road on right leads to Lake Lenore caves. Views of dip slopes on basalt and the Great Blade. A well-developed butte-and-basin scabland area (Fig. 23) occurs to the east of Lake Lenore. [0.3]
130.0 Lake silt on left. [0.4]
130.4 Island in Lake Lenore formed by east-dipping basalt beds of Coulee monocline. [1.8]
132.2 Large flood bar on right. The Cariboo Cattle Trail sign indicates that this trail crossed the Grand Coulee at this point along its route from Wallula Gap in south-central Washington, northward through the western Channeled Scabland to the Okanogan Valley of British Columbia. [0.8]
133.0 Blue Lake on right. [2.0]

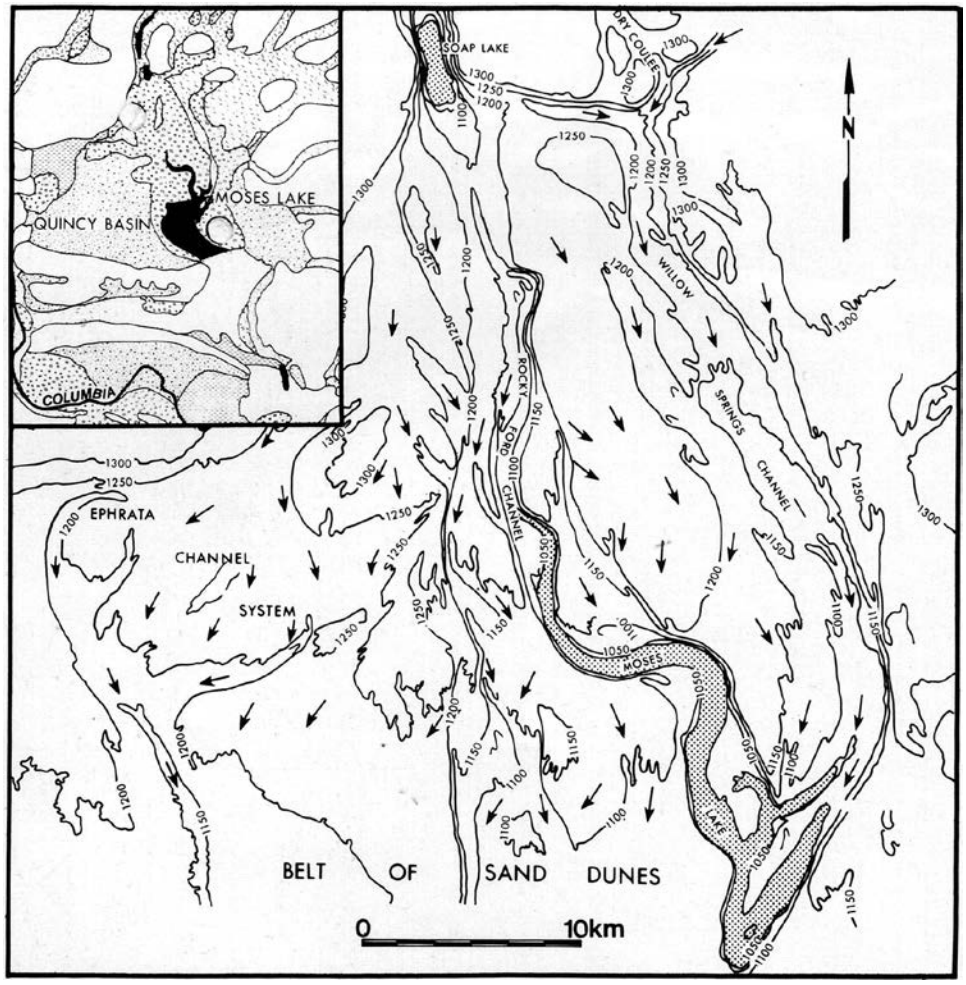

Figure 20. Map of the Ephrata fan complex in the upper part of the Quincy Basin (see inset) with arrows showing the inferred flow directions of the late Pleistocene megaflooding. (Figure is modified from Bretz, 1959, p. 33.)

Figure 21. Over-sized boulder of basalt entablature deposited by cataclysmic flooding on the proximal portion of the Ephrata fan. This boulder measures 18 m along its long axis. A prominent scour hole, described by Baker (1973a, 1978b), extends downstream from the boulder (just above the vehicle).

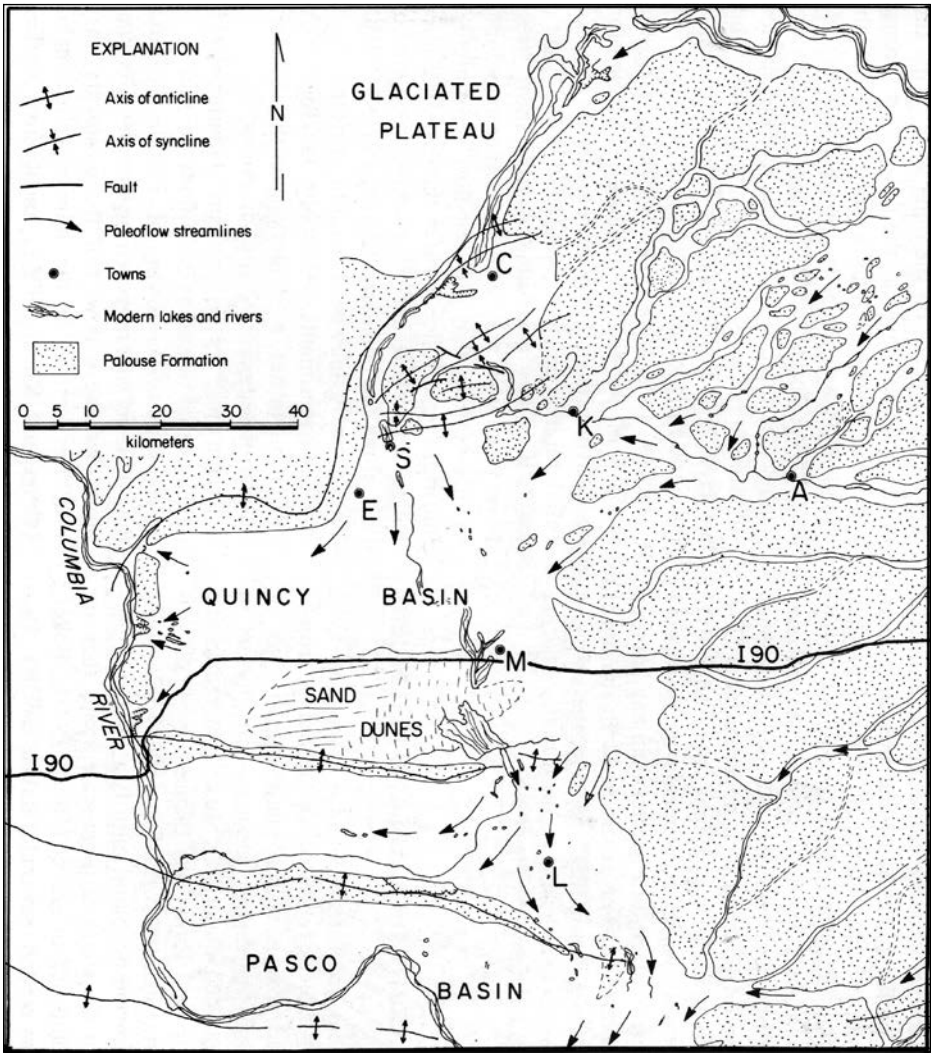

Figure 22. Regional pattern of channels and structural elements for the western Channeled Scabland as mapped from LANDSAT imagery (E-1039-1843-5 and E-1004-18201-7). The structurally controlling features include the coulee monocline, extending from just east of Ephrata (E) to just north of Coulee City (C). Other towns indicated on the map are Odessa (A), Wilson Creek (K), Othello (L), Moses Lake (M), and Soap Lake (S).

Figure 23. Aerial photograph, looking to the southwest, showing butte-and-basin scabland in Lenore Canyon of the lower Grand Coulee. Note the roadways for scale.

135.0 Park Lake Road to right. Continue on SR-17. [0.4]
135.4 Jasper Coulee and flood eddy bar visible to right. The Blue Lake Rhino caste in basalt was discovered near here. When, during the Miocene, molten lava entered a swamp, rapid cooling of the lava around a rhino carcass preserved a mold of the animal, forming a small cave. [0.2]
135.6 Park Lake on right. [0.5]
136.1 Good view of coulee monocline to left and front. [1.4]
137.5 Road to Sun Lakes State Park on right. Continue on SR-17. [1.9]
139.4 Turn right into parking lot for Dry Falls Visitor Center.

STOP 4—Dry Falls (N47.6467°, W119.6764°) (Baker)

Perhaps the most famous cataract in the Channeled Scabland is "Dry Falls," which is part of a complex that extends over a width of 5.5 km, with a maximum vertical drop of ~120 m (Fig. 24). Dry Falls is at the northern end of Lower Grand Coulee, which was excavated by cataclysmic floodwater from a zone of fractured basalt along the axis of the coulee monocline (Bretz, 1932). It is also at the upstream terminus of an inner channel that receded headward into the Hartline Basin, near Coulee City, Washington. Bretz et al. (1956, p. 1029) hypothesized that the Channeled Scabland cataracts formed subfluvially rather than by the plunge-pool undercutting classically illustrated by Niagara Falls. This hypothesis is supported by high-water mark evidence (Baker, 1973a). Bretz (1932) also described the initiation of a 250 m cataract near Coulee City, which receded more than 30 km upstream to create the Upper Grand Coulee.

Missoula flood erosion of the Columbia River Basalt probably occurred as an organized sequence of stages (Fig. 25), examples of which can be found throughout the Channeled Scabland (Baker, 1973b, 1978c, 2009c). The first floodwater encountered a plateau surface capped by loess that had been shaped into hills by the gentle dissection of streams fed by rainfall and runoff on the plateau itself (phase I, Fig. 25). The high-velocity water quickly filled the relatively small pre-flood valleys, shaping the remnant loess divides between them into streamlined loess hills (phase II, Fig. 25). Next, the incising floodwater encountered the top of the Columbia River Basalt Group lavas, often finding entablature. The irregular jointing of the entablature makes it relatively resistant to flood erosion, so its surface may have been initially scoured by longitudinal grooves, similar to those observed just above Dry Falls (Fig. 24). As the scour cut deeper into a basalt flow, in many locations it would next encounter the well-developed columnar jointing of the upper colonnade. The joint-bounded columns were very susceptible to plucking-type erosion (phase III, Fig. 25) in which the pressure fluctuations associated with vertical vortices (kolks) lifted sections of column and entrained them into the floodwater. The resulting potholes would then enlarge and coalesce (phase IV, Fig. 25), forming the common butte-and-basin scabland topography of the region. Eventually, a prominent inner channel (phase V, Fig. 25) would develop, probably by the initiation and headward migration of a cataract such as Dry Falls (Fig. 24).

From studies in the Columbia River gorge, Benito (1997) found that the various phases of erosion shown in Figure 25 are associated with different levels of flow strength, estimated as bed shear stress, mean flow velocity, and power per unit area of bed (see Table 1). These parameters were determined from hydraulic modeling (see also Benito and O'Connor, 2003).

The lava stratigraphy exposed in Dry Falls is dominated by the Wanapum Basalt. A Priest Rapids Member flow, possibly the

Figure 24. Aerial view, looking to the north, showing the Dry Falls cataract complex. The megaflood flows were from top to bottom in this scene, parallel to the bedrock grooves visible near the center of the photo. Two prominent alcoves are at the left center of the photo, and the Dry Falls Visitor Center (Stop 4) is located above the left alcove. Some very prominent rock basins (potholes) can be seen at the lower right. Banks Lake and its dam are at the top center. Coulee City is in the upper right corner of the picture.

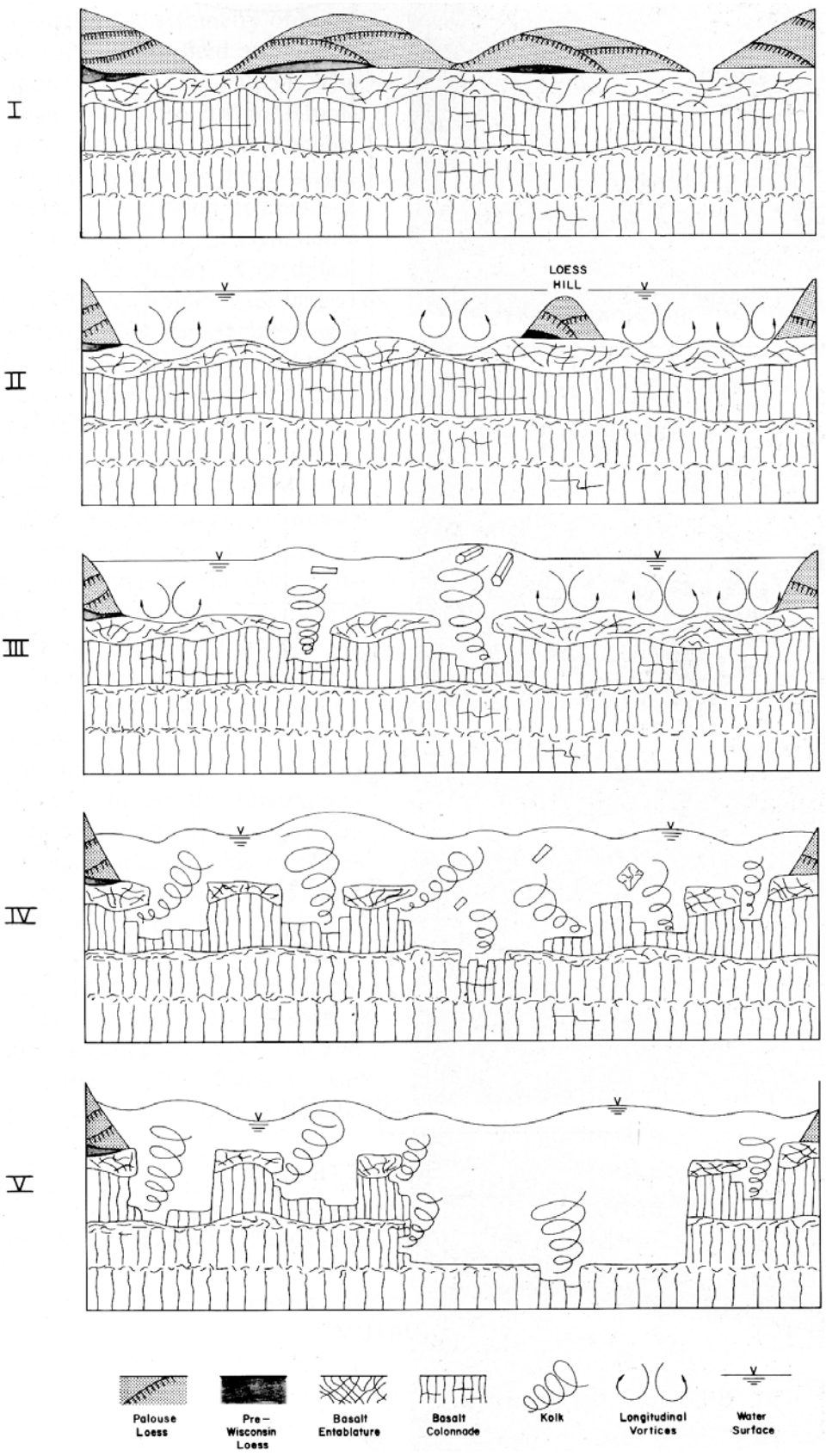

Figure 25. Hypothetical sequence of bedrock erosion (from top to bottom) as seen in the Channeled Scabland illustrated by schematic cross section, showing the plucking action of macroturbulence, including longitudinal vortices and kolks (stages II and III). The lateral enlargement of inner channels (stages IV and V) probably proceeded by the undercutting of relatively resistant basalt entablature as underlying columns were plucked out by kolks. See text for a more detailed discussion.

Lolo or Rosalia, sits at the top of the stack. Below are two flows of the Roza Member and at least one flow from the Frenchman Springs Member. At the bottom and farther south, the Grande Ronde Basalt is visible. Note the variety of lava textures and the interactions of flow lobes at each stratigraphic level.

Turn right out of the parking area and continue north on SR-17. [2.0].

141.4 Junction with U.S. 2. Turn right on U.S. 2 toward Coulee City. [0.2]
141.6 Begin crossing Dry Falls Dam. Banks Lake is on the left. [1.5]
143.1 Power plant and Main Canal intake for Columbia Basin Irrigation Project. [0.3]
143.4 Turnoff for Coulee City on right. Continue on U.S. 2 toward Spokane. [2.3]
145.7 U.S. 2 turns to the right. Continue straight on SR-155 toward Coulee Dam. Hartline Basin expansion bar visible on right; upper Grand Coulee ahead. [2.1]
147.8 Entering the upper Grand Coulee. Notice steeply dipping basalt flows on the right where the coulee monocline crosses the upper Grand Coulee. [3.8]

The Upper Grand Coulee

Reverend Samuel Parker (1838) provided some of the first scientific observations of the dry river courses ('coulees') of eastern Washington State. Parker hypothesized that the Grand Coulee was an abandoned former channel of the Columbia River. A subsequent government survey of Grand Coulee by Lieutenant T.W. Symons (1882) included the following description of his travel: "… north through the coulée, its perpendicular walls forming a vista like some grand ruined roofless hall, down which we traveled hour after hour. …"

Symons (1882) hypothesized that the diversion of the Columbia River through the Grand Coulee was caused by a glacial blockage of the river immediately downstream of its junction with the coulee. This view became generally accepted for the next few decades (Russell, 1893; Dawson, 1898; Salisbury, 1901; Calkins, 1905).

A traverse of the Grand Coulee in 1912 by the American Geographical Society's transcontinental excursion led to the authoring of several international papers on the coulee by participants on the excursion. Henri Baulig, Université de Rennes, described the loess, coulees, rock basins, plunge pools, and dry falls ("cataract desechée de la Columbia") for the area (Baulig, 1913). He also noted the immense scale of the erosion (Baulig, 1913, p. 159): "… peut-être unique du relief terestre, —unique par ses dimensions, sinon par son origine." Karl Oestreich, University of Utrecht, considered the Grand Coulee to be "… eines machtigen Flusses Bett … ohne jede Spur von Zerfall der frischen Form" (Oestreich, 1915). He provided another excellent set of descriptions, including features that he recognized to require a special explanation, including granite hills exhumed from burial by the plateau basalt layers, and almost perpendicular coulee walls locally notched by hanging valleys. Oestreich (1915) proposed that the hanging valleys resulted from glacial erosion of the coulee, but that the deepening of the coulee came about by enhanced fluvial erosion from the glacially enhanced and diverted Columbia River. He also recognized that the coulee was cut across a pre-glacial divide, which he correctly noted to lie just north of Coulee City.

An influential report on the Grand Coulee was written by Oscar E. Meinzer, who later founded many of the hydrological science programs of the U.S. Geological Survey. Meinzer (1918) proposed that the glacially diverted Columbia River "cut precipitous gorges several hundred feet deep, developed three cataracts, at least one of which was higher than Niagara … and performed an almost incredible amount of work in carrying boulders many miles and gouging out holes as much as two hundred feet deep." He also recognized that the dipping surface to the basalt on the northern Columbia Plateau was important for generating a steep water-surface gradient to the Columbia River water that was diverted across the plateau by glacial blockage of its pre-glacial valley. The resulting increased velocity of the river water was thus capable of the enhanced erosion indicated by the scabland.

151.6 Gravel exposure in megaflood eddy bar on right. [0.4]
152.0 Slackwater silts on left. [1.4]
153.4 Spectacular view of upper Grand Coulee. The pull-off on the left is a good opportunity for taking photographs. [1.1]
154.5 Turnoff on left goes to Paynes Gulch site. [1.1]
155.6 Boulders on megaflood bar to left. [1.6]
157.2 Flood gravel exposure. [0.4]
157.6 Lake silts exposure. [1.8]
159.4 View of Steamboat Rock. Note pull-off on left. [1.8]
161.2 Road to Steamboat Rock enters from left. Continue on SR-155. [2.2]
163.4 Pull off on left. Views of Steamboat Rock, Castle Rock, inselbergs, and a megaflood eddy bar.

STOP 5—Steamboat Rock (N47.8583°, W119.1064°) (Baker)

Steamboat Rock (Fig. 26) is the remnant of a great cataract system that receded ~30 km from the coulee monocline all the way to the Columbia River. There must have been a temporary spill point at Steamboat Rock prior to the last recession ca. 17.2 cal ka, as indicated by the exhumation date for one of the inselbergs at Electric City noted above. The top of Steamboat Rock is littered with erratic boulders, and cosmogenic exposure dates for some of these are shown in Table 2 (see discussion below). The lava stratigraphy seen in cross section in Steamboat Rock and the walls of the Upper Grand Coulee are dominated by the N2 member of the Grande Ronde Basalt. They are capped by the Wanapum Basalt, commonly the Roza and/or Priest Rapids Members.

Cosmogenic ^{36}Cl Exposure Dating of Megaflooding (Zreda and Baker)

We applied the terrestrial in situ cosmogenic nuclide (TCN) method (Gosse and Phillips, 2001) to date the latest phase of megaflooding in the Channeled Scabland region. Specifically, we employed surface exposure dating by cosmogenic ^{36}Cl (Phillips et al., 1986). Our field samples were collected from nine sites (one granite inselberg near Electric City—sample MF-1; and eight boulders in various geological contexts). These samples were processed and analyzed using methods described by Desilets et al. (2006a) and Pigati et al. (2008), and the ^{36}Cl ages were calculated using the ACE software (Anderson et al., 2007), with the following production rates: 71.6 ± 3.7 atoms ^{36}Cl (g Ca)$^{-1}$ yr^{-1}, 155.1 ± 9.6 atoms ^{36}Cl (g K)$^{-1}$ yr^{-1}, and 676 ± 40 fast neutrons (g air)$^{-1}$ yr^{-1}. These production rates are based on the calibration data set of Phillips et al. (1996), augmented by high-potassium samples from three additional sources (Ivy-Ochs et al., 1996; Zreda et al., 1999; Phillips et al., 2009). They have been scaled to sea level and high geomagnetic latitude (Desilets et al., 2006b), and to modern geomagnetic field conditions (referenced to the 1945.0 Definitive Geomagnetic Reference Field) using the method of Pigati and Lifton (2004).

The results are shown in Table 2. In this table, error 1 is based on chemistry errors only, and it is used for comparison to other ^{36}Cl ages computed using the same production rates. Error 2 includes error 1, but it also adds uncertainties in regard to the production rates. Error 2 should be used when comparing to absolute dates obtained from other techniques besides the ^{36}Cl method. Important samples relevant to the timing of the late Pleistocene megaflooding are those from ice-rafted boulders on Rattlesnake Mountain (which will be visible to the west of Stop 11). The dates (samples MF-6, MF-7, and MF-8; Table 2) are between 16.2 and 16.9 ka (see also Bjornstad, 2014).

Erratic boulders at the summit of Steamboat Rock yielded cosmogenic nuclide dates of 16.3 and 13.2 ka (samples MF-2 and MF-3, Table 2). These probably apply to the advance of Okanogan lobe ice over the upper Grand Coulee, which would have greatly impacted the routing of megafloods through the Channeled Scabland region (e.g., Fig. 12).

Continue north on SR-155. [1.1]

164.5 Northrop Canyon Road enters from the right. A possible stop on Northrup Canyon Road provides an excellent exposure of sedimentation in an eddy bar at the mouth of Northrup Canyon. [0.2]
164.7 Lake silts. [2.1]
166.8 Lake silts. [1.2]
168.0 Extensive lake silts. [1.0]
169.0 Road crosses a small arm of Banks Lake. The Electric City inselbergs can be seen on the right. A sample collected at the top of one these inselbergs for terrestrial cosmogenic nuclide dating (Fig. 27) yielded an age of ca. 17.2 ka (sample MF-1, Table 2). This suggests that unroofing of the granite in the upper Grand Coulee occurred during the late Pleistocene megaflooding. [0.9]
169.9 Center of Electric City. [0.9]
170.8 North Dam, Banks Lake, on left. Entering town of Grand Coulee. [0.5]
171.3 Junction with SR-174. Turn left on SR-174 and ascend hill. (SR-155 continues to Coulee Dam.) [1.9]
173.2 Turn right on the road to Crown Point Vista. [1.5]
174.7 Crown Point overlook.

STOP 6—Crown Point Overlook of Grand Coulee Dam (N47.9694°, W118.9867°) (Baker)

Grand Coulee Dam, constructed on the Columbia River between 1933 and 1941 (with an addition built in 1967–1974), is considered the largest concrete structure in North America, and is the largest producer of hydropower in the United States (nearly 7 GW). The dam impounds Franklin D. Roosevelt Lake, from which water is pumped into Banks Lake (Fig. 24), which is the major storage for the Columbia Basin Irrigation Project of the U.S. Bureau of Reclamation (Neff, 1989).

The Okanogan lobe of the Cordilleran Ice Sheet temporarily blocked the Columbia River valley downstream of this point, thereby impounding glacial Lake Columbia. This resulted in major changes in the late Pleistocene megaflooding pathways through the Channeled Scabland region (Fig. 12).

Following this stop, the trip will continue across the Waterville Plateau, ~55 km^2 of which was covered by the late Pleistocene Okanogan lobe of the Cordilleran Ice Sheet (Kovanen and Slaymaker, 2004). The evidence for glaciation includes the abundant large blocks of basalt, locally known as "haystack rocks," eskers, and moraines. All these will be seen along the field trip route. Kovanen and Slaymaker (2004) hypothesize that the Okanogan lobe exhibited very fast ice flow during its advance, probably associated with instabilities cause by ice-marginal lakes and the dynamics created by a subglacial water reservoir. As noted in the introductory section, the presence of subglacial lakes beneath the Cordilleran Ice Sheet has also been inferred from both theory (Livingstone et al., 2012, 2013) and field evidence (Lesemann and Brennand, 2009). From their comparison of the Okanogan lobe land systems to modern analogues in Iceland, Kovanen and Slaymaker (2004, p. 563) suggest that the Okanogan lobe may have exhibited surge behavior. They further note, "…if a catastrophic episode of subglacial meltwater release did occur from an up-glacier reservoir, it could have been channeled down the Okanogan and Columbia River valleys through a tunnel system." The geometry is such that any such subglacial channeling would have delivered the flood flows to all or some of the following: (1) downstream portions of the Columbia Valley toward present-day Wenatchee, (2) upstream parts of glacial Lake Columbia, and (3) the plateau, where drainage collected in Moses Coulee, as will be seen at Stop 7.

Figure 26. Aerial photograph of Steamboat Rock, a basalt monolith within the upper Grand Coulee. View toward the south.

TABLE 2. COSMOGENIC ^{36}CL DATES FOR SITES IN THE CHANNELED SCABLAND REGION

Sample #	Lat. (°N)	Long. (°W)	Elev. (m)	Context	Lithology	Age (yr)	Error 1	Error 2
MF-1	47.9417	119.0380	558	Exhumed inselberg	Granite	17,210	2550	2700
MF-2	47.8636	119.1325	686	Erratic boulder Steamboat Rock	Granite	16,280	440	950
MF-3	47.8675	119.1366	686	Small erratic Steamboat Rock	Granite	13,190	540	870
MF-4	47.8709	119.1286	686	Moraine erratic Steamboat Rock	Granite	12,210	890	1090
MF-5	47.6450	119.6644	579	Moses Coulee flood bar	Basalt	15,480	2800	2910
MF-6	46.3788	119.5004	310	Ice-rafted erratic Rattlesnake Mtn.	Granite	16,930	3290	3420
MF-7	46.3840	119.4635	209	Ice-rafted erratic Rattlesnake Mtn.	Granite	16,170	1020	1330
MF-8	46.3809	119.4647	225	Ice-rafted erratic Rattlesnake Mtn.	Basalt	16,740	2600	2730
MF-9	46.1623	119.2999	268	Large ice-rafted erratic (Badger Coulee)	Granite	35,640	1150	2090

Figure 27. Marek Zreda collecting a sample for ^{36}Cl nuclide dating from the summit of an exhumed granite inselberg at Electric City in the upper Grand Coulee.

Return to SR-174. [1.5]

176.2 Junction with SR-174. Turn right and continue west on SR-174. [5.3]
181.5 Boulder of the Withrow Moraine. [2.5]
184.0 Barker Canyon Road enters from the left (south). [2.1]
186.1 McCabe Road enters from the right. [4.8]
190.9 Del Rio Road (U Rd NE) enters from the right. [4.7]
195.6 Junction with SR-17. Turn left (south) on SR-17. [0.7]
196.3 Esker. [1.9]
198.2 Esker. [4.9]
203.1 Sims Corner. Junction with SR-172. Continue south on SR-17. [8.0]
211.1 Junction with St. Andrews E Road. Turn right on St. Andrews E Road. [3.0]
214.1 Junction with St. Andrews S Road. Turn left (south) onto St. Andrews S Road. [5.5]
219.6 Junction with U.S. 2. Turn right (west) on U.S. 2. [0.2]
219.8 "Haystack" rocks. [11.8]
231.6 Jameson Lake Road enters from the right. Turn right on Jameson Lake Road for side trip to Withrow Moraine and megaflood bar. [2.5]
234.1 Pull off on either side of the road for view of Withrow Moraine.

STOP 7—Withrow Moraine and Flood Bar in Upper Moses Coulee (N47.5969°, W119.6764°) (Baker)

At this location, a portion of the Withrow Moraine overlies an elongate pendant bar that was emplaced by cataclysmic megaflooding prior to the advance of the Okanogan lobe to its late Pleistocene terminal position (Fig. 28). A ^{36}Cl cosmogenic nuclide date on a basalt boulder from the flood bar yielded an age of 15.5 ka (sample MF-5, Table 2). As on the plateau upland surface, the summit of the moraine has the large "haystack" blocks of basalt. There are also smaller erratic boulders of granitic composition and other basement rocks that probably derive from the Okanogan highlands to the north of the Columbia River. After its terminal phase, the moraine was breached, resulting in a sequence of outwash terraces along the western side of the coulee that reflects the history of the ice lobe at its terminus and subsequent retreat up the coulee.

Turn around and return to U.S. 2. [2.5]

236.6 Junction with U.S. 2. Turn right and continue on U.S. 2. [0.4]
237.0 Road ascends great flood bar. [1.2]
238.2 Junction with Moses Coulee Road. Turn left onto this road down Moses Coulee. [1.1]
239.3 Road descends gravel bar. [3.8]
243.1 Exposures of flood gravel in eddy bar on right. [0.2]
243.3 Olson Road enters from right. Continue on Moses Coulee Road. [0.6]
243.9 Leaving inner channel of Moses Coulee. [5.6]
249.5 Junction with road to Palisades. (This road is variously marked 12th Road SE and 24 NW Road.) Turn right (west) toward Palisades. [1.2]
250.7 Pavement ends. [2.2]
252.9 Rattlesnake Springs (Three Devils) cataract complex of Moses Coulee. [1.5]
254.4 Steamboat Rock. [0.1]
254.5 Excellent basalt columns are visible on the right. [0.3]
254.8 Billingsley Ranch. [2.5]
257.3 Pavement resumes. Flood bar on right. [2.0]
259.3 Gravel bar on left. [0.5]
259.8 Gravel pit in bar on left. [1.8]
261.6 Palisades Country Store. [0.7]
262.3 Gravel dunes (giant current ripples) on gravel bar. [0.5]
262.8 Lake silts. [1.0]
263.8 Small gravel bar. [9.1]
272.9 Junction with SR-28. Turn left and continue south on SR-28. [1.1]
274.0 Moses Coulee bar. [3.1]
277.1 Dipping pillow-palagonite beds visible in basalt cliffs on left. [2.0]
279.1 View of West Bar. Gravel pit formerly had Set S. [1.7]
280.8 Junction with Crescent Bar Road. Turn right into Trinidad. Continue along Crescent Bar Road (also listed as Crescent Bar Road NE) 0.8 miles to a hairpin curve where there is a view across the Columbia River toward West Bar.

STOP 8—View of West Bar GCRs (N47.2288°, W120.0125°; Elevation 274 m) (Baker)

This viewpoint affords the opportunity to see one of the most spectacular zones of giant current ripples in the region (Fig. 29). West Bar is located on the western side of the Columbia River valley, which here has its bottom obscured by Wanapum Lake, a long reservoir with a pool elevation of 174 m that extends upstream from Wanapum Dam, located downstream ~40 km to the south. The West Bar giant current ripples (fluvial dunes) average ~8 m in height, ~110 m in spacing, and are composed of gravel with boulders up to 1.4 m in diameter (Baker, 1973a). The ripples occur at an elevation of ~210 m, while maximum megaflooding at this location may have reached as much as 400 m, although that flooding may have occurred before emplacement of the current ripple configuration.

Retrace route back to SR-28.

280.8 Turn right onto SR-28. [0.6]
281.4 Cross Lynch Coulee. [0.2]
281.6 Basalt. [1.4]
283.0 Rest area on right. [1.5]
284.5 Cross Crater Coulee. [3.2]
287.7 Center of Quincy. End of Road Log for Day 1.

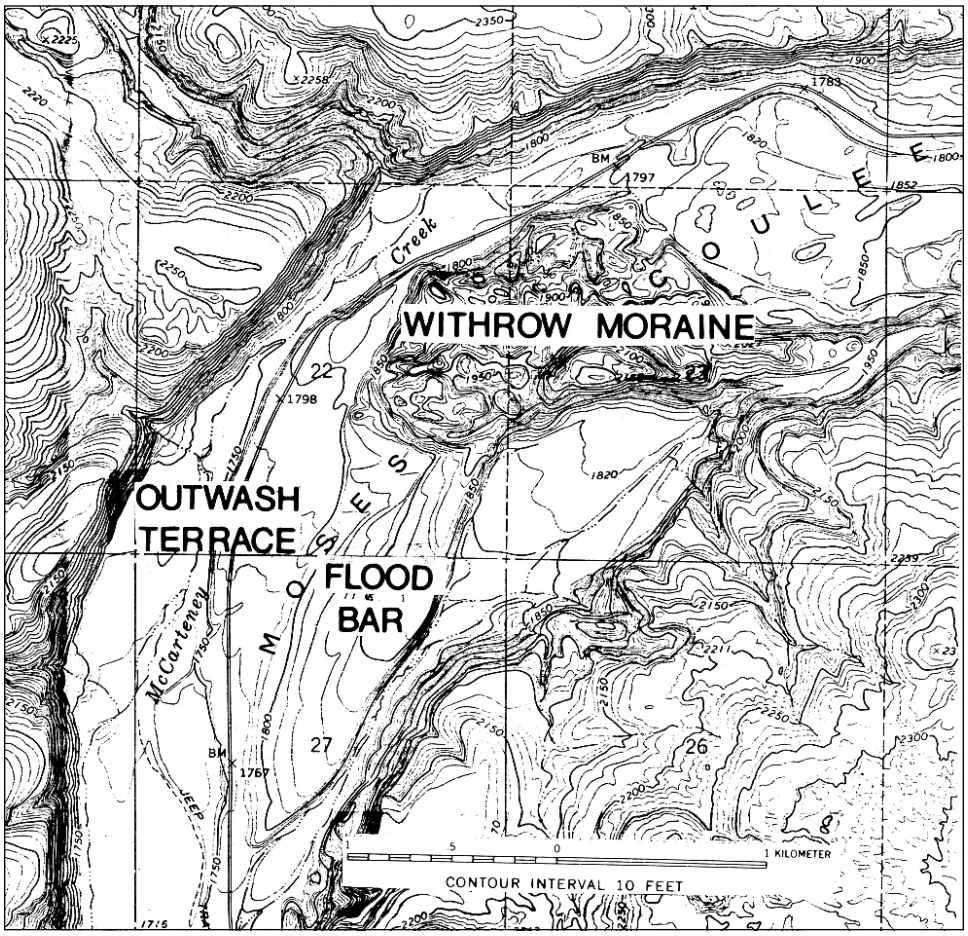

Figure 28. Topographic map of a portion of northern Moses Coulee showing the position of the Withrow Moraine overlying an elongate megaflood pendant bar. North is to the top of the map. Stop 7 is located on the road just to the southwest of the Withrow Moraine.

Figure 29. Giant current ripples of West Bar. Ripples formed from the last outburst flood coming down the Columbia Valley—likely during the breakup of the Okanogan lobe and release of glacial Lake Columbia.

■ DAY 2—QUINCY TO RITZVILLE

Mileage	*Directions*
0.0	Begin in center of Quincy, Washington, at junction of SR-28 and SR-281. Take the latter south. [5.0]
5.0	Junction with White Trail Road (5 NW). Turn right (west) on White Trail Road. [2.0]
7.0	Cross West Canal of the Columbia Basin Irrigation Project. Note white caliche excavated from the canal. This is part of a thick petrocalcic horizon that caps early Pleistocene flood gravel that crossed Babcock Ridge from the west. [1.0]
8.0	Junction with unnamed gravel road coming from south and a small "Public Fishing" sign. Turn left (south) on to the gravel road. [0.4]
8.4	Entrance to Quincy Lakes Recreation Area. Note basalt scabland. [0.4]
8.8	Exposure of pillow basalt on the left side of the road. [0.1]
8.9	Pass mouth of Stan Coffin Lake. [0.4]
9.3	Mouth of Quincy Lake. [1.0]
10.3	Cross small dam that impounds Evergreen Reservoir. [0.2]
10.5	Stop at the south end of Evergreen Reservoir and pull off at the outhouse on the right. Walk a few hundred meters west to the overlook.

STOP 9—Potholes Coulee and Dusty Lake Overview (N47.1319°, W119.9334°; Elevation 363 m) (Bjornstad)

The drainage divide into Potholes Coulee (365 m) is the lowest of the three cataracts that cascaded from the Quincy Basin into the Columbia valley. This spectacular feature deservedly caught the attention of previous investigators (Baker and Nummedal, 1978; Edgett et al., 1995; Bjornstad, 2006a) and especially Bretz (1923, 1925, 1928, 1930b, 1959; Bretz et al., 1956), who referred to this feature as Potholes cataract. Potholes Coulee (Fig. 30), like neighboring Crater Coulee and Frenchman Coulee, formed spectacular, horseshoe-shaped, multi-tiered cataract canyons when floodwaters quickly rose up to 442 m elevation, overtopping several divides across Evergreen and Babcock ridges. When this happened, a drop of >260 m was created over a distance of less than 5 km between the Quincy Basin and the Columbia River Valley to the west. With this difference in water level over such a short distance, floodwaters furiously ate away at the underlying basalt layers. Topsoil was completely stripped away, along with hundreds of meters of bedrock, carving deep chasms into the ridgeline (Fig. 30).

Potholes Coulee consists of two, parallel, amphitheater-shaped, cataract-lined alcoves. Separating the two alcoves is a great blade of basalt 3.5 km long, 300 m wide, and up to 115 m tall (Bretz, 1923). The upper ends of these alcoves form the Ancient Lakes Basin on the north and Dusty Lake Basin on the south. An upper cataract tier steps up from these alcoves, forming a wild maze of butte-and-basin scabland all the way to Quincy Lakes. Deep plunge pools lie at the bases of some cataracts. Beyond the cataracts are huge bars of coarse-grained flood deposits, which blanket the bottom of both alcoves westward to Babcock Bench. Many of the whale-back-shaped bars are covered with giant current ripples. Elongated depressions (fosses) developed between flood bars and the coulee walls.

The basalt visible from this stop looking out across the Dusty Lake Basin consists of the Roza and Frenchman Springs Members of Wanapum Basalt. Three cataract tiers are preserved in 3-km-wide Potholes Coulee (Fig. 30). At this stop we are standing on the lip of the upper tier. The upper cataract spans the thickness of the Roza Member, which is 50 m thick in places (Reidel et al., 2013). During repeated floods, this cataract canyon receded from the edge of the Columbia River valley 5 km to the west. One characteristic of the Roza Member is especially huge columns that can be a meter or more wide. A middle tier developed across the Frenchman Springs Member, the next oldest basalt member. In some places, these two tiers are stacked on top of each other, forming a single cataract up to 120 m high. At the west end of the coulee, a lower tier steps down into the next oldest basalt member (Sentinel Bluffs Member of Grande Ronde Basalt).

Potholes Coulee formed when late Pleistocene megaflooding filled the Quincy Basin. Quincy Lakes were created as floodwaters, which had overtopped Evergreen and Babcock ridges, picked up speed as they were funneled through narrow Potholes Coulee (Bjornstad, 2006a). The mouths of the lakes mark the eastern extent of cataract recession in Potholes Coulee. During future ice age floods, the cataracts in Potholes Coulee will likely resume their eastward migration, gobbling up part or all of the current Quincy Lake system. Less erosion occurred east of the lakes because floodwaters moved more slowly across the wide expanse of the Quincy Basin. The slower speed of the floodwaters in the central Quincy Basin explains why no well-developed scabland features lie east of Quincy Lakes. Instead of erosion, the floods mostly deposited sediment in the center of the basin.

Continue south on gravel road. [2.5]

13.0	Exit the Quincy Lakes Recreation Area. The road rises up on to the soil-covered Evergreen Ridge. [0.4]
13.4	Vineyards are visible as the road climbs up Evergreen Ridge. These are situated at the approximate high-water level for megaflooding of the Quincy Basin. [0.4]
13.8	Junction with Road 2 NW. Turn left (east) on to Road 2 NW. [0.2]
14.0	Make a sharp right turn (south) on to paved Road U NW. [1.1]
15.1	Turn left (east) on to Road 1 NW. [3.3]
18.4	Road 1 NW curves to right, following the west canal of the Columbia Basin Irrigation Project on the left. A landfill on the right has excellent exposures of early Pleistocene megaflood gravel (Baker, 1973a). [0.4]

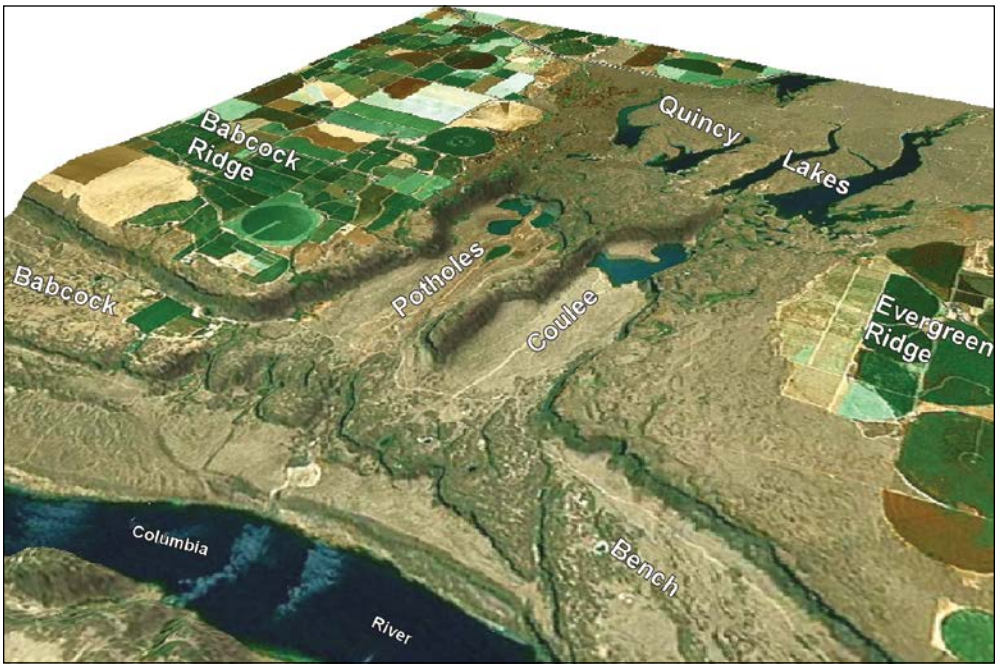

Figure 30. Oblique aerial view of Potholes Coulee, a dual cataract canyon. Stop 9 is at the head of the alcove on the right. View to northeast. Compare to Figure 4.

18.8 Road junction with Road R NW. Turn left on to Road R NW (also known as Beverly Burke Road). [0.4]
19.2 Junction with SR-281. Cross SR-281 and continue east on Road 1 NW to I-90 exit 151. [1.0]
20.2 Junction with I-90. Enter I-90 eastbound toward Spokane. [13.0]
33.2 I-90 exit 164 (Dodson Road). Exit and continue south on Dodson Road. [5.7]
38.9 Stabilized dunes, distal Ephrata fan. [0.4]

Northern Columbia River Basin Eolian Sedimentary Deposits (Gaylord)

Eolian deposits in the northern part of the Columbia River Basin consist primarily of sand dunes that accumulated south of the Beezley Hills and the Grand Coulee in the Quincy Basin. The sand dunes in this subbasin of the CRB reflect the influence of abundant source sediment, persistently dry climatic conditions, common sand-moving winds, and topography (Gaylord et al., 2014). Megaflood deposits in the Quincy Basin are gravel dominated but also include local accumulations of finer-grained, sand- and silt-/clay-rich slackwater sediment. The mineral and lithic contents of Quincy Basin dune sand particles indicate they were derived primarily from the local slackwater deposits (Dalman, 2007; Gaylord et al., 2014). The mean grain sizes and compositions of the constituent particles of the dunes are reflected in their color. Medium- to coarse-sized, dune-sand particles (common in the CRB) have higher basalt-lithic contents than do fine-sized, dune-sand particles; thus, coarser grained (medium- to coarse-sand dominated) dunes are medium to dark gray in color whereas finer-grained dunes tend to be more yellow-brown, reflecting higher quartz and feldspar and lower basalt-lithic contents.

Close inspection of actively migrating unvegetated dune sands in hand-dug pits in Quincy Basin sand dunes reveals laminated successions of "subcritically climbing translatent stratification" that resulted from the migration and aggradation of low amplitude (<1.0 cm high) eolian ripple forms (cf. Hunter, 1977). Subcritically climbing translatent stratification provides definitive evidence for the eolian origin of sedimentary deposits on Earth (e.g., Kocurek and Dott, 1981) and Mars (Grotzinger et al., 2005). Other, more steeply dipping primary sedimentary structures generated by grain-flow and grain-fall deposition on dune slipfaces (Hunter, 1977) are less common, but are preserved in these dunes.

Sediment-moving winds across the region, including the Quincy Basin, are generally from the SW during the autumn to late spring and from the NW during the summer months (Gaylord and Stetler, 1994; Stetler and Gaylord, 1996; Dalman, 2007; Gaylord et al., 2014). The Quincy Basin dunes bear the imprint of the modification of these prevailing winds by the terrain. In particular, prevailing SW-NE winds have been modified by the W-E–aligned, 200–300-m-high, monoclinal Beezley Hills on the northern margin of the basin, and by the W-E–aligned, 100–200-m-high, anticlinal Frenchman Hills on the southern basin margin. These eolian-terrain effects, coupled with persistent sand-moving winds and abundant loosely consolidated megaflood sand deposits along the Columbia River west of Moses Lake, resulted in the largest concentration of sand dunes on the Columbia Basin, the Moses Lake dune field. This dune field mantles a 15-km-wide W-E–aligned, >1000 km^2 portion of the southern Quincy Basin with up to 15 m of dune sand (Petrone, 1970). The dune field

consists of now largely stabilized parabolic, barchan and barchanoid ridge dunes separated by intervening areas of interdune deflation plains and ponds, sand sheets, and (locally) sand streaks. Sand dune deposits in the Potholes Reservoir, an engineered lake impounded behind O'Sullivan Dam in 1949, are now visible only as water-saturated and vegetated barchan- and barchanoid-shaped islands. The ready availability of water in this part of the CRB has enabled much of the area surrounding the Moses Lake dune field to be irrigated.

No comprehensive attempts have yet been made to date eolian dune sands in the Quincy Basin using optical or thermal luminescence techniques. However, burial of Glacier Peak tephra (13.8 cal ka) in stabilized sand deposits near the town of Ephrata on the northern basin margin does establish the timing of the earliest sand dune activity as latest Pleistocene (Gaylord et al., 2004; Dalman, 2007). The only other Pleistocene-aged dune sands identified in the CRB are at Hanford Reach (Gaylord et al., 2011). Some of the dune sands in the Quincy Basin contain beds of Mazama tephra (ca. 7.7 cal ka; Bacon, 1983; Hallett et al., 1997), fixing the age of those deposits within the early to middle Holocene. Many sand dunes in this area also contain laterally continuous 0.5–1.0-cm-thick laminations and thin beds of tephra from the 1980 Mount St. Helens eruption.

39.3 Pivot irrigation on left. [0.4]
39.7 Stablized dunes. [0.4]
40.1 Stablized dunes. [0.4]
40.5 Pivot irrigation on left. [0.3]
40.8 Pivot irrigation on left. [2.1]
42.9 Junction of Dodson Road and Frenchman Hills Road, turn left (east) onto Frenchman Hills Road. [1.1]
44.0 Junction with Road A SW. Continue on Frenchman Hills Road; Frenchman Hills on right. [1.8]
45.8 Erratic boulders. [0.8]
46.6 Junction of Frenchman Hills Road with Rt. 262, turn left and continue east on Rt. 262. [5.6]
52.2 Road to left leads to the Potholes State Park (an area of partially submerged sand dunes). Continue on Rt. 262. [0.5]
52.7 Junction of Rt. 262 with H Road SE. Turn right on H Road SE. [1.4]
54.1 Junction of H SE with 1 SE. Turn left on 1 SE and go 1.2 miles for view of Frenchman Hills anticline exposed in the Drumheller Channels scabland. Return to the junction with H SE. [2.4]
56.5 Junction with H SE. Turn left (south) on to H SE. [3.1]
59.6 Junction of H SE with Road 12 SE. Turn left on to Road 12 SE, which changes name to McManamon Road. [1.2]
60.8 Scenic overlook on left with views of Drumheller Channels. Enter Columbia Wildlife Refuge. [0.7]
61.5 Cross Crab Creek. [3.8]
65.3 Junction of McManamon Road and Morgan Lake Road (to Columbia National Wildlife Refuge). Continue east on McManamon Road. [3.7]
69.0 Cross Potholes East Canal and climb hill. [0.4]
69.4 Cross rail line. [0.5]
69.9 Rail crossing just before Othello industrial area. McManamon Road becomes N Broadway Avenue. [1.0]
70.9 Traffic light, N Broadway Avenue and Main in Othello. Continue on N Broadway Avenue. [1.0]
71.9 Rt. 26 underpass on south side of Othello. N Broadway Avenue becomes Rt. 24, S Radar Road. Continue south. [1.0]
72.9 Junction with Bench Road. Continue south on Rt. 24. [3.9]
76.8 Junction with Muse Road. Continue south on Rt. 24. [0.2]
77.0 Road curves to the right. [0.2]
77.2 Cross Crab Creek. [0.3]
77.5 Junction with Sage Hill Road on left. Continue straight on SR-24 west. [4.5]
82.0 Pass junction with Hendricks Road (on left). Continue west on SR-24. [6.3]
88.3 Pass junction with the road to White Bluffs. [2.7]
91.0 Turn right on the road toward Saddle Mountain summit. [4.4]
95.4 Crest of ridge. Turn right and continue east to the overlook of landslide complex to the north. [1.1]
96.5 Park at viewpoint.

STOP 10—Overview from the Crest of Saddle Mountain (N47.2027°, W119.9833°) (Baker and Bjornstad)

Park in turn-around. Saddle Mountain is one of a series of anticlinal ridges in the Yakima fold belt (Reidel et al., 1989) of the western Columbia River Basin. The ridges have an average length of just over 100 km and are separated by broad, sediment-filled synclinal valleys ~20 km wide. At the core of many ridges, there is a major thrust fault, and the asymmetry of the ridge reflects the vergence of the fault (in general, the steeper sides are to the north, indicating that the faults dip to the south). For the most part, the deformation exposed at the surface is folding over the tip of the thrust fault (fault-bend folding), although drag folds are also evident in places. The folding is primarily in the Columbia River Basalt Group lavas, and the timing (and rate of folding) is largely coincident with emplacement of the lava pile, but some very slow deformation may be continuing up to the present day (Reidel et al., 2013). For example, the Saddle Mountains appear to have largely formed over a few hundred thousand years. However, there is some evidence that subsidence (and related contraction) started before the volcanism (e.g., Reidel, 1984; Reidel et al., 1989).

This site also provides an overview of the Taunton-Corfu landslide complex to the northeast (Fig. 31). Lewis (1985) estimates that ~1 km^3 of basalt and sedimentary rock (Ringold Formation) was incorporated into this complex slide in a series of at least 24 separate events. The Mount St. Helens S tephra

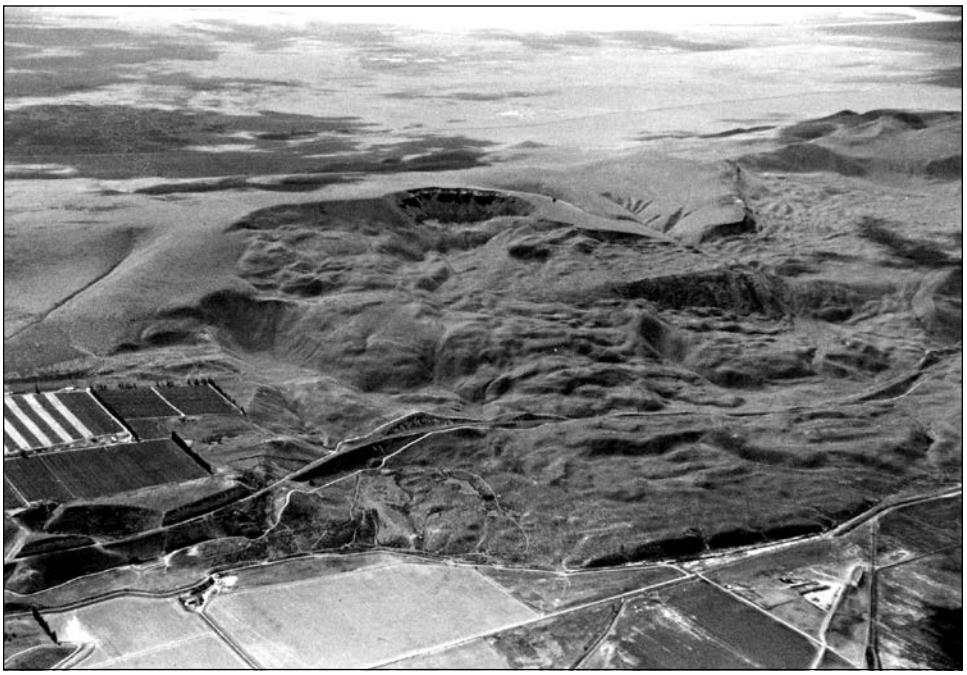

Figure 31. Aerial photograph of the Taunton-Corfu landslide complex along the north side of the Saddle Mountains. View to the southwest. Stop 10 is at the top of the ridge, near the top center of the photo.

(ca. 16 cal ka) was found in eolian silt overlying the oldest of these slides, and the Mazama tephra (ca. 7.7 cal ka) was found in silts overlying one of the youngest of the slides (Lewis, 1985). The older slides on the western end of the complex have clearly been trimmed at their toes by later flood erosion, but young slides to the east lack this modification. Thus, it is plausible that the sliding was in response to erosion by the late Pleistocene flooding emanating from Drumheller Channels to the NE. The flood flows subsequently went down lower Crab Creek valley between the Frenchman Hills and the Saddle Mountains. Continued sliding into the Holocene may reflect other causes for failure, including possible seismic events.

Return by the same route to SR-24. [5.5]

102.0 Junction with SR-24. Turn left (east). [2.7]

104.7 Junction with unnamed road to White Bluffs. Turn right (south). The road passes through the sand dunes of the Hanford Reach National Monument (Fig. 32), as described in the following regional overview of eolian deposits in the Channeled Scabland region. [0.3]

Southern Columbia River Basin Eolian Deposits (Gaylord and Sweeney)

The southern part of the Columbia River Basin (CRB) in Washington and northernmost Oregon contains five notable areas of sand-dominated and mixed sand/silt-clay eolian deposition connected genetically with megaflood deposits. These are the Hanford Reach National Monument, Hanford site, Juniper–Smith Canyon, Eureka Flat, and Juniper Canyon (Fig. 32). The first three areas are characterized by stabilized and active sand dunes and associated loess deposits, and the fourth and fifth areas by an extensive sand sheet and minor stabilized and active sand dunes and loess.

Hanford Reach National Monument

The Hanford Reach National Monument is a part of the broader Hanford area that includes the Hanford site, which is also known as the Hanford Nuclear Reservation. The monument area largely parallels the eastern valley margins of the Columbia River (Figs. 32, 33) and includes a variety of eolian features of accumulation and erosion. These eolian deposits cap a thick and texturally heterogeneous succession of megaflood sediment and the Miocene–Pliocene Ringold Formation (Grolier and Bingham, 1978; Lindsey and Gaylord, 1990; Gaylord et al., 2003). The Hanford Reach eolian deposits consist primarily of stabilized to active SW-NE–oriented parabolic sand dunes and secondarily of sand sheet and loess deposits. Erosional (deflationary) eolian features include yardangs, ventifacts, dispersed pebble lags, and blowouts developed on underlying megaflood and Ringold Formation deposits.

Heavy and light mineral compositions indicate that eolian deposits in the monument were derived primarily from sand and silt/clay-rich megaflood deposits that were augmented by minor contributions from sand- and silt/clay-rich facies of the Ringold Formation. Loess mantles the surface along and beyond the northern and eastern boundaries of the monument, and commonly is buried beneath sand dunes and sand sheet deposits (Gaylord et al., 2007; Anfinson, 2008).

The history of eolian deposition at Hanford Reach National Monument has been determined from detailed stratigraphic and

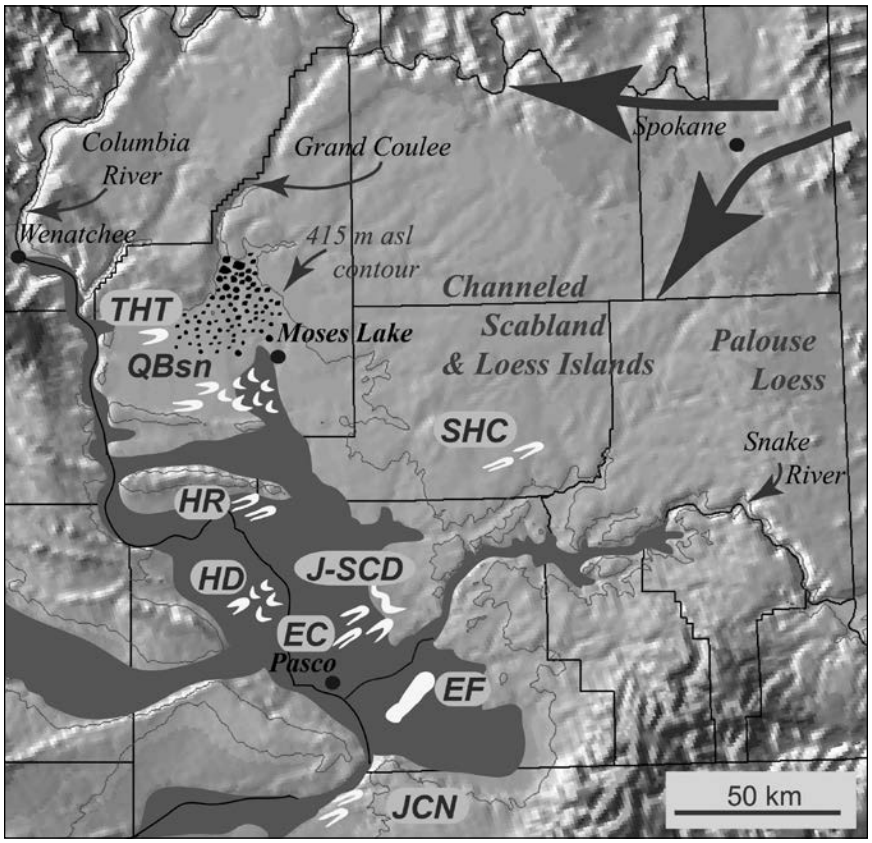

Figure 32. Major Quaternary sand- and silt-clay-dominated eolian accumulations in the Columbia River Basin (CRB) of Washington and northernmost Oregon. Sand dune and sand sheet deposits from the northern CRB include the Thornton dunes (THT) and Quincy Basin dunes (QBsn), which also include the Moses Lake dune field discussed in this trip chapter. Sand dune, sand sheet, and loess deposits discussed in this section include the Hanford Reach National Monument dunes, sand sheets and loess (HR), Hanford site dunes (HD), Juniper–Smith Canyon dunes (J-SCD), Eltopia Canal (EC), Eureka Flat sand dunes, sand sheets and loess (EF), and Juniper Canyon sand dunes and sand sheets (JCN). Also shown is the location of the Sand Hills Coulee dunes (SHC) seen at Stop 13.

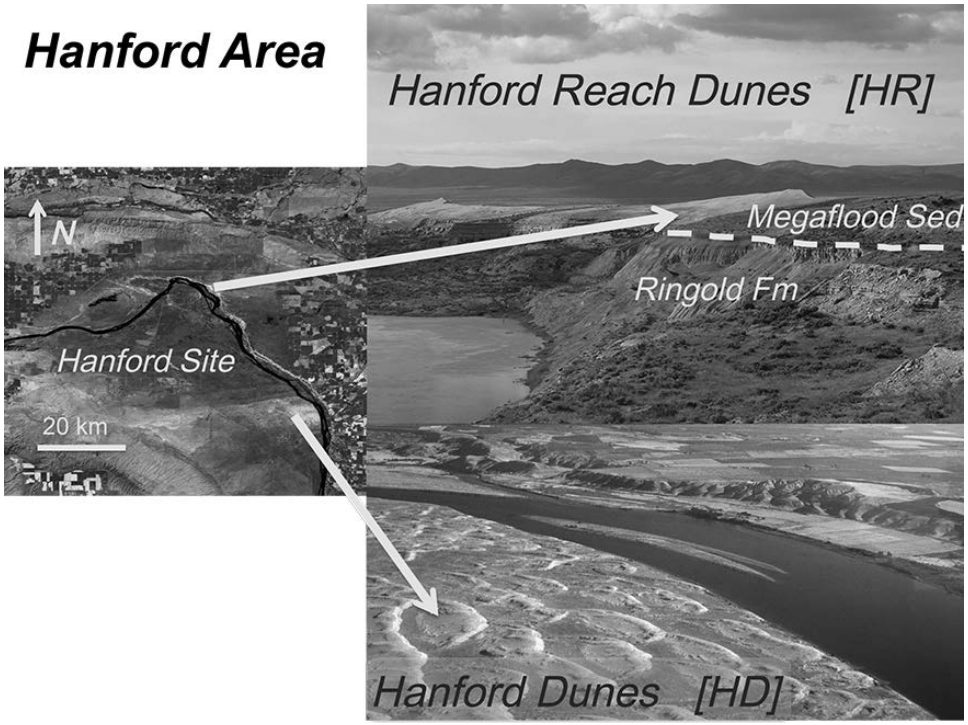

Figure 33. The Hanford area includes the Hanford Reach National Monument (HR) and the Hanford site (HD) sand dune, and sand sheet and loess deposits. The Hanford Reach encompasses active and stabilized sand dunes (visible on the valley crest), as well as sand sheet deposits and loess that cap megaflood and Ringold Formation sedimentary strata exposed along the eastern valley of the Columbia River. The Hanford site dune field occupies a central position on the west side of the river. Note the partially stabilized parabolic dunes on the Hanford site that are migrating NE toward the river in the inset oblique air photo in the lower right.

sedimentary reconstructions, tephrochronologic analyses, and field mapping (Gaylord et al., 2011). The sand dune depositional record at the monument (Fig. 34) reflects the influence of persistently dry conditions and strong winds that have readily remobilized source sediment and transported it to the E and NE. The chronology of late Pleistocene and Holocene sand dune activity at Hanford Reach (Gaylord et al., 2011; Fig. 34) has been estimated using bracketing ages from lenses and thin beds of Mount St. Helens set S tephra (Sg and So; ca. 16 cal ka; Clynne et al., 2008) and Glacier Peak G tephra (ca. 13,560 cal yr ka B.P.; Kuehn et al., 2009). The preservation of Mount St. Helens set S tephras at Hanford Reach is the first such case documented in sand-dominated eolian deposits in the Columbia Basin, whereas preservation of Glacier Peak G tephra is the second such case (Gaylord et al., 2004, 2014; Dalman, 2007). The preservation of the Mount St. Helens set S tephras at this location strongly suggests that megaflood waters did not exceed 210 m a.s.l. after this time. In other parts of the Channeled Scabland, at least 31 post–Mount St. Helens set S tephra megafloods have been documented (Clague et al., 2003; Benito and O'Connor, 2003). Mazama tephra (ca. 7.7 cal ka) is not preserved in the Hanford Reach section documented by Gaylord et al. (2011) but occurs in nearby dune sands. Thus, its absence in the Figure 34 stratigraphic section is attributed to heightened post-Mazama deflation during episodes of enhanced middle to late Holocene aridity. The middle to late Holocene sand dune record characterized at Hanford Reach was influenced by sagebrush stabilization as evidenced by pervasive cicada nymph burrowing (O'Geen and Busacca, 2001; Fig. 34); there also was incipient soil development at this time. An ~12-m-thick dune sand that caps the Mount St. Helens D 1980 tephra at Hanford Reach is attributed to enhanced eolian activity following a range fire in the past 15 yr.

The history of sand dune deposition at Hanford Reach complements dune chronologies from the nearby Hanford and Juniper–Smith Canyon dunes (Gaylord and Stetler, 1994; Stetler and Gaylord, 1996; Gaylord, et al., 2001). Both of those other dune fields were the foci for sand dune and sand sheet activity and deposition that preceded and then succeeded accumulation of the Mazama tephra (7.7 cal ka).

The fine-medium grained, well-sorted, Hanford Reach dune sands bear a striking resemblance to the sand-rich, gray-brown, basalt-lithic enriched megaflood deposits from which they were derived. As is the case for the northern CRB dune deposits previously discussed in this guide, the most prominent sedimentary structures visible in these dune sands are subcritically climbing translatent strata (wind ripple strata; cf. Hunter, 1977); grainfall and grain-flow cross-strata are less common. Many of the dune deposits at Hanford Reach also are structureless because of extensive syn- and post-depositional phytoturbation.

Hanford Site Dunes

Stabilized and active sand dunes mantle ~15% of the ~1500 km^2 Hanford Site (Figs. 32 and 33). Roughly half of the sand dunes on the site are active and consist of a series

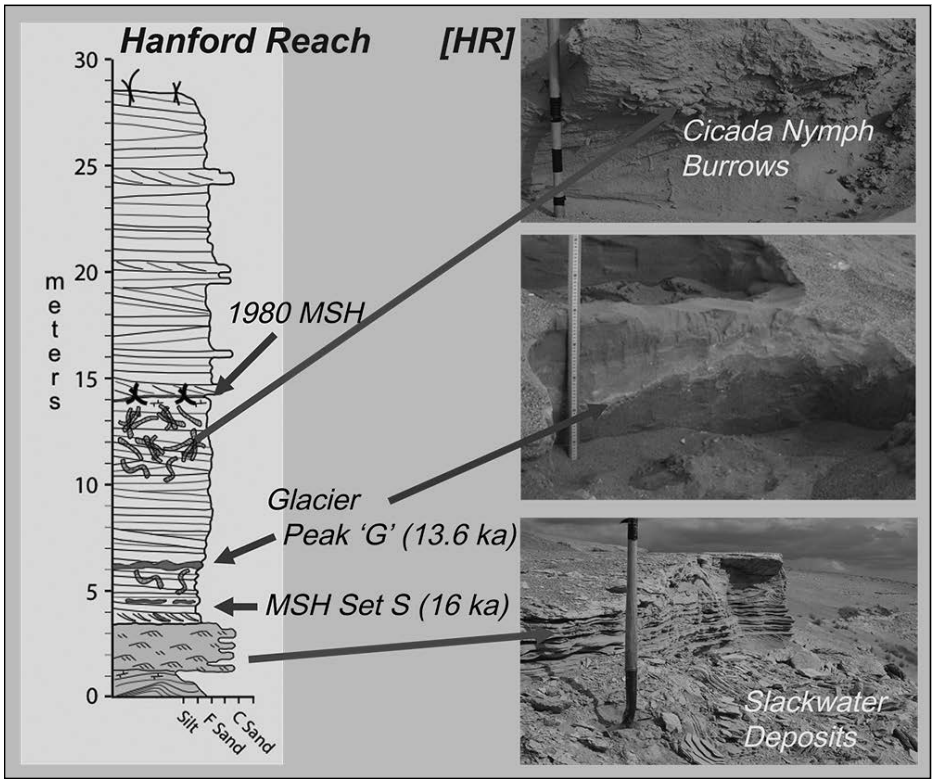

Figure 34. Hanford Reach stratigraphic section discussed in the text. Ages for Glacier Peak tephra after Kuehn et al. (2009) and for Mount St. Helens (MSH) set S tephras from Clynne et al. (2008). Slackwater megaflood deposits at the base of this stratigraphic succession are late Wisconsin in age.

of transverse to barchanoid-ridge and barchan dunes that have been transitional to parabolic dunes since at least the late 1940s (Gaylord and Stetler, 1994; Stetler and Gaylord, 1996). The horns of some of the barchan dunes have served as bypass zones for migrating sand grains, adding to the morphologic complexity of these compound dune forms. Other sand-dominated eolian deposits include thin sand sheets and stabilized parabolic dune limbs that parallel the prevailing SW-NE winds. Actively migrating dunes are concentrated on a part of the site that is frequently subject to low-level terrain-induced airflow confluence. The recent transition of barchan and barchanoid dunes to parabolic dunes is assumed to be connected to high subsurface soil-moisture levels promoted by the Columbia River dam system.

The dunes and sand sheets on the Hanford site overlie a thick succession of sand-bearing, gravel-rich megaflood sediment. Dune deposits grade from fine to medium sand in upwind areas to very fine to fine sand in downwind locations. These dunes consist primarily of basaltic lithic particles, lesser concentrations of quartzo-feldspathic grains, and minor percentages of crystalline and metamorphic lithic fragments, evidence that they were derived primarily from remobilization of megaflood slackwater sediment (Smith, 1992; Gaylord and Stetler, 1994).

The relative ease of remobilization of the sand-dominated eolian deposits in upwind parts of the Hanford site, persistently low levels of subsurface moisture in those source areas, and the absence of topographic depressions or obstacles that might have promoted dune or sand sheet accumulations have worked against accumulation of a long or thick eolian stratigraphic record. Available data suggest that the Hanford site dunes were likely mobile and subject to repeated episodes of deflation throughout their history; thus, they are largely unrepresented in the depositional record. Still, on the basis of limited tephrochronologic and archaeological evidence from the site, it appears that the Hanford dunes were active both before and after accumulation of the Mazama tephra (ca. 7700 cal yr B.P.). Post-Mazama dune sands apparently were stabilized by ca. 4400 cal yr B.P. and have been episodically remobilized since (Smith, 1992; Gaylord and Stetler, 1994; Stetler and Gaylord, 1996).

Juniper-Smith Canyon Dunes

The Juniper-Smith Canyon dunes mantle >100 km^2 of slackwater megaflood and loess deposits northeast of the Snake River near Pasco, Washington (Gaylord et al., 1999, 2001) (Fig. 32). This dune field is one of the largest of the southern scabland dune fields and is actively migrating within dryland wheat fields. Though more active in the last century, as demonstrated by relic transverse and barchanoid ridge dunes that now are largely stabilized by shrub-steppe vegetation and juniper trees, this dune field is now characterized by stabilized to active parabolic and blowout dunes that were derived from deflation of slackwater megaflood deposits. Up to 40 m of stabilized to active dune sand mantles a moderately to deeply dissected, megaflood-induced topography. Stabilized dunes are primarily parabolic- or blowout-shaped and are anchored by a mixture of both native and introduced grasses, shrubs, and juniper trees. Actively migrating dunes have only sparse vegetation cover, and are concentrated near the downwind edge of the dune field and in topographically favored positions subject to higher wind speeds and/or lower levels of subsurface moisture. Active and stabilized dunes reflect primarily SW to NE transport, which is consistent with modern autumn, winter, and early spring winds in the area (Gaylord and Stetler, 1994; Stetler and Gaylord, 1996). Textural and compositional analyses of dune and source sediments reveal distinct fining of dune sands to the NE, away from sand- and basalt-lithic rich megaflood deposit sources. Downwind, dune sands overlie compositionally similar loess deposits. However, the genetic relations between sand dune and loess deposits are not well documented nor understood because of the scarcity of direct and indirect temporal markers. The only clear record to date of dune chronology has come from correlative dune deposits on the upwind margin of the dune field exposed along Eltopia Canal (Gaylord et al., 2001) (Fig. 35).

The 14-m-thick Eltopia Canal stratigraphic section (Fig. 35) has been subdivided into five depositional-climatic episodes that reveal a history of sedimentary reworking of Missoula megaflood, Holocene and Recent fluvial deposits, and sand dune sediment within the Smith Canyon area. Eltopia Canal chronostratigraphic control is largely limited to two intercalated beds that contain reworked Mazama tephra (ca. 7.7 cal ka). During the first episode, massive to ripple cross-laminated, fine-grained silt, and very fine-grained megaflood sand, silt, and clay (slackwater) deposits were pedogenically altered. Soil development probably began shortly following the final late Wisconsin megaflood. A dry and slightly warmer climate at this time promoted mixed grass and shrub steppe vegetation in lowland areas of the Pacific Northwest (Barnosky, 1985; Whitlock and Bartlein, 1997).

During the second episode, pedogenically altered megaflood sediment was reworked by local streams that flowed primarily south to north (opposite of modern flow directions) within Smith Canyon. Fluvial sediment deposited during this episode consists of well-sorted, fine–medium-grained, horizontal planar and low-angle planar cross-stratified sand. The excellent sorting of these fluvial sands and occasional intercalated eolian ripple laminations in these deposits indicate they were regularly reworked by the wind. The timing of this episode is inferred to correspond with the early Holocene (ca. 10–7 ka), a time of increasingly extended periods of high effective precipitation (Lowe et al., 1997), expansion of grass steppe and mixed grass/shrub steppe in lowland areas (Barnosky et al., 1987; Chatters and Hoover, 1992), and the overall warming of the climate across the region.

During the third episode, sedimentary deposition was concentrated in south- to north-flowing streams. Small- to medium-scale, horizontal planar to high-angle cross-stratified, moderately to well-sorted fine- to coarse-grained sand deposits include intercalated beds of pebble- to boulder-sized clasts of relatively pristine Mazama tephra. The pristine nature of the tephra clasts suggests this bed was deposited shortly after the ca. 7700 cal yr B.P. Mazama event. This deposit also may correspond with an

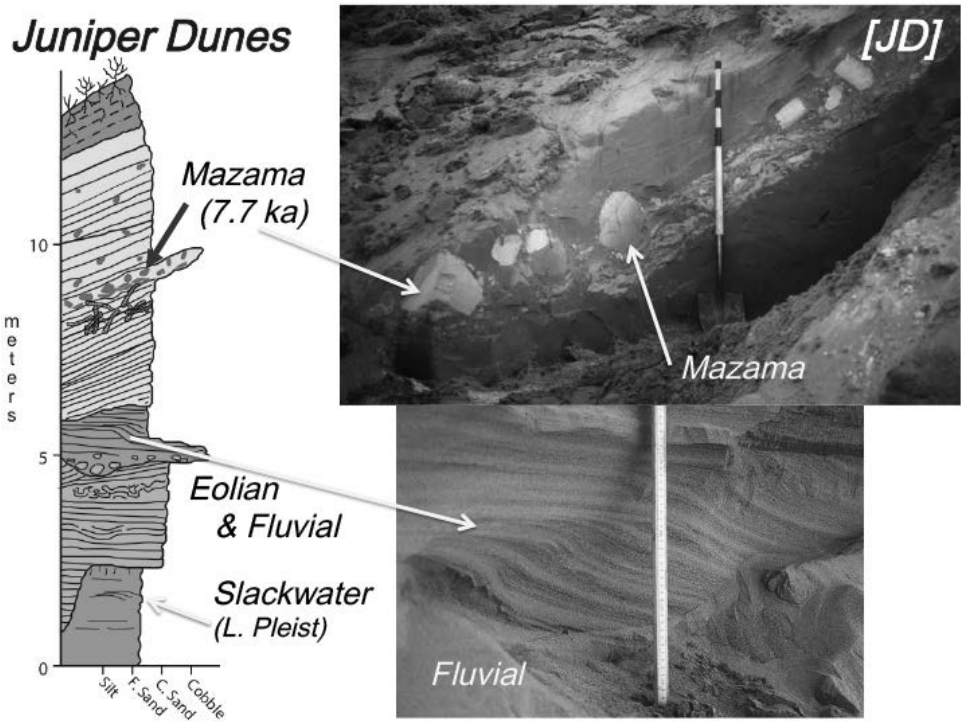

Figure 35. Stratigraphic section of the Juniper–Smith Canyon dunes measured and described at Eltopia Canal by Gaylord et al. (2001). Note how large Mazama tephra clasts are concentrated near the top of the grainflow deposit that accumulated on the slipface of a middle Holocene dune. Description of five depositional-climatic episodes associated with this stratigraphic section is provided in the text.

episode of increased floodplain aggradation in the northern CRB as noted by Chatters and Hoover (1992).

During the fourth episode, sedimentation in the Smith Canyon area was primarily eolian in nature. Deposits during this episode are characterized by large-scale, high-angle cross-stratified fine- to coarse-grained sand that was being transported to the E and SE, a direction consistent with modern summer winds (Gaylord and Stetler, 1994). As was the case for the underlying deposits, these sediments also include an intercalated bed containing pebble- to boulder-sized clasts of reworked Mazama tephra. However, unlike the pristine tephra clasts from episode 3, these clasts were disturbed by cicada burrowing (O'Geen and Busacca, 2001), evidence that sage brush had begun to stabilize the dunes. The fourth depositional-climatic episode is inferred to have extended from a short time (perhaps hundreds of years) after ca. 7 ka until at least 5 ka. This time interval is concurrent with extended episodes of very low effective precipitation in south-central British Columbia (Lowe et al., 1997), continued dominance of dryland shrub steppe in the Pacific Northwest lowlands (Barnosky, 1985; Chatters and Hoover, 1992), and expansion of trees into surrounding upland areas (Barnosky, 1985; Whitlock and Bartlein, 1997). The sedimentary evidence at Eltopia Canal points toward heightened middle Holocene warmth and drought in the Juniper–Smith Canyon dunes area at this time.

During the fifth episode, dune sands were stabilized by encroaching and increasingly dense grass and mixed shrub-steppe vegetation. Massive, bioturbated fine to medium sand that characterizes these deposits has been pedogenically altered. The timing of stabilization and soil formation at this time corresponds with generally expanding and increasingly dense grass and mixed shrub-steppe vegetation in the CRB lowlands (Barnosky, 1985; Chatters and Hoover, 1992) and increasingly extended episodes of moderate to high effective precipitation (Lowe et al., 1997).

Juniper dune activity observed from 1940s to late 2000s air photos roughly parallels the timing of active sand dune expansion and contraction observed on the nearby Hanford site, Washington, by Gaylord and Stetler (1994). However, as verified from remote sensing imagery, the volume of actively migrating dune sand since the early 2000s in this area has largely been static.

Eureka Flat

Eureka Flat is a sedimentologically and stratigraphically diverse 80-km-long deflation plain northeast of Wallula Gap, which is also located to the south of the Juniper–Smith Canyon dune field (Figs. 32, 36). Bordered by the Snake River and by loess uplands, prevailing SW-NE winds have remobilized slackwater-dominated megaflood sediment into genetically related sand sheets, sand dunes, and loess. Characterized as a veritable "dust-producing engine" (Sweeney et al., 2007), saltating sand grains on Eureka Flat have proven to be a highly effective mechanism for ejecting dust-sized particles from mixed sand, silt, and clay megaflood source sediment. This general dust-producing process was previously recognized by Bagnold (1941), Shao et al. (1993), Pye and Tsoar (1990), and Pye (1995). The large volume of suitable megaflood source sediment combined with persistent, sand-moving winds in this area has been responsible for the

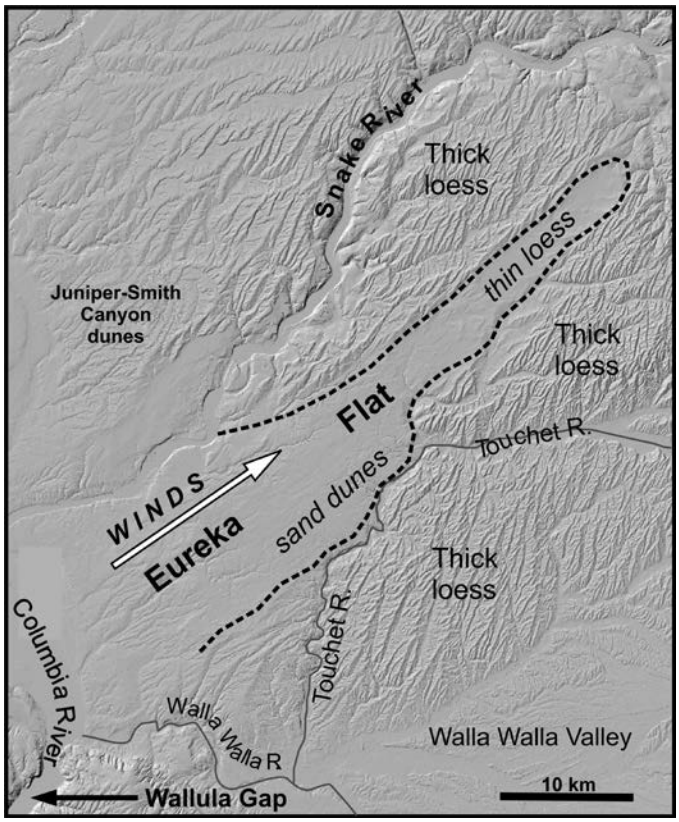

Figure 36. Shaded relief map of Eureka Flat showing its relation to Wallula Gap and the Juniper–Smith Canyon dunes; note alignment of Eureka Flat with the prevailing wind. Also note the concentration of sand dunes in upwind parts of Eureka Flat, as well as the downwind and lateral concentrations of loess.

widespread and thick Palouse loess that blankets >50,000 km^2 of eastern Washington and northern Idaho with up to 76 m of loess (Sweeney et al., 2007). These deposits include thick accumulations of both L1 loess (ca. 15–0 ka) and L2 loess (ca. 77–16 ka) (McDonald and Busacca, 1988, 1992; Busacca, 1989).

Thickness of loess can be accentuated by geomorphic mechanisms, including topographic trapping of eolian sand (Mason et al., 1999; Sweeney et al., 2005, 2007). If eolian sand intercepts a topographic obstacle, such as a canyon or other incised drainage, the sand can become trapped, thus removing it from the eolian system. Downwind of this trap, loess can accumulate to greater thicknesses compared to areas with no topographic trap because saltating sand grains are not available to erode loess in proximal locations. For example, Winnette Canyon, an ephemeral drainage on the east side of Eureka Flat, forms a sharp boundary between eolian sand on the upwind side and thick loess (~12 m of L1 and L2 loess deposits) downwind.

In contrast, loess that mantles the downwind portion of Eureka Flat is only ≤2 m thick and is underlain by a late Pleistocene eolian sand sheet characterized by well-sorted sand and climbing wind ripple strata. In this case, eolian sand migrated down the entire length of Eureka Flat until the sand sheet became stabilized with vegetation, making it a suitable trap for loess. Initially, the sand-rich loess may have been prone to wind erosion, especially in areas with lower vegetation density. The loess here fines upward, reflecting the decreasing influence of saltating eolian sand over time, because active eolian sand became restricted to only the upwind portion of Eureka Flat. Major and trace-element geochemistry of sand dune, sand sheet deposits, and loess accumulations on Eureka Flat indicate the megaflood deposits were their primary sediment source (Sweeney et al., 2007; McDonald et al., 2012).

The location of Eureka Flat immediately downwind from Wallula Gap, a hydraulic dam for megaflood waters, made it an ideal long-term depocenter for megaflood deposits throughout scabland history that may extend to the beginning of the Pleistocene, ca. 2 Ma (Bjornstad et al., 2001; Pluhar et al., 2006). Consequently, the periodic replenishment of an eolian sediment source by megafloods may have played a prominent role in loess generation for perhaps just as long (McDonald and Busacca, 1988; Busacca, 1989, 1991). However, the absence of suitably continuous exposures and reliable temporal markers has made reconstruction of the long-term eolian history difficult. Nevertheless, the sedimentary, stratigraphic, and pedologic evidence from Eureka Flat has suggested that pre–late Wisconsin megaflooding loaded Eureka Flat with abundant fine-grained sediment, which was largely responsible for generating the L2 loess (Sweeney et al., 2007; McDonald et al., 2012). Subsequent late Wisconsin megaflooding renewed source sediment loading ultimately led to generation of the L1, the most recent of the loess deposits.

Juniper Canyon

Juniper Canyon is located south of Eureka Flat and adjacent to Wallula Gap just across the border in northernmost Oregon (Fig. 32). This canyon is ~1 km wide and 150 m deep and incised into basalt of the Horse Heaven Hills. It forms a prominent boundary between sand-dominated eolian sediment upwind and loess downwind (Sweeney et al., 2005). The area was inundated by megafloods up to 350 m a.s.l. (O'Connor and Baker, 1992) that scoured basalt and older loess as well as deposited sand- and gravel-dominated flood deposits. Downstream from Wallula Gap, megaflood waters ponded in the Umatilla Basin, depositing sand-silt-clay sediment. Upwind of the canyon, thin sand sheets, parabolic dunes, and blowouts are separated by gravel lags and small-scale yardangs eroded into older, somewhat resistant loess paleosols. The eolian sand is basalt rich, reflecting its megaflood source. The orientation of dunes reflects the prevailing SW-NE winds of the region. Some of the dunes have migrated into Juniper Canyon. Timing of dune migration is documented by the presence of Mazama tephra (7.7 cal ka) in a blowout that is interbedded within eolian sand that had cascaded down the south canyon slope; the timing of this eolian activity is consistent with that documented in the Juniper–Smith Canyon dunes (Gaylord et al., 2001).

Juniper Canyon has provided an ideal test of the topographic trap model proposed by Mason et al. (1999), where loess

accumulation is accentuated downwind of a trap for eolian sand, and is similar to the example described for Eureka Flat. The L1 loess downwind of Juniper Canyon is up to 7.5 m thick, compared to 3 m thick or less on the Horse Heaven Hills where topographic traps do not exist (Sweeney et al., 2005). Additionally, the topographic trap results in loess that is better sorted with limited variability in grain size compared to areas with no trap, because much of the sand has been sequestered from the eolian system.

105.0 Interpretive sign for Wahluke Unit of Hanford Reach National Monument. [0.2]

105.2 Trees to the right formed in a manmade wetland during the late 1960s and early 1970s, which used excess irrigation water for wildlife enhancement. The project led to landsliding along the nearby White Bluffs of the Columbia River. [1.2]

106.4 Low hills to the right are sand dunes sourced from the White Bluffs. [2.2]

108.6 Four-way junction of unnamed roads. Road to right (west) leads to the old White Bluffs ferry landing, and a primitive trail to the White Bluffs rhythmite site described by Keszthelyi et al. (2009). Go straight through the junction and continue south. [0.4]

108.0 Pass over Wahluke Wasteway. [1.5]

110.5 The road follows the edge of the White Bluffs escarpment to right (west), which lies beyond the sand dunes. [2.0]

112.5 Pull into the parking area on the right at the gate across the road. Walk 40 m west to overlook.

STOP 11—White Bluffs Overlook Site: Overview of Hanford Site and Gable Mountain (N46.6319°, W119.3960°; Elevation 268 m) (Bjornstad)

The White Bluffs line the north and east sides of the Columbia River for ~50 km along the Hanford Reach (Fecht et al., 2004). The 150-m-tall bluffs consist of Miocene–Pliocene Ringold Formation deposits from the ancestral Columbia River and its tributaries (Reidel et al., 1992; Lindsey, 1996). The Ringold Formation accumulated in the Pasco Basin until ca. 3.4 Ma (DOE, 1988). Since then, the Columbia River and Quaternary megaflooding have removed up to 180 m of Ringold deposits from the center of the basin, leaving behind this high erosional escarpment (DOE, 2002). Even here, at this high overview point, the largest Ice Age floods would have been 90 m overhead! Evidence for both modern and ancient landslides is visible from here (Hays and Schuster, 1987; Bjornstad, 2006a). Most landslides along the White Bluffs occur on steep, unstable slopes where water is suddenly added. Recent landslides, beginning in the early 1980s, have resulted from water seeping out of several manmade lakes and unlined canals located just east of the bluffs (Bjornstad, 2006a). Many examples of this type of landslide occur within the Wiehl Ranch landslide complex, which is best seen upriver from here to the northwest. There is evidence immediately below the bluffs for an old landslide (Bjornstad, 2006a). This landslide, with rounded and weathered blocks, likely occurred 14,000–15,000 yr B.P., soon after one of the last Ice Age floods. Unlike modern local landslides, no water is seeping out along the slide, suggesting the water that created this prehistoric slide is no longer present. Another landslide that may be associated with the Ice Age floods can be seen across the river along the north side of Gable Mountain (Fecht, 1978).

Also visible from this vantage point is the Gable Mountain bar, located straight across the river on the Hanford site. It represents one of the best examples of a pendant flood bar, which formed in a more protected area just downstream of Gable Mountain (Bretz, 1925; Bretz et al., 1956; Fecht, 1978; Bjornstad, 2006a). Consider the highest point on Gable Mountain, ~335 m; even this highest point was submerged under as much as 30 m of water during the largest Ice Age flood. Flood channels up to 2 km wide and 40 m deep were scoured out on either side of the ridge as the floods raced past.

Return by the same route to SR-24. [7.8]

120.3 Junction with SR-24. Turn right (east) toward Othello. [6.3]

126.6 Pass the junction with Hendricks Road (on right). Continue east on SR-24. [4.5]

131.1 Junction SR-24 with Sage Hill Road. Turn right and continue south on Sage Hill Road toward Basin City. [4.5]

135.6 Junction with Hendricks Road. Turn left (east) on Hendricks Road. [0.9]

136.5 View to the east of Othello Channels. [4.8]

141.3 Junction with Schoolaney Road. Continue east on Hendricks Road. [3.4]

144.7 Junction with SR-17. Continue straight through the intersection and follow SR-260 east toward Connell (Hendricks Road becomes SR-260). [6.4]

151.1 Railroad overpass. Continue into Connell. [0.2]

151.3 Entering Connell. [0.9]

152.2 U.S. 395 overpass. Continue east on SR-260. [3.4]

155.6 View of Washtucna Coulee on left. [2.7]

158.3 Junction with Copp Road. Continue east on SR-260. View to north of Sulfur Lake in Washtucna Coulee. [1.1]

159.4 Roadcut in loess. [0.1]

159.5 Blackburn Road enters from the right. Continue east on SR-260. [2.5]

162.0 CON-1 Site. [0.4]

162.4 Junction with Delaney Road. Turn right (south) on Delaney Road. [1.9]

164.3 Junction with Largent Road. Turn left (east) on Largent Road. [2.2]

166.5 Junction with Pasco/Kahlotus Road. Turn right (south) on Pasco/Kahlotus Road. [7.5]

174.0 Junction with Burr Canyon Road. Turn left onto Burr Canyon Road. [1.3]

175.3 Pull out on the right shoulder as Burr Canyon Road turns to the right across from the rhythmites exposed in roadcut on the left.

STOP 12—Burr Canyon Rhythmites (N46.5228°, W118.6417°; Elevation 270 m) (Baker and Bjornstad)

A roadcut along Burr Canyon Road exposes about a half dozen slackwater flood rhythmites. These slackwater sedimentary beds occur over 120 m above the current Snake River, located at the mouth of Burr Canyon, over a mile away. The character of the slackwater beds here indicates that megaflooding coming down the Snake River from the northeast backflooded into this tributary valley at least six times toward the end of the last glaciation. This flooding would have had to come through Devil's Canyon or over the Palouse Snake Divide (see below). It is the elevation of these sediments, rather than their sedimentology that provides an indication of the megaflooding magnitudes. Unlike slackwater sites at lower elevations, there are few individual units here, which may imply that only a small number of the scores of events inferred from those lower sites (e.g., Waitt, 1980, 1985) may have been large enough to achieve the stages represented at this stop. A similar relationship of evidence for large and small late Pleistocene flooding events is observed in the Columbia Gorge region (Benito and O'Connor, 2003).

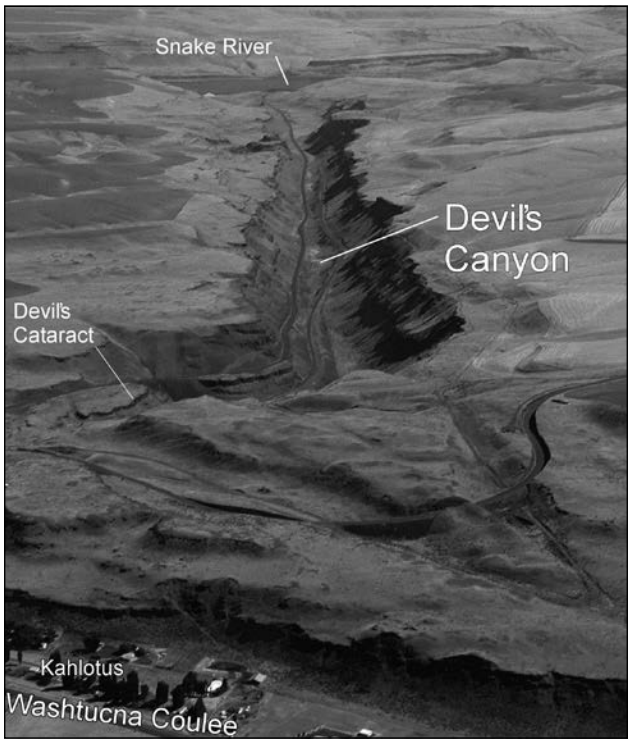

Figure 37. Aerial view of Devil's Canyon Coulee, which was created by Ice Age floods that spilled out of Washtucna Coulee into the Snake River canyon. View to the south, toward the Snake River.

Continue east on Burr Canyon Road. [1.1]

176.4 Burlington Northern Railway trestle. [0.8]
177.2 Junction with Grand Road from southwest. Continue north on Burr Canyon Road along Snake River. [0.6]
177.8 View of fluvial gravel dunes (giant current ripples) across river on right. [1.1]
178.9 Windust Park on right (restroom stop, if needed). Name of Burr Canyon Road changes to Devil's Canyon Road. [2.2]
181.1 View of flood gravel across river on right. [0.9]
182.0 Lower Monumental Dam on right. [0.2]
182.2 Boat launch area on right. [0.4]
182.6 Flood bar at mouth of Devil's Canyon. Drive up Devil's Canyon (Fig. 37). [1.5]
184.1 Excellent exposure of canyon-filling lava flow in wall in Devil's Canyon. [2.6]
186.7 View of Devil's Canyon cataract on left. [0.6]
187.3 Junction of Devil's Canyon Road (SR-263) with Pasco-Kahlotus Road. Turn right toward Kahlotus. [0.7]
188.0 Intersection with SR-260 in Kahlotus. Turn left on SR-260 toward Connell. [0.2]
188.2 Intersection with SR-21 (Kahlotus-Lind Road). Turn right toward Lind. [10.0]
198.2 Cross Sand Hills Coulee. Stop for view of dunes.

STOP 13—Sand Hills Coulee (N46.7808°, W118.5383°) (Gaylord)

The Sand Hills Coulee dune field consists of ~12 km^2 of parabolic and blowout dunes that are concentrated in a shallow, <20-m-deep coulee that was generated by megaflooding of unknown age(s) (Schatz, 1996; Gaylord et al., 1999). The loess island upon which this dune field developed is ~70 km wide and is truncated by the 6–8 km-wide, basalt-floored Lind Coulee on its north, 3–5 km-wide Washtucna Coulee on its south, Cheney-Palouse scabland tract on its east, and the Drumheller Channels on its west. It is located ~70 km east of the Columbia River. Much of the terrain surrounding this dune field is either under dry-land cultivation or has been left dormant because of the sensitivity of the soils to erosion. More than 80% of the dunes in the dune field are stabilized by shrub and steppe vegetation. Active dunes have migrated, on average, 2–3 m since the 1980 Mount St. Helens eruption, whose ~0.5-cm-thick deposit is easily traced on and just beneath the surface.

The mineral and lithic content and provenance of the Sand Hills Coulee dunes, as well as their relative isolation on a loess island sets them apart from other sand dune and sand sheet deposits in the CRB (Schatz, 1996; Gaylord et al., 1999, 2014). Mineralogically and lithologically, the Sand Hills Coulee dune sands are quartz- and feldspar-enriched, and strikingly yellow in their appearance; this contrasts with the dominantly gray to gray-brown, basaltic-lithic-enriched and largely megaflood-derived Moses Lake, Hanford Reach, Hanford site, Juniper–Smith

Canyon, Eureka, and Juniper Canyon sand dune and sand sheet deposits. The compositional and/or color differences between the Sand Hills Coulee dunes and other CRB dune sands are explained by the source contributions to Sand Hills Coulee dunes from the Miocene–Pliocene Ringold Formation (Schatz, 1996; Gaylord et al., 1999, 2014). The nearest Ringold Formation exposures, however, are located ~30 km to the west and largely covered with loess and colluvium, making their relation to the development of these dune sands a still unresolved puzzle.

Except for a few poorly exposed sand sheet deposits in roadcuts and gullies, sand-dominated eolian deposits on this loess island apparently post-date the last glacial maximum. Dune reconstructions from Hanford (Gaylord and Stetler, 1994; Stetler and Gaylord, 1996), Hanford Reach (Gaylord et al., 2011), and the Juniper–Smith Canyon dunes (Gaylord et al., 2001) suggest that the primary post–last glacial maximum eolian sand dune mobility on the CRB occurred during the early and middle Holocene. The few age constraints on dune activity in the Sand Hills Coulee dunes include a tentatively identified Mount St. Helens J tephra (Gaylord et al., 1999; Mount St. Helens J: ca. 13.8–12.8 cal ka, Clynne et al., 2008), reworked beds of Mazama tephra (ca. 7.7 cal ka), and the Mount St. Helens 1980 tephra. These bracketing ages suggest that the dunes were subject to drought-driven eolian activity during the early and middle Holocene. A prolonged episode of landscape stability and dune stabilization began in the late–middle Holocene and has been interspersed with relatively short episodes of drought-induced eolian activity since that time.

Continue north on SR-21 (Kahlotus-Lind Road). [0.9]

199.1 Intersection with SR-26. Continue north (straight ahead) on SR-21 toward Lind. [11.0]
210.1 Junction with U.S. 395. Take on-ramp to the right for U.S. 395 north toward Ritzville. [16.0]
226.1 Night at motel in Ritzville.

■ DAY 3—RITZVILLE TO MOSCOW

Mileage	*Directions*
0.0	Start at the intersection of S. Division St. and Weber Avenue in southeast Ritzville near I 90 exit 221. Continue north toward the center of Ritzville on S. Division Street. [0.3]
0.3	Turn right on Bauman Road. Road curves to the left (north) past the cemetery. Golf course on left. [0.4]
0.7	Junction of Bauman Road with Wellsandt Road, turn right (east). [0.6]
1.3	Pass over I 90. [4.4]
5.7	Junction with Hills Road, turn right (toward Marengo and Benge). [0.3]
6.0	View of Cow Creek scabland to left and front. [1.2]
7.2	Road bears left. [1.3]
8.5	Cross Cow Creek. [0.1]
8.6	Large silt mounds visible on the scabland surfaces. [1.2]

Silt Mounds

Silt mounds are an extremely common feature on scabland surfaces, including gravel bars and planar areas of scoured basalt. The origin of these mounds remains unresolved. They are typically several meters in diameter, ~1–2 m in height, and occur in closely spaced fields. They are predominantly composed of silt, with some sand. Hypotheses for their origin include causation by runoff erosion of silty deposits, frost wedging, desiccation cracking, earthquake shaking (Berg, 1990), the work of gopher colonies, and the vegetation anchoring of wind- or water-transported silts. Olmsted (1963) proposed that the anchoring occurs when eolian silts (presumably supplied from wind erosion of the nearby loess uplands) accumulate in depressions, where the higher moisture content promotes vegetation growth that then serves to anchor the windblown silt (which then promotes moisture retention, which promotes more vegetation growth, etc.). Washburn (1988) also invokes anchoring by vegetation, but places more emphasis on surface runoff for transporting the sediment.

9.8 Junction with Dury Road. Bear left at the intersection and continue on Hills Road, which now becomes E Urquhart Road. [0.2]

▸ **NOTE:** If you have time, drive 1 mile down Dury Road to view a giant ice-rafted erratic (Fig. 38). ◂

10.0 Road ascends scarp of the gravel bar on the downstream end of a streamlined loess hill. [1.2]
11.2 Junction with Marengo Road.

▸ OPTIONAL SIDE TRIP—Marengo Road Log

Reset odometer.

0.0 Turn right (south) on Marengo Road. [0.6]
0.6 Road ascends loess scarp on the northern end of the Marengo loess "island." [0.2]
0.8 Roadcut in loess. [1.1]
1.9 Summit of Marengo loess "island." [1.2]
3.1 Ranch buildings on left. [0.3]
3.4 Pavement ends. Turn right on Cow Creek Road, paralleling the railroad tracks. [0.2]
3.6 Cross Union Pacific Railroad tracks and then John Wayne trail, and turn right on Cow Creek Road. [0.5]
4.1 Park along the road just before the next rail crossing (to private land) and climb up to the old railroad grade to the right. This was the former Chicago, Milwaukee, St. Paul and Pacific Line, but it is now the John Wayne Pioneer Trail of Iron Horse State Park. Follow the trail line southwestward ~1 km to the old railway cut in the distance.

Figure 38. This huge, ice-rafted erratic of granodiorite measures 8 × 5.5 × 2.7 m; estimated weight of the boulder is ~350 tons. It rests on one side of a flood bar within the Cow Creek flood-channel complex at an elevation of 514 m. The erratic lies ~100 m below the maximum flood level for this area. Grounding of ice-rafted erratics is rare, especially along a high-velocity flood channel like the upper Cow Creek. An exception occurred here apparently due to the large size and mass of the boulder. Since coming to rest thousands of years ago, several rectangular pieces of the erratic were split off by resourceful farmers, to be used as foundation stones in local dwellings.

▸ OPTIONAL STOP A—Marengo Railway Cut (N47.0167°, W118.2083°) (Bjornstad and Baker)

The Marengo railway cut exposes highly weathered flood deposits capped by strongly weathered calcic soils, signifying ancient floods from earlier in the ice age going back ≥1 million yr (Fig. 39).

While the evidence for floods from the last glacial cycle (late Wisconsin Epoch between 15,000–28,000 yr ago) is plentiful and widespread, there are also some sites in the Channeled Scabland with a record for older, pre-Wisconsin floods that go back ≥ 1 million yr (Patton and Baker, 1978a; Baker et al., 1991a; Bjornstad et al., 2001; Medley, 2012). The paucity of evidence for the oldest floods is not surprising since the younger cataclysmic floods tended to erode or bury the evidence for the older floods.

Most old flood localities are located in remote areas of the Cheney-Palouse scablands. One of the best exposures for old flood deposits can be seen at this stop (Fig. 39). The oldest flood deposits often display a reversed magnetic polarity in combination with calcic paleosols developed atop the flood deposits, suggesting flood ages of ≥780,000 yr (age of the last major shift in magnetic polarity). In the exposed section, sediments within the lower paleosols, above the flood gravel (the "Younger Pre-Palouse Loess" on Fig. 39), retain a normal (N) over reversed (R) magnetic polarity locked in at the time of sediment deposition. A Th/U radiometric age of 800,000 yr B.P. from sediment below the magnetic reversal is consistent with the magnetic-polarity age (Bjornstad et al., 2001). Since the flood gravels lie below the dated horizons, it follows that a major megaflood occurred more than 800,000 yr ago. Flood gravel from the late Pleistocene phase of megaflooding is exposed near the top of the section beneath the "Altithermal Soil" developed on "Late Pinedale Loess" (older terminology from Patton and Baker, 1978a).

Return to vehicle and retrace route back on Cow Creek Road and Marengo Road to the junction with Urquhart Road. [4.1] Turn right to continue east on Urquhart Road.

▸ Add 8.2 to mileage *if* you took the OPTIONAL SIDE TRIP, *then continue on with the regular Road Log below.* ◂

REGULAR ROAD LOG (*continued*)

11.2	Junction with Marengo Road. Continue east on Urquhart Road. [0.5]
11.7	Road ascends a large gravel bar that formed on the upstream end of the Marengo loess "island." [0.1]
11.8	Gravel exposure in roadcut on the western margin of the bar. [0.3]
12.1	Gravel exposure in roadcut on the eastern margin of the large flood bar. [0.4]
12.5	Gravel exposure in a small gravel bar. [0.5]
13.0	Flood bar at the downstream end of a streamlined loess hill. [0.1]
13.1	Teske railway crossing. Road turns southeast and becomes Harder Road. [0.6]
13.7	Scabland inner channel and butte-and-basin scabland. [0.2]
13.9	Streamlined loess hill on left. Note the steep loess scarp. [1.3]
15.2	Junction with Benge-Ritzville Road to right. Continue east in the direction of Urquhardt Road, which now becomes Harder Road (Fig. 40). [0.6]
15.8	Subtle gravel dunes (giant current ripples) to the right (south of the road) (Fig. 40). [0.4]
16.2	Streamlined loess hill on left (Fig. 41). [0.6]
16.8	Butte-and-basin scabland. [1.2]
18.0	Roadcut on left exposes early Pleistocene flood gravel with petrocalcic soil horizon (Fig. 42). Pull off on left. [2.5]
20.5	Pavement ends. [0.7]
21.2	McCall Road sign, road curves to left. [0.7]
21.9	Butte-and-basin scabland on right. [0.5]
22.4	Cross scabland inner channel. [0.1]
22.5	"Harder's Hangout" on left. [0.1]

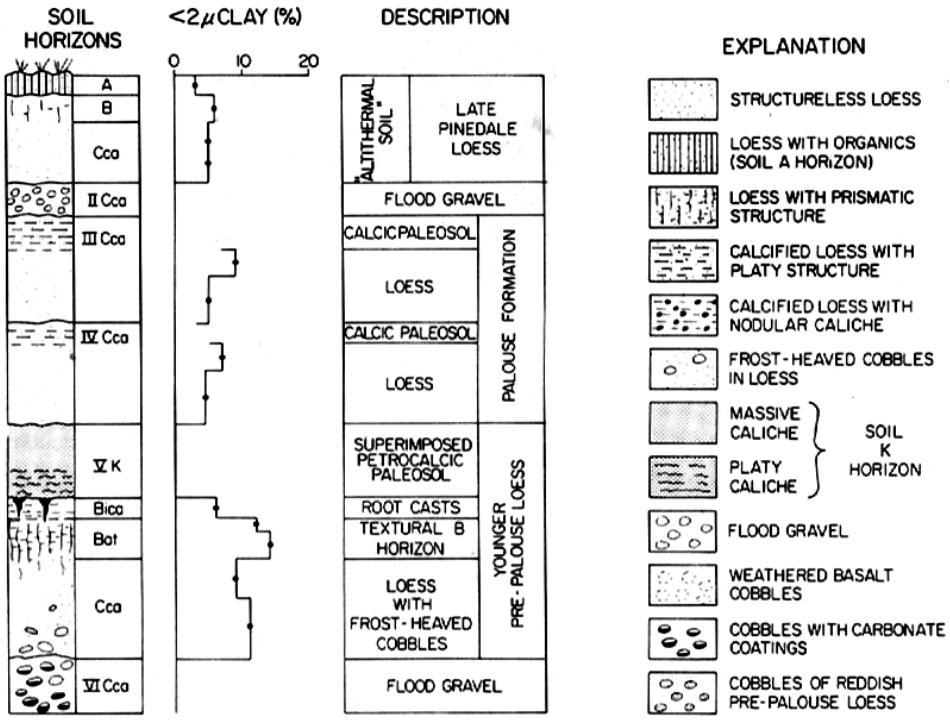

Figure 39. Stratigraphic section exposed at the Marengo railway cut (optional Stop A) (modified from Patton and Baker, 1978a).

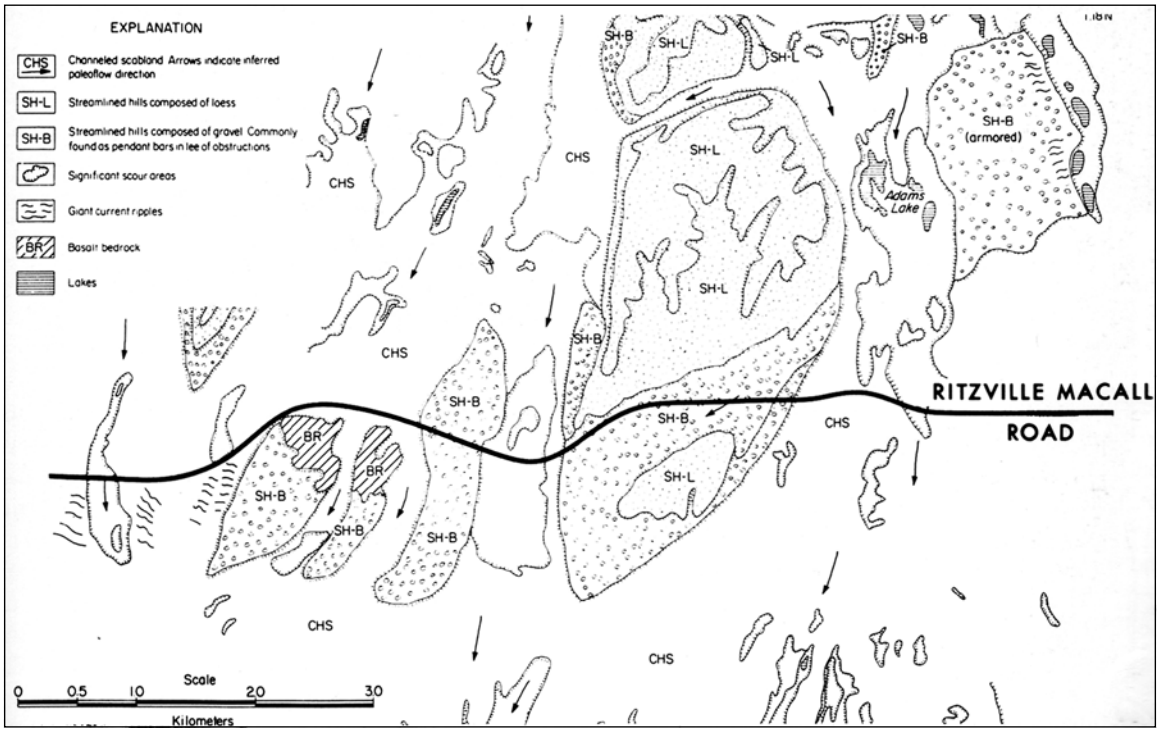

Figure 40. Morphological map (from Patton and Baker, 1978b) showing the route of the field trip through the central portion of the Cheney-Palouse scabland tract. Note the relationships of various scabland features that will be observed along the drive, including streamlined loess hills, scoured basalt, gravel bars, and giant current ripples (dunes). North is toward the top of the map. The roadcut shown in Figure 42 is located along the highway (heavy black line) near the center of the map, on the western edge of the gravel comprising the southern part of the large streamlined hill.

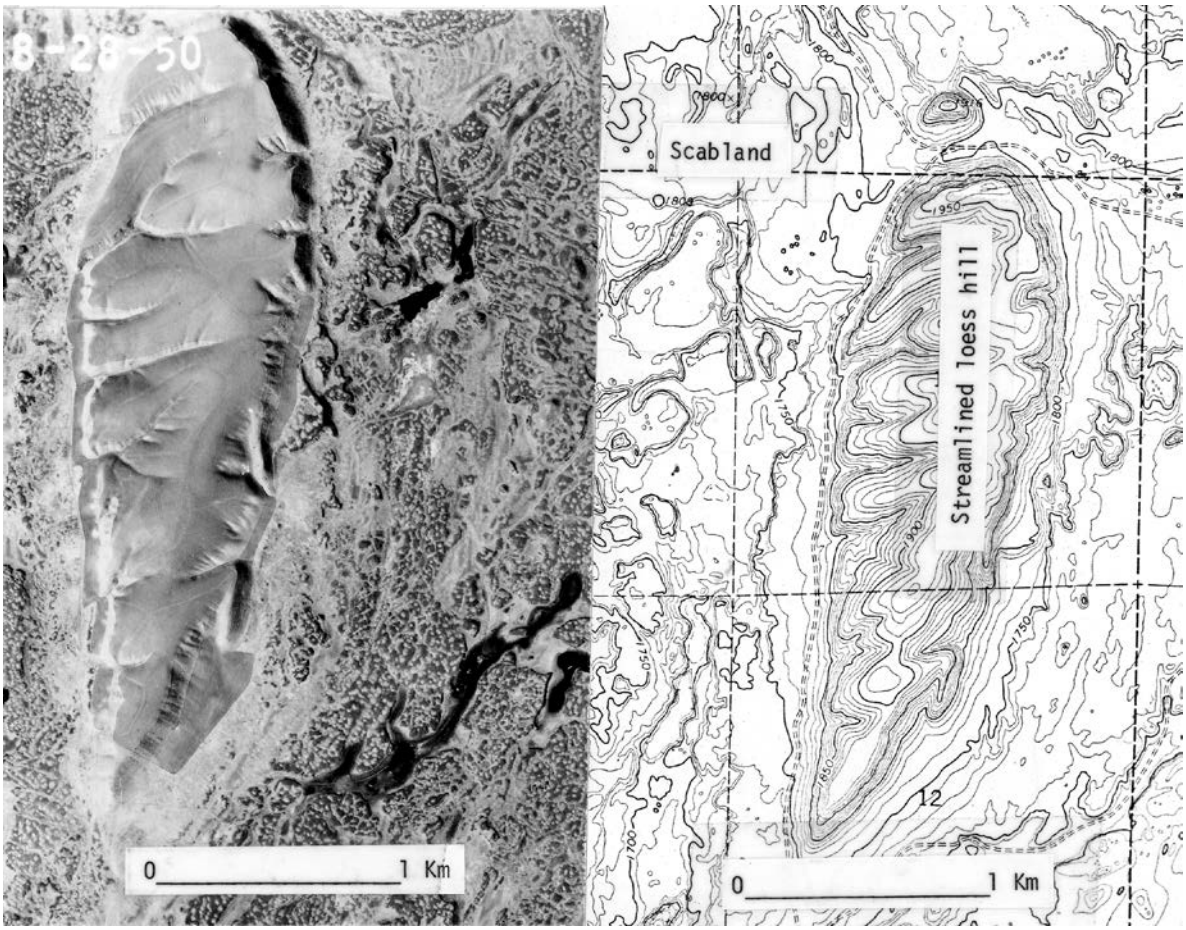

Figure 41. Aerial photograph (left) and topographic map (right) of streamlined and scarped loess island surrounded by basaltic scabland. The megaflooding came from the north (top of the map area). The map shows a small cataract that receded headward around the blunt upstream end of the hill (top of the map area). The aerial photograph shows longitudinal grooves and butte-and-basin topography on the scabland surface marginal to the hill near the center of the image.

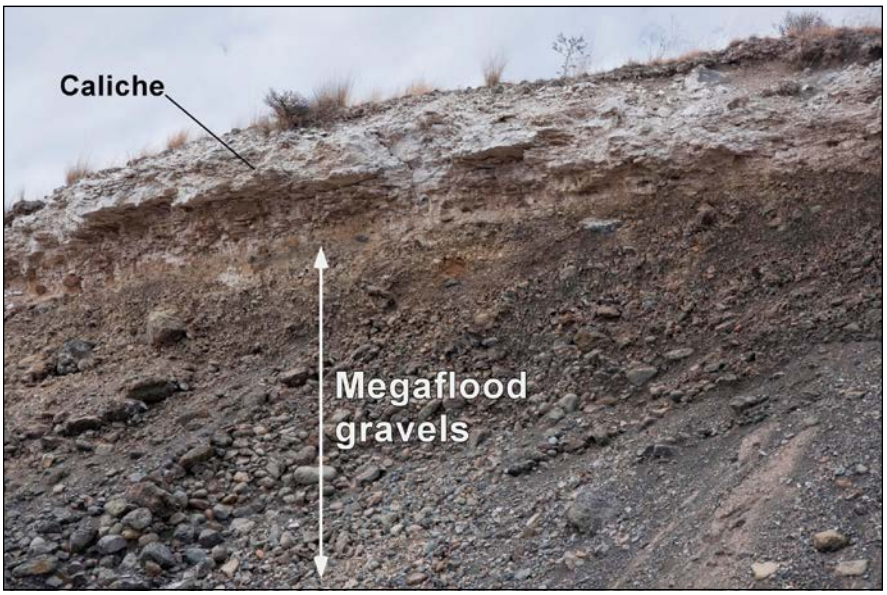

Figure 42. Old flood deposits along Harder Road (Macall site) in roadcut exposing 3-m-high section of gravel comprising the downstream extension of the large streamlined hill located near the center of the mapped area in Figure 40. A thick petrocalcic horizon overlies the megaflood gravel sequence. In the paleosol sequence above the flood gravels, a single paleomagnetic sample was reversely magnetized and a Th/U age from the calcic horizon measured >350 ka. Thus, the gravels probably were emplaced by an early Pleistocene megaflood (>780 ka) (Bjornstad et al., 2001).

22.6 Junction with Gering Road, turn right and follow Gering Road. [3.0]
25.6 Junction with Revere Road, turn right (south) on Revere Road. An early Pleistocene flood gravel is exposed along Revere Road just to the north of this road junction. [0.4]
26.0 Gravel pit in flood bar on right. [0.4]
26.4 Cross abandoned railway line (now John Wayne Pioneer Trail of Iron Horse State Park). Road makes a sharp left turn and continues toward the Revere grain. [0.2]
26.6 Junction with Jordan Knott Road, turn right and follow Jordan Knott Road south. [0.4]
27.0 Bridge over Rock Creek. [1.1]
28.1 Small streamlined loess hill on the right has a very well-formed prow on its upstream end. [0.3]
28.4 Second, larger streamlined loess hill on right. [0.4]
28.8 Road on the right leads to Rock Creek Management Area

▸ OPTIONAL SIDE TRIP—Towell Falls Road Log (Baker)

Reset odometer.

0.0 Turn right on the gravel road to Towell Falls, following scarp on the eastern side of streamlined loess hill. [1.6]
1.6 Cross cattle guard. [0.8]
2.4 Arrive at the parking area with view of Escure Ranch. A primitive road (open seasonally) continues south from this point. The stop involves either a hike or drive on the road, beyond the swinging gate heading downstream along Rock Creek.

▸ OPTIONAL STOP B—Towell Falls (N47.0143°, W117.9435°) (Baker)

The late Pleistocene megaflood water was ~150 m deep at this point. After ~0.5 miles, the primitive road (trail) passes a flat-topped mesa, part of a trenched spur. After ~1.6 miles, the track rises on a rock bench from which there is a good view of the megaflooding topography of the Rock Creek scabland. At ~2 miles, the track enters a maze of scabland buttes and then emerges on the top of a huge flood bar at the downstream end of one of the basalt buttes. At 2.8 miles, there is a view of Towell Falls to the west, but a short walk to the east will bring one to a point where a small, unnamed tributary entering Rock Creek from the north has cut completely through a pendant bar that formerly blocked this tributary valley. After the late Pleistocene megaflooding emplaced this bar, the blocked tributary valley was almost completely filled with fluvial sediments, consisting of loess eroded from the surrounding uplands. The flood bar was not breached until the valley was filled, so there seems to be a very long post-megaflooding record of sedimentation. Erosion of the flood bar also locally exposes coarse flood deposits from early Pleistocene megaflooding (Fig. 43), although this exposure tends to collapse unless cleaned by active stream cutting. Return to vehicle at the trailhead and retrace the road back to Jordan Knott Road. [2.4]

▸ Add 4.8 to mileage *if* you took the OPTIONAL SIDE TRIP, *then continue on with the regular Road Log below*. ◂

Figure 43. Exposure of pre-Wisconsin flood gravel overlain by late Pleistocene flood deposits near the mouth of the tributary from the north that joins Rock Creek just downstream from Towell Falls.

REGULAR ROAD LOG (*continued*)

28.8 Junction of Jordan Knott Road with road to Rock Creek Management Area. Turn right and continue southeast on Jordan Knott Road. [1.1]
29.9 Scabland inner channel with prominent loess scarp visible to the southeast. [0.7]
30.6 Ranch near spring-fed creek. [0.2]
30.8 Small gravel bar. [0.6]
31.4 Loess scarp on right. [1.6]
33.0 Lamb Road joins on the right. Continue straight ahead on Jordan Knott Road. [0.9]
33.9 T junction. Turn right on Jordan Lake Road. [0.1]
34.0 Loess scarp on right. [0.4]
34.4 Entering Mason Draw. Loess scarp on right; butte-and-basin scabland on left. [1.1]
35.5 Ranch. [1.4]
36.9 Ranch. [0.6]
37.5 Johnson Lake in inner channel on left. [0.8]
38.3 Lamb Road joins from right, continue south on Jordan Lake Road. [0.5]
38.8 Sharp turns to right, then left. [1.6]
40.4 Junction with Endicott Road. Turn right on Endicott Road (pavement resumes). [0.7]
41.1 Streamlined hill on left. [1.1]
42.2 Roadcut in loess. Buried paleosols are visible in trench on the right. [0.4]
42.6 Roadcut in loess. [0.4]
43.0 Enter Rock Creek scabland area. [1.1]
44.1 Steep descent into the Rock Creek inner channel. [0.4]
44.5 Gravel bar with rippled surface in distance on right. [0.1]
44.6 Bridge over Rock Creek. [0.2]
44.8 Junction with Hawk's Road. Continue on Endicott Road, ascending a large gravel bar. [0.4]
45.2 Exposure of gravel in bar on left. [0.3]
45.5 Exposure of gravel in bar on right. [1.1]
46.6 Loess scarp on left. [1.1]
47.7 Zornes Road enters from north (right). [1.1]
48.8 Loess scarp on right. [1.5]
50.3 Troupe Road enters from left. [1.0]
51.3 Road enters a megaflood channel that was cut into the Palouse loess. [2.8]
54.1 Cross the old railroad line (now the Columbia Plateau Trail). [0.1]
54.2 Ritzville/Benge Road enters the from right (north). [0.8]
55.0 Benge heritage marker. Benge-Winons Road becomes Benge-Washtucna at the point where E. Ralston-Benge Road enters from the right (north). [1.3]
56.3 Old railway line (Columbia Plateau Trail) visible on left (south). [2.4]
58.7 Tunnel under Union Pacific rail line. [0.2]
58.9 Cross Cow Creek. [0.1]
59.0 Mack Road joins from the right (northwest). [0.4]
59.4 Union Pacific Railroad trestle in distance on left. [1.0]
60.4 Gray Road joins from the left (south). [0.6]
61.0 The road follows a relatively small flood overflow channel connecting the Cow Creek scabland to Stanley Coulee. [1.9]
62.9 Entering Stanley Coulee. [2.4]
65.3 Dury Road enters from right (north). [2.8]
68.1 Junction with SR-261. Washtucna bar is in the foreground. Turn left on SR-261 toward Washtucna. [0.1]
68.2 Pit exposes gravel in Washtucna bar on the right. [1.8]
70.0 Foreset beds in flood gravel (Washtucna bar) visible in exposures on right. [0.4]
70.4 Junction with SR-26. Continue through the intersection on SR-261, entering Washtucna and continuing down Washtucna Coulee. [2.3]
72.7 Road junction, turn left on Nunamaker Road, pavement ends. [0.4]
73.1 Railroad underpass (Columbia Plateau Trail). Ascend from Washtucna Coulee. [1.3]
74.4 Sharp bend in road. Gravel pit on the left exposes high-level flood gravel (elevation 390 m). [0.2]
74.6 Prominent loess scarp visible to front. [0.6]
75.2 Enter high-level flood-cut channel (floor at 415 m elevation). [2.1]
77.3 Junction with SR-261. Turn left and continue east on SR-261 (pavement resumes). [1.6]
78.9 Snake River canyon visible on right. [0.5]
79.4 Sharp bends in road, with descent into HU Coulee. [0.2]
79.6 HU Canyon on right. [0.3]
79.9 HU Ranch. [1.2]
81.1 Steep loess scarp on right. [0.4]
81.5 Prows on streamlined loess hills on right. [0.4]
81.9 Junction with Davin Road. Turn right. [0.9]
82.8 Park and walk to the loess hill to the left of the road.

STOP 14—Loess Hill (N46.6536°, W118.2850°) (Baker)

Hike up the streamlined loess hill east of Davin Road.

The eastern portions of the Channeled Scabland contain spectacular examples of km-scale hills that show distinctive flow streamlining of their edges ("islands") and, in some cases, their tops (Fig. 44). These streamlined hills generally occur in local clusters, organized in a braid-like pattern within the overall scabland complex. The hills are composed predominantly of remnant loess that was not stripped from the underlying basalt by the floodwaters. They generally rise up to 50 m above the surrounding scabland areas, and are commonly 1–4 km long and 0.5 km wide. Bretz (1923) first recognized their remarkable shape, with steep, ungullied bounding hillslopes that converge upstream to prow-like terminations and downstream to tapering tails. The drag or resistance to a flowing fluid is minimized for specific relationships among lengths, widths, and areas, which

Figure 44. Streamlined loess hill located on the Palouse–Snake River Divide.

can be quantified for these streamlined landforms (Baker, 1978c, 1979; Komar, 1983, 1984; Baker and Komar, 1987).

Return to vehicle and retrace path on Davin Road to junction with SR-261. [1.0]

83.8 Davin Road junction with SR-261. Turn right and continue southeast on SR-261. [1.2]
85.0 Road to Palouse Falls (fee area) on left. Continue toward Lyons Ferry. [0.9]

Palouse-Snake Divide Crossing

Prior to the megaflooding, the Palouse River flowed along the present course of now-dry lower Washtucna Coulee (seen earlier today). The megaflooding greatly exceeded the capacity of this pre-flood valley, and the floodwater spilled to the south, across the pre-flood divide between the Palouse and Snake Rivers (Fig. 45). The result is a spectacular scabland area ~16 km wide. Most of the original loess cover was stripped off, leaving only isolated areas of streamlined loess hills. A very narrow, 125-m-deep inner gorge was carved into the jointed basalt, probably through the action of a cataract initiated near the Snake River, similar to what can be seen near HU Ranch and at Devil's Canyon (Fig. 37). However, in this case, the cataract receded all the way to the Palouse River, resulting in the capture of its drainage. The present Palouse Falls derive from the ungraded floor of the captured river.

85.9 Loess scarp on right. [0.3]
86.2 Turn to the right. [1.0]
87.2 Palouse Canyon on left. [1.9]
89.1 View of Palouse Canyon and Mid Canyon bar (Fig. 45). [0.8]
89.9 Pass under Union Pacific Railroad trestle. [0.4]
90.3 Entrance to Lyons Ferry State Park on left. [0.5]
90.8 Snake River Bridge. [0.1]
90.9 Megaflood gravel of Mid Canyon Bar exposed on left. [0.4]
91.3 Road junction. [0.4]
91.7 Gravel dunes (giant current ripples) on Mid Canyon Bar. [0.4]
92.1 Descend Mid-Canyon Bar. [1.0]
93.1 Railroad overpass. [0.2]
93.3 View across Snake River (left) toward large megaflood bar. [0.5]
93.8 Entering Tucannon River valley. [0.3]
94.1 View across river on left to Tucannon eddy bar exposures in old roadcuts of highway (described by Baker, 1973a). [0.7]
94.8 Views of slackwater deposits draped on sides of Tucannon River valley. [0.5]
95.3 Cross Tucannon River. [0.5]
95.8 Junction with Powers Road (also known as Tucker Road) entering from right. [0.8]
96.6 Park in the large pullout on the left side of road. Examine the exposures of megaflood slackwater deposits on the left side of the road. This is the coarse-grained facies, and Stop 16 will be at an exposure of the fine-grained facies.

STOP 15—Flood Slackwater Deposits in Tucannon Valley (N46.5314°, W118.1408°) (Smith and Gaylord)

Retrospective Summary of Missoula Floods Sedimentation in the Tucannon Valley, Southeastern Washington (Smith)

Introduction

The controversy over the origin of the Channeled Scablands of eastern Washington by cataclysmic floods unleashed from

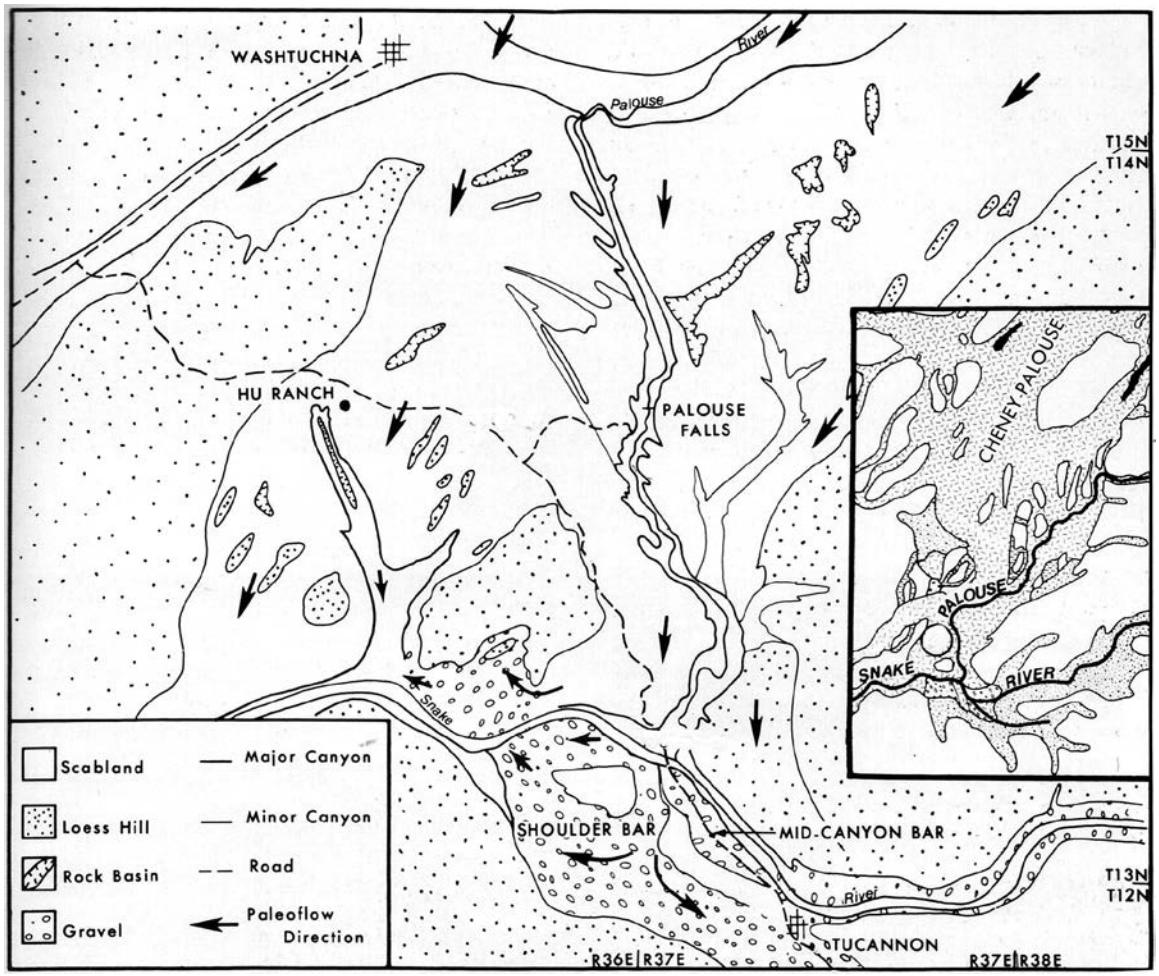

Figure 45. The late Pleistocene megaflooding overfilled Washtucna Coulee (original valley for the Palouse River) and, aided by NW-trending tectonic fracture zones, spilled south via Devil's Canyon (Fig. 37), HU cataract, and what is now the Palouse River canyon. North is at the top of the mapped area, which measures 29 × 24 km.

glacial Lake Missoula raged from the late 1920s until the late 1960s (Baker, 2009a), but a new debate was kindled in the 1980s. Did this unimaginable inundation occur a few times, as proposed by Bretz (1969), or dozens of times, as hypothesized by Waitt (1980)? This new debate focused on the roughly 40 graded layers of sand and silt, commonly called rhythmites, located throughout the lower Walla Walla and Yakima River valleys. Deposition occurred when these valleys were backflooded as inflowing floodwaters from the north and east were hydraulically ponded as much as 200 m deep in the Pasco Basin behind the Columbia River constriction at Wallula Gap. Prior to Waitt (1980), the multiple graded beds were interpreted as the record of a complexly pulsating hydrograph during one or perhaps a few different flood events (Baker, 1973a; Patton et al., 1979; Bjornstad, 1980; Bunker, 1982). In contrast, Waitt (1980, 1985) interpreted each bed to be the record of a single flood, requiring 40 or more cataclysmic failures of the ice dam holding back glacial Lake Missoula during the last Pleistocene deglaciation.

It was the debate about the relationship between the number of beds and number of floods that brought me to the Tucannon River valley in the summer of 1990. With no predisposed allegiance to the proponents of either side in this sometimes caustic debate, I proposed that detailed sedimentological analysis of the flood deposits would elucidate the depositional processes and, therefore, an improved understanding of the number of graded layers deposited during a single flood (Smith, 1993). By that time, the evidence for dozens of floods had been strengthened by the discovery of glacial Lake Missoula deposits interbedded within the sediments of proglacial lakes in northern Washington (Rigby, 1982; Atwater, 1984, 1987). There, more than 80 coarse-grained layers of putative Missoula-flood origin were each separated by varved clays to suggest that dozens of years elapsed between each flood event (Atwater, 1987). Subsequently, the evidence of a prolonged period with dozens of floods was strengthened by documentation of disconformities in flood-gravel bars downstream from Wallula Gap (Benito and O'Connor, 2003), and

secular variation of magnetic-field directions in the rhythmites in the Walla Walla and Yakima valleys that demonstrated flood deposition over a period of 2.5–3.5 k.y. (Clague et al., 2003). Left unresolved, however, was whether one or multiple graded beds were deposited during a single such flood and the implications of the physical sedimentology for understanding the paleohydraulics of these events.

Geomorphic Setting and Age of Flood Deposits in the Tucannon Valley

The Tucannon River enters the Snake River more than 100 river kilometers upstream from the Pasco Basin. Floodwater from glacial Lake Missoula initially entered the lower Tucannon valley directly from the Channeled Scabland rather than by backflooding from the Pasco Basin. Floodwater surged southward from Washtucna Coulee over a divide, now crossed by the Palouse River, and dropped into the Snake River canyon nearly opposite the mouth of the Tucannon River (Fig. 46). During at least some floods, the water not only flowed up the Snake River and into the Tucannon valley, but also crossed over the 90-m-high basalt ridge just east of this confluence. A gravel eddy bar, ~40 m high, was formed at the mouth of the Tucannon River (site of section 1 in Fig. 46).

Deposits attributed to the Missoula floods underlie a terrace surface ~8–15 m above present river grade and are distinctive for upstream decrease in grain size and upvalley-dipping cross-beds, which preclude deposition by local fluvial processes in the Tucannon River. These deposits are traceable upstream for ~28 km to an elevation of ~335 m. In addition, adjacent hillslopes include local accumulations of pebbles and cobbles of crystalline and metasedimentary rocks that are exotic in contrast to the monotonous basaltic bedrock geology of the region. These accumulations of exotic clasts are interpreted as debris left behind from melting icebergs that grounded against the hillsides at elevations at least as high as 400 m above sea level (Bretz, 1929).

The deposits in the Tucannon valley are correlated to other well-studied Missoula flood-deposit sections by the occurrence of the Mount St. Helens set S Ash. This ash layer, sampled at sections 2 and 4 (Fig. 46) in 1990, was analyzed (Smith, 1993) to corroborate its provenance as set S, which is also known within flood deposits in the Walla Walla (Bjornstad, 1980), Yakima (Bunker, 1982), and Columbia (Smith, 1993; Benito and O'Connor, 2003) River valleys. The set S tephra were probably erupted between 13,350 and 14,400 ^{14}C yr B.P. (Clague et al., 2003), or ca. 16.3 ka and 17.5 ka (calibrated ages).

Sedimentology of Tucannon Valley Deposits

The descriptions and interpretations of the deposits associated with the Missoula floods are listed in Table 3 and are illustrated in Figure 47 for sections 3 (Stop 15) and 7 (Stop 16). Additional stratigraphic sections and illustrations are provided in Smith (1993).

Facies FC—graded layer with horizontally laminated base overlain by opposite-facing ripple cross-laminations (Fig. 48)—is the dominant facies in terms of occurrence and is also the typical facies found among rhythmites reported in the Walla Walla and Yakima valleys (Bjornstad, 1980; Bunker, 1982; Waitt, 1980). The coarser-grained variant FB, usually with only upvalley-dipping cross-bedding, is located in the lower Tucannon valley and, in many cases is overlain by FC.

Facies FA is restricted to the vicinity of section 3 (Stop 15). I interpret this facies to represent traction-carpet gravel sheets emplaced by flood flows that overtopped the ridge between the Snake and Tucannon Rivers and then descended to the valley floor (Fig. 46).

Facies FD is notable for representing true slackwater deposition beneath hydraulically ponded water in the lower valley. Suspension deposition was interrupted by emplacement of thin graded-bed turbidites traveling downvalley as a consequence of continued sediment influx from the Tucannon River farther upstream.

Nonflood facies are also present and, where intervening between flood facies are a clear indication of a hiatus between flood events (Table 1, Fig. 47). NA and NB are indistinguishable, respectively, from loess and slopewash colluvium that occurs on the hillslopes above the elevation of flood erosion. NC layers are interpreted as fluvial deposits of the Tucannon River.

Stratigraphic sections were measured and described following preparation by mason's trowel and paintbrush. These tools were used to provide fresh outcrop faces and to accentuate fine-scale sedimentary structures. Brush strokes were made vertically to avoid creating striations that might be confused as primary laminations.

Bioturbation is apparent in the sediment at all measured section localities. Discrete burrows range in size from 1 to 2 cm across, and are attributed to insects, when up to 10 cm in diameter, ascribed to rodents. The smaller burrows are rarely more than 5–10 cm long but the larger rodent burrows can extend subvertically for at least 2 m. Therefore, smaller burrows can commonly be matched to a single paleo-ground surface, whereas large burrows typically cannot. Gradual upward transition from laminated to massive sediment, with or without discrete burrow traces, is common in many FC and FD beds and this transition is interpreted as homogenization by bioturbation. The relative extent of bioturbation was estimated using the approach of Droser and Bottjer (1986) and diagrammatically shown alongside the lithologic drawing in the stratigraphic sections (Fig. 47).

How Many Beds Were Deposited During a Single Flood?

While working in the Tucannon valley in 1990, I also visited the sections in the Walla Walla and Yakima valleys that were interpreted by Waitt (1980) to support the deposition of a single graded-bed rhythmite (typically resembling FC or FC+FD at his Tucannon study sites) during a Missoula flood. I had previously attended a field trip in northern Washington led by Brian Atwater, which convincingly showed evidence for dozens of Missoula outburst floods, each separated by lacustrine-varve deposition in glacial Lake Columbia. However, I did not accept a priori that each flood would leave behind only a single graded bed on the backflooded landscapes surrounding the Pasco Basin. I was

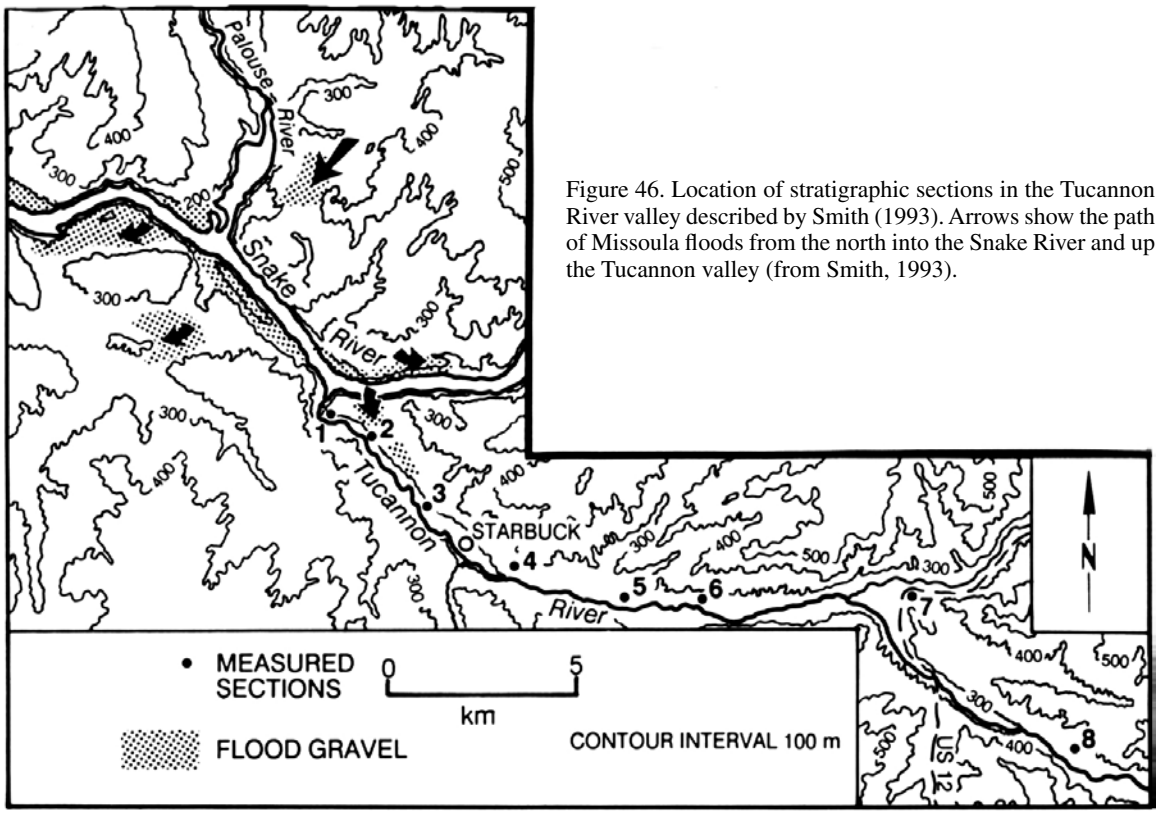

Figure 46. Location of stratigraphic sections in the Tucannon River valley described by Smith (1993). Arrows show the path of Missoula floods from the north into the Snake River and up the Tucannon valley (from Smith, 1993).

TABLE 3. DESCRIPTION AND INTERPRETATION OF SEDIMENTARY FACIES IN THE TUCANNON VALLEY

Facies code	Description	Interpretation
Flood facies		
FA	Sandy gravel (clasts to 1.2 m across) in layers 0.4–1.0 m thick; massive, commonly reverse-graded at base; merge vertically and horizontally (upvalley) into FB. Found only at and in vicinity of section 3.	Rapid deposition in traction carpets from highly concentrated sediment flows at the base of flood currents descending steep ridge separating Snake and Tucannon valleys.
FB	Sand and gravelly sand (clasts to 20 cm) in layers up to 1 m thick; horizontal bedding or planar-tabular cross-bedding (most commonly unidirectional upvalley but downvalley in some cases), normal or reverse-to-normal grading; upward transitions from horizontal bedding to cross-bedding is typical. Found only within 12 km of the mouth of the Tucannon River.	Deposition by decelerating upvalley turbulent flows, with some deposition by downvalley return flows.
FC	Sand and silty sand in layers 8 to 75 cm thick; normal or reverse-to-normal grading with horizontal and climbing-ripple cross-lamination (bidirectional upvalley overlain by downvalley). Most common facies, occurring alone in 38% of flood beds and with FD in an additional 33% of flood beds.	Deposition by decelerating turbulent flows that flowed upvalley and then downvalley.
FD	Silt and sand in layers 5 to 50 cm thick; normal-graded strata 1 to 5 cm thick, commonly with ripple cross-lamination (mostly unidirectional downvalley; rarely upvalley) and horizontally laminated silt; flame structures (downvalley flow) are common; typically overlies FC or FB. Found only below 235 m elevation (~12 km upstream of mouth of the Tucannon River).	Suspension deposition from hydraulically ponded water with common turbidity current sediment influx from Tucannon River and rare upslope driven flood flows from the mouth of the Tucannon River.
Non-flood facies		
NA	Silt and sandy silt; massive, bioturbated.	Eolian loess.
NB	Gravelly silty sand (clasts to 10 cm); massive or discontinuous diffuse layering; lenticular.	Colluvium (with admixed eolian silt).
NC	Sandy gravel and gravelly sand; scour-and-fill bedding, and less common planar-tabular and trough cross-bedding (downvalley flow).	Shallow braided-stream alluvium of the Tucannon River.

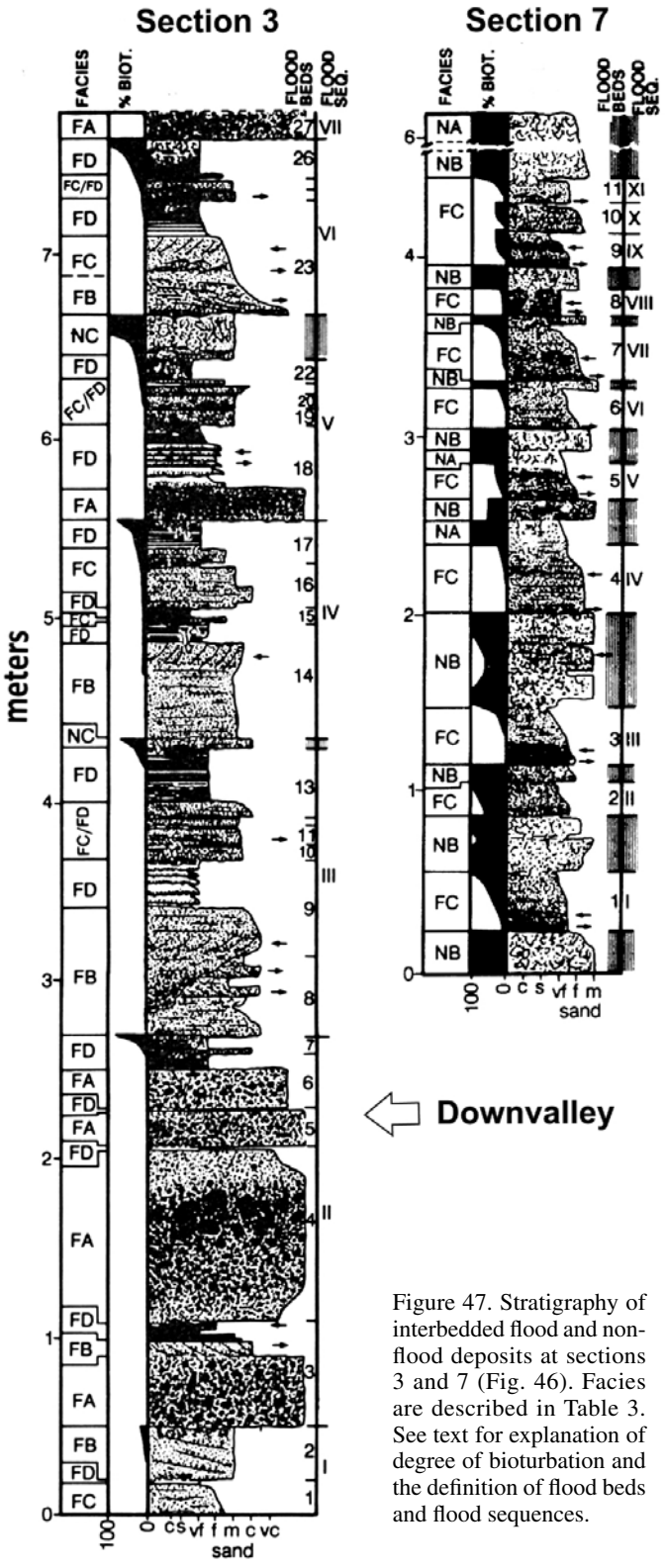

Figure 47. Stratigraphy of interbedded flood and non-flood deposits at sections 3 and 7 (Fig. 46). Facies are described in Table 3. See text for explanation of degree of bioturbation and the definition of flood beds and flood sequences.

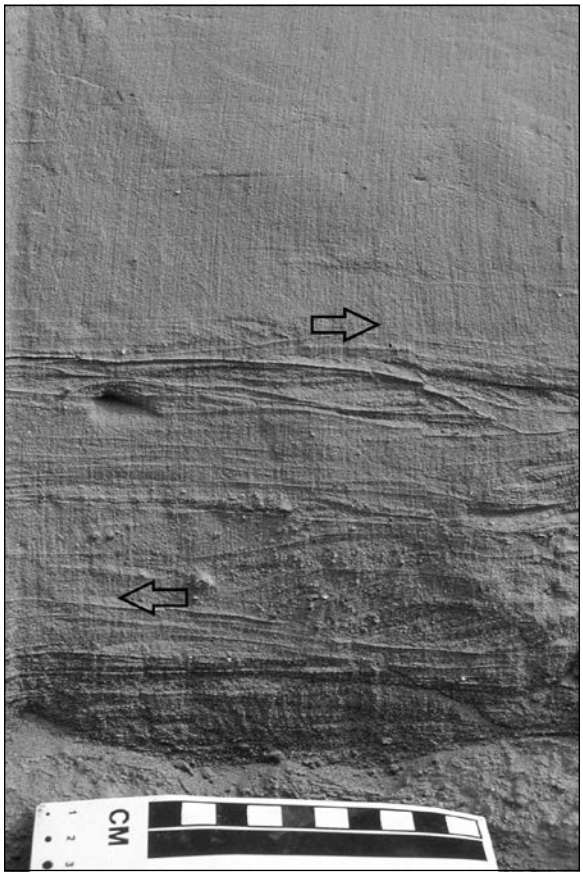

Figure 48. The most common flood-deposited rhythmite consists of facies FC (Table 3), a graded bed with cross-laminations showing that currents flowed first upvalley (to the left) and then downvalley (to the right). Photo shows flood bed 5 at section 7 (Figs. 46, 47). Vertical striations on the outcrop face were produced by a brush while cleaning the exposure.

persuaded by the logical arguments of Baker and Nummedal (1978) and Patton et al. (1979) for the likelihood of complex, multi-peaked hydrographs related to (1) complex progressive failure of the ice dam, (2) variable arrival times of flood waves traveling different pathways through the Channeled Scabland to the Pasco Basin, and (3) water-level fluctuations caused by cataract recession and spillovers across drainage divides. Nonetheless, when I cleaned off and observed for myself the rhythmites in the Walla Walla and Yakima valleys, I was strongly compelled to accept Waitt's (1980) hypothesis; the upper part of each graded bed was clearly bioturbated and, in many cases, separated from the overlying rhythmite by deposits of loess, typical for the region, that enclosed, at many localities, one or two of the set S ashes. Despite being convinced of the one-bed-per-flood explanation for the valleys backflooded by rising water in the Pasco Basin, I remained open to the possibility that highly variable hydrographs might be preserved by multiple flood beds deposited during a single flood at other localities.

Before leaving each measured and described stratigraphic section, my field assistant and I worked together, sometimes in lively debate, to reach consensus on the number of flood sequences that were present, not simply the number of flood beds. A *flood bed* was defined as a single graded interval, commonly with gradational internal facies boundaries, and they are denoted by Arabic numerals in Figure 47. Thirty-nine percent of the 112 flood beds in the eight measured stratigraphic sections consist only of facies FC and another 33% consist of FC overlain by FD. Other beds begin with FA or FB and typically grade upward through FC and, in some cases, to FD. A *flood sequence* was defined (Smith, 1993) as one or more flood beds that are bounded by nonflood facies or horizons of bioturbation, but that lack such features between beds. Each flood sequence, even if composed of multiple beds, is inferred to record deposition during a single flood and they are denoted by Roman numerals in Figure 47. Therefore, the definition of flood sequences is critical to the debate of one-bed-per-flood versus many-beds-per-flood.

Although deposition of a single bed during a flood, at a particular location, was most common, multiple-bed flood sequences are prominent, especially in the lower part of the Tucannon valley. Seventy-two percent of all flood sequences defined in the eight stratigraphic sections contain only one bed, especially at sections 4 through 8. At section 7 (Stop 16), for example, each bed represents a separate flood and is separated from the deposits of the next youngest flood by slopewash colluvium or loess (Figs. 47 and 49). However, in the lower valley, multi-bed flood sequences are common, especially at section 3 (Stop 15).

I contemplated during the fieldwork that evidence of interflood lacuna might have been eroded away between beds in the lower valley, where coarser grain sizes imply stronger transporting currents that may have amalgamated flood beds while removing nonflood facies or bioturbated intervals. If so, then the existence of multiple-bed flood sequences might be contested. However, the preservation of nonflood facies and bioturbated bed tops in many places implies that erosion at these locations may have been limited. Where possible, my assistant and I examined bed contacts laterally for 2 to >10 m, looking for evidence of local preservation of interflood bioturbation or deposition that may have been eroded away in the line of the measured section. At section 3, erosion surfaces are prominent, but correlation of four short sections across the outcrop face led to consistent designation of flood-sequence boundaries (Fig. 50). Soft-sediment deformation is commonly more intense in facies FD within a flood sequence, in contrast with FD layers at the top of flood sequences, consistent with differences in sediment saturation for sediment loading on a just-deposited substrate versus a just-wetted, previously exposed substrate (Fig. 51).

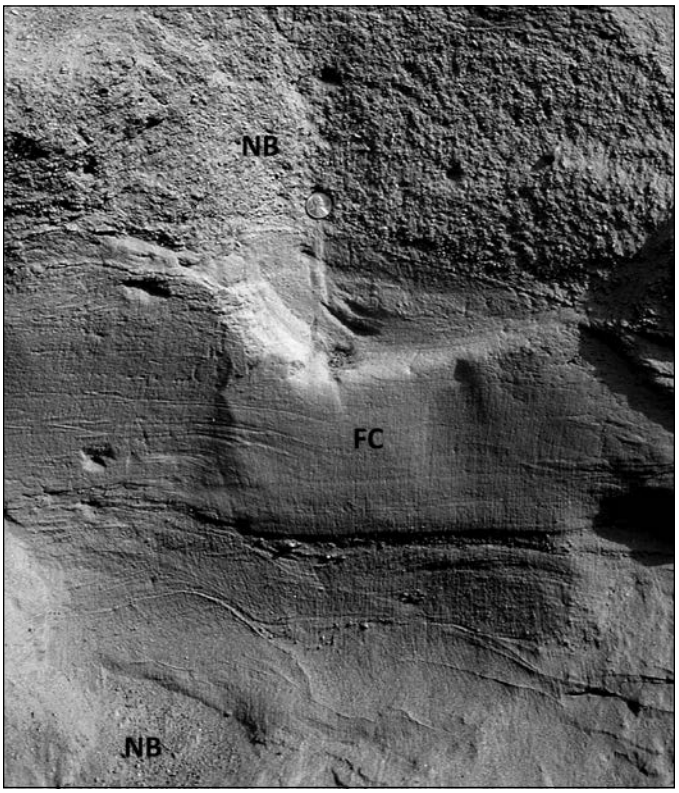

Figure 49. An example of a flood bed (facies FC) interbedded with nonflood hillslope deposits (NB); flood bed 3 at section 7 (Figs. 46, 47).

On the other hand, Shaw et al. (1999) contested the evidence for any buried exposure surfaces at section 3 (Stop 15), attributing all of the sediment at this section to a single flood. They suggest that laminated beds grading upward into massive beds were not evidence for bioturbation but "are as easily explained by suspension settling" (p. 606). Such an alternative explanation seems far from easy. The massive sediment, which I interpret as bioturbated, is a mixture of grain sizes from fine silt to medium sand, and would be segregated by grain size into distinct laminae if deposited from suspension. In some cases, burrows within these massive, presumably bioturbated zones are truncated at the base of the next flood bed, showing that these burrows are clearly associated with a buried land surface (Fig. 52).

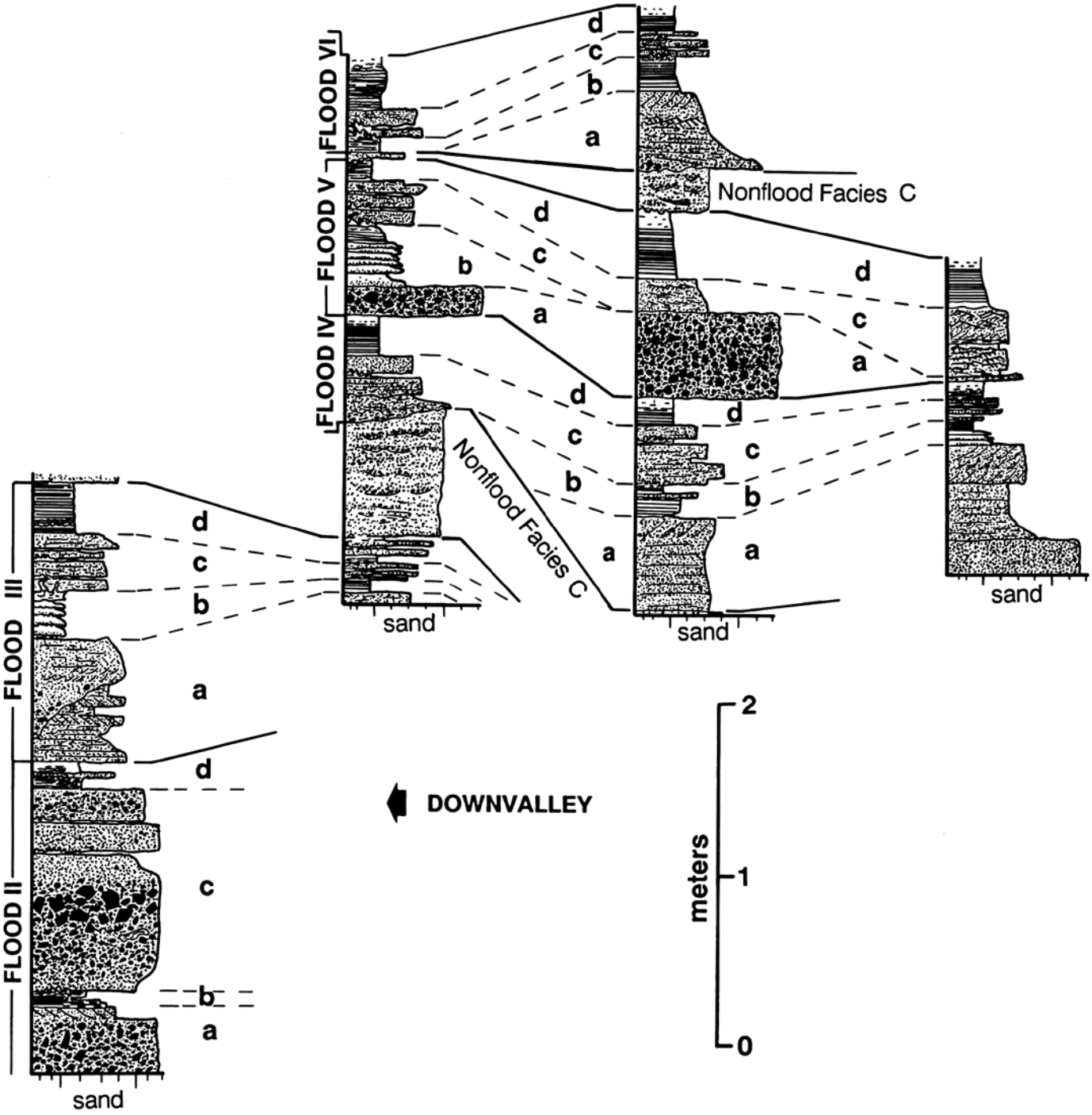

Figure 50. Correlation of several stratigraphic sections across the roadcut at section 3 (Fig. 47) shows a repeated pattern of deposition of four members (a, b, c, and d) during each of five floods. See text for description and interpretation of members a–d. (From Smith, 1993.)

Figure 51. Contrasting texture and deformation in light-colored FD layers in section 3 (top of flood bed 9 and flood bed 13 within flood sequence III) (Fig. 47). The lower FD interval has coarser grain size and thicker beds ("member b" in Fig. 50) than the upper interval ("member d"). Soft-sediment deformation by loading of coarser sediment is much more intense in the lower bed, within the flood sequence, than in the upper bed, interpreted to mark the top of the flood sequence with a hiatus prior to deposition of overlying gravel. Scale bar is 10 cm tall.

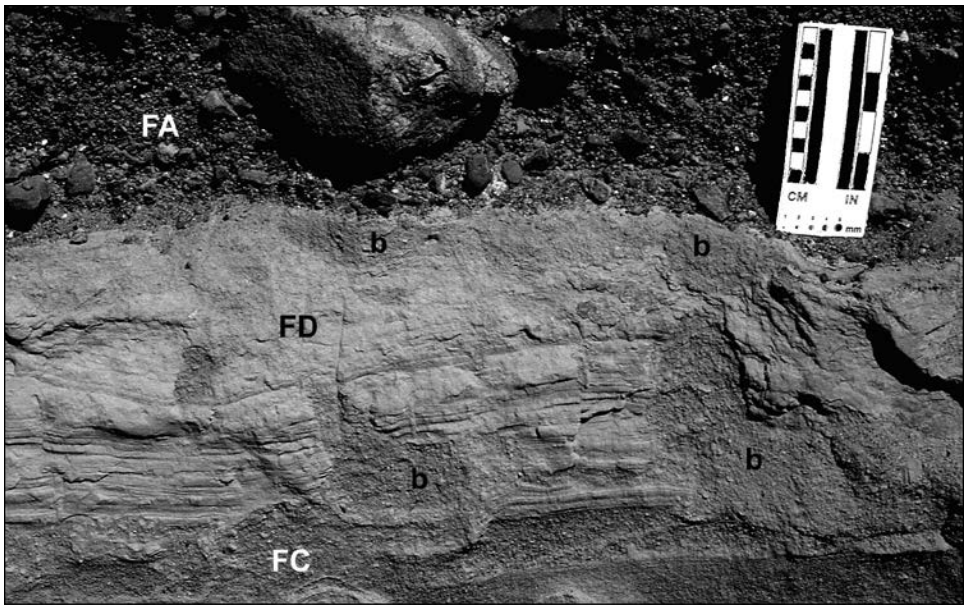

Figure 52. Close view of the top of flood bed 13 at section 3 (Fig. 47). Laminae within facies FD are increasingly interrupted upward by burrows with bioturbation destroying all lamination in the upper few centimeters. Cylindrical rodent burrows (labeled "b") are notably truncated below the contact with the overlying gravel in the center of the view and near the scale.

Sedimentological Implications of Flood Processes

The evidence for deposition of multiple beds during a single flood at some locations implies a complex, multi-peaked hydrograph. Particularly notable is the correlation of sections at location 3 that show a repeated pattern of deposition during five successive floods (Fig. 50). Each flood sequence contains four depositional members, labeled a through d. "Member a" begins with coarse-grained FA or FB layers. Crossbedding, when present, indicates either only upvalley flow or upvalley flow followed by downvalley flow. "Member b" represents relatively still-water conditions and deposition of FD layers that include thin graded layers with downvalley directed ripple cross-laminations. Coarser sediment influxes are recorded in "member c" by three or four upvalley-thinning FC-overlain-by-FD beds with mostly upvalley-dipping cross-laminations. The abrupt thinning of these beds across the outcrop face suggests attenuation of flood pulses within the existing stilling basin of the backflooded valley. Each flood sequence ends with deposition of FD layers in "member d." These uppermost FD layers are finer grained than in "member b," and contain almost exclusively downvalley-directed ripple cross-laminations. Each of these five floods apparently consisted of (1) an initial upvalley surge of water and sediment ("member a"); followed by (2) relatively quiet-water deposition interrupted by small downvalley-directed gravity currents and minor upvalley-flowing bottom currents ("member b"); interrupted by (3) three or four new upvalley surges from the Tucannon-Snake confluence, attenuating in the hydraulically ponded water in the valley; and followed by (4) renewed slackwater sedimentation with sediment flows heading downvalley, perhaps from a prograding Tucannon River delta into the transient lake that might be represented by local NC facies.

The sedimentology of the Tucannon valley flood deposits permits distinction of dynamic and passive flooding processes. Early interpretations of Missoula flood rhythmites (e.g., Baker, 1973a; Waitt, 1980) attributed all deposition as occurring on the bottom of relatively quiet hydraulically ponded lakes that rose slowly, remained for several days, and then drained as the hydrograph waned. This model does not, however, account for the observation that suspension deposits (FD) do not intervene between upvalley and downvalley dipping ripple cross-laminations in ubiquitous facies FC but, instead, overlie these traction deposits; this is true everywhere that rhythmites are found and not only in the Tucannon valley. Therefore, even where only one bed was deposited during a flood, the flows dynamically surged up *and then down the valleys* before hydraulically ponded still-water conditions were established. During at least some floods, water surged over the ridge at the east side of the mouth of the Tucannon River, and poured into the valley near section 3, leaving the hillslope draped in gravel and the emplacement of the facies FA traction-carpet deposits. Using the suspension-criterion approach of Komar (1980), I calculated upvalley current velocities in excess of 6 m/s near the mouth of the Tucannon, decelerating to ~1 m/s at a distance 12 km upstream and to ~0.5 m/s at the farthest upvalley section, 25 km from the confluence (Smith, 1993). In other words, the water did not slowly rise as the shoreline of a filling backwater lake, but moved upvalley as a dynamic current for perhaps 6–8 h before reversing and flowing back downslope.

Passive flooding, or the inundation of the landscape beneath the fluctuating surface of still, hydraulically ponded water affected a shorter reach of the Tucannon valley than was reached by the dynamic flood surge. Facies FD is the only facies that includes clearly defined suspension deposits with minor gravity flows beneath relatively quiet water, and it is absent above 230 m (section 5). Therefore, initial flood surges traveled at least 30 km upvalley with icebergs stranding at elevations as high as 400 m, and then water relatively quickly drained back with ponding restricted to the lower 10–12 km of the valley.

Return to vehicle and continue on SR-261 southbound. [0.4]

97.0	Junction with Little Goose Dam Road entering from left. [0.3]
97.3	Entering Starbuck. [1.5]
98.8	Exposure of slackwater flood deposits on left. [1.3]
100.1	Riveria Road enters from the left. [0.3]
100.4	More slackwater deposits exposed on left. [0.4]
100.8	Smith Hollow Road enters from the right. [1.6]
102.4	Note prominent terracettes on the hillside (right). [3.2]
105.6	Junction with U.S. 12. Turn left onto U.S. 12 eastbound and pull off immediately into the large pullout on the right.

STOP 16—Flood Slackwater Deposits in Tucannon Valley (N46.3552°, W117.9690°) (Smith and Gaylord)

The roadcut exposure is of a distal, fine-grained facies at section 7 in Figures 46 and 47 for the same slackwater sedimentary sequence that was observed and described in detail for Stop 15. See discussion above.

Return to vehicle and continue east on U.S. 12. [6.3]

111.9	Passing Garfield County line. [2.1]
114.0	Junction with U.S. 12 and SR-127. Turn right and continue on U.S. 12 to Clarkston. [12.0]
126.0	Pomeroy. [10.5]
136.5	Alpowa Summit. Elevation 849 m. [11.6]
148.1	Road to the left (West Lake Drive) provides access to the Alpowa Creek Habitat Management Area. U.S. 12 continues east across the bridge toward Clarkston.

A now-overgrown exposure on the left bank of Alpowa Creek to the left of the highway has a basal slackwater sediment unit that is overlain by colluvium and alluvial fan gravel, which in turn is overlain by megaflood rhythmite units, similar to those observed at the Tucannon stops. A similar relationship of units occurs further west down the Snake River at Steptoe Canyon (Hammatt, 1977). At both these sites, what is interpreted to be the Mount St. Helens S tephra (Foley, 1976) occurs in the nonflood colluvium and alluvium that was deposited between the lower slackwater unit and

the multiple rhythmites. Moreover, two radiocarbon dates from the same nonflood layers date to ca. 15.8 and 17.5 ka (Hammatt, 1977), seemingly confirming this relationship. If this is correct, then an earlier late Pleistocene megaflooding phase was separated by a significant time gap from the phase that emplaced the rhythmites at these sites and possibly those at Stop 17 as well. [0.4]

148.5 Gravel bar in Snake River. [0.4]

148.9 Silcott Grade Road enters from the right. Note the large megaflood bar on the left that has been partly inundated by the waters of Lower Granite Lake, the reservoir formed on the Snake River upstream of Lower Granite Dam, constructed 1965–1975 by the U.S. Army Corps of Engineers in the Snake River canyon ~20 miles downstream, of this point. [1.1]

150.0 Silcott Hills Road enters from the right. [3.4]

153.4 Evans Road enters from the right. [1.3]

154.7 Elm Street. [0.4]

155.1 Entering Clarkston, Washington. [0.6]

155.7 Junction with 15th Street. Continue east through Clarkston on U.S. 12/Bridge Street. [1.5]

157.2 Drawbridge over Snake River. Entering Lewiston, Idaho. [0.2]

157.4 Hard turn to right on first turn after bridge (U.S. 12 East/Snake River Avenue) going south. [0.1]

157.5 U.S. 12 turns off to the right. Continue straight (south) on Snake River Avenue toward Hells Gate State Park. [1.2]

158.7 Traffic circle. Continue south on Snake River Avenue toward Hells Gate State Park. [1.3]

160.0 Bear left at the fork in road, continuing toward Hells Gate State Park (right fork goes over Southway Bridge). [0.2]

160.2 Underpass. [1.5]

161.7 Atlas Sand and Rock on left. This is a very large gravel pit in Tammany bar. Excellent exposures of the bar sedimentation can be found, but permission is required to enter the property. [0.5]

162.2 Pull off on the left. View point into gravel pit.

STOP 17—Tammany Bar Gravel Pit (N46.3552°, W117.0465°) (Baker and Gaylord)

Tammany bar (Bretz, 1969, p. 531–532) exposes the slackwater facies of late Pleistocene megaflooding overlying Bonneville flood gravel along the Snake River ~5.5 km south of Lewiston, Idaho. The Bonneville flood deposits overlie sand and gravel of the Snake River that is being commercially extracted by Atlas Sand and Rock. An organic sample from the Snake River alluvium collected by V. Baker, L. Ely, and J. O'Connor yielded a radiocarbon age of 27.860 ± 345 (ca. 32.5 ka) (J. O'Connor, 2016, personal commun.). The overlying Bonneville flood deposits are spectacularly exposed in the eastern face of the commercial excavations. Huge northward-dipping foreset bedding in gravel and boulders shows that the Bonneville megaflooding came from the south, flowing down the Snake River. The event occurred ca. 18.5 ka (Lifton et al., 2015; Oviatt, 2015), leaving extensive evidence on the Snake River Plain of southern Idaho (Malde, 1968; O'Connor, 1993).

Overlying the Bonneville gravel is a sequence of 21 rhythmic graded beds (Waitt, 1985). The beds get thinner up section. The lower coarse-grained basal portion of each rhythmite consists of coarse sand and/or granule gravel of basaltic composition, locally with small foresets that dip toward the south, in an upstream direction relative to the Snake Valley. This basal layer in each rhythmite is overlain by sand-to-silt sedimentation. The 21 rhythmites probably represent approximate age equivalents to the sections observed in the Tucannon Valley at Stops 15 and 16. In this case, however, the slackwater deposits occur ~120 km upstream from the mouth of the Palouse River, which would have been the site of the late Pleistocene megaflood influxes to the Snake River valley.

Confirming geochronological analyses have not yet been performed. Waitt (1985) correlates the upward thinning sequence at Tammany bar to the section of Touchet Bed rhythmites at Burlingame Canyon, inferring that the later of the late Pleistocene outbursts from glacial Lake Missoula became smaller and more frequent as glaciation waned, and that the self-dumping process envisioned for outburst flooding became less effective for generating the largest lake releases.

Turn around and retrace the route on Snake River Avenue, following signs to Route 12, then to Route 12 East. (It is possible to go further up the road to a rest stop on the right, before turning around and retracing the route.) [7.0]

169.2 Follow signs to U.S. 12 East (bypass of downtown Lewiston). [2.3]

171.5 Junction of Route 12 East (bypass) with Main Street, Lewiston. Turn left (east) on U.S. 12/Main Street. [0.5]

172.0 Memorial Bridge over Clearwater River. [1.2]

173.2 Take the exit left onto U.S. 95 North (follow signs to Moscow). [5.6]

178.8 Scenic viewpoint. [1.2]

180.0 Exit 195 for Pullman on right. Continue straight on U.S. 95 toward Moscow, Idaho. [15.2]

195.2 Moscow, Idaho. End of trip.

ACKNOWLEDGMENTS

V.R.B. thanks the Geological Society of America Quaternary Geology and Geomorphology Division, which provided financial support through its Don Easterbrook Distinguished Scientist Award, for some of the field investigations and absolute dating. This guidebook chapter benefited from reviews by Lisa Ely, Virginia Gulick, and Jim O'Connor. Keegan Schmidt's editing was heroic.

REFERENCES CITED

Alho, P., Baker, V.R., and Smith, L.N., 2010, Paleohydraulic reconstruction of the largest glacial Lake Missoula drainings: Quaternary Science Reviews, v. 29, p. 3067–3078, doi:10.1016/j.quascirev.2010.07.015.

Allen, J.R.L., and Leeder, M.R., 1980, Criteria for the instability of upper-stage plane beds: Sedimentology, v. 27, p. 209–217, doi:10.1111/j.1365-3091.1980.tb01171.x.

Anderson, K., Bradley, E., Zreda, M., Rassbach, L., Zweck, C., and Sheehan, E., 2007, ACE: Age Calculation Engine—A design environment for cosmogenic dating techniques, *in* Proceedings of the International Conference on Advanced Engineering Computing and Applications in Sciences, Papeete, Tahiti: New York, Electrical and Electronics Engineers, p. 39–48.

Anfinson, O.A., 2008, Sediment sources for catastrophic glacial outburst flood rhythmites and Quaternary eolian deposits at the Hanford Reach National Monument, Washington [M.S. thesis]: Pullman, Washington State University, 124 p.

Atwater, B.F., 1984, Periodic floods from glacial Lake Missoula into the Sanpoil arm of glacial Lake Columbia, northeastern Washington: Geology, v. 12, p. 464–467, doi:10.1130/0091-7613(1984)12<464:PFFGLM>2.0.CO;2.

Atwater, B.F., 1986, Pleistocene Glacial Lake Deposits of the Sanpoil River Valley, Northeastern Washington: U.S. Geological Survey Bulletin 1661, 39 p.

Atwater, B.F., 1987, Status of glacial Lake Columbia during the last floods from glacial Lake Missoula: Quaternary Research, v. 27, p. 182–201, doi:10.1016/0033-5894(87)90076-7.

Atwater, B.F., Smith, G.A., and Waitt, R.B., 2000, The channelled scabland: Back to Bretz?: Comment: Geology, v. 28, p. 574–575, doi:10.1130/0091-7613(2000)28<576:TCSBTB>2.0.CO;2.

Bacon, C.R., 1983, Eruptive history of Mount Mazama and Crater Lake caldera, Cascade Ranges, U.S.A.: Journal of Volcanology and Geothermal Research, v. 18, p. 57–115, doi:10.1016/0377-0273(83)90004-5.

Bagnold, R.A., 1941, The Physics of Blown Sand and Desert Dunes: London, Methuen and Co., 265 p.

Baker, V.R., 1973a, Paleohydrology and Sedimentology of Lake Missoula Flooding in Eastern Washington: Geological Society of America Special Paper 144, 79 p, doi:10.1130/SPE144-p1.

Baker, V.R., 1973b, Erosional forms and processes for the catastrophic Pleistocene Missoula floods in eastern Washington, *in* Morisawa, M., ed., Fluvial Geomorphology: London, Allen and Unwin, p. 123–148.

Baker, V.R., 1977, Lake Missoula flooding and the Channeled Scabland, *in* Brown, E.H., and Ellis, R.C., eds., Geologic Excursions in the Pacific Northwest: Bellingham, Washington, Western Washington University, p. 399–414.

Baker, V.R., 1978a, The Spokane Flood controversy and the Martian outflow channels: Science, v. 202, p. 1249–1256, doi:10.1126/science.202.4374.1249.

Baker, V.R., 1978b, Paleohydraulics and hydrodynamics of scabland floods, *in* Baker, V.R., and Nummedal, D., eds., The Channeled Scabland: Washington, D.C., National Aeronautics and Space Administration, p. 59–79.

Baker, V.R., 1978c, Large-scale erosional and depositional features of the Channeled Scabland, *in* Baker, V.R., and Nummedal, D., eds., The Channeled Scabland: Washington, D.C., National Aeronautics and Space Administration Planetary Geology Program, p. 81–115.

Baker, V.R., 1979, Erosional processes in channelized water flows on Mars: Journal of Geophysical Research, v. 84, p. 7985–7993, doi:10.1029/JB084iB14p07985.

Baker, V.R., 1982, The Channels of Mars: Austin, University of Texas Press, 198 p.

Baker, V.R., 1987a, Paleoflood hydrology and extraordinary flood events: Journal of Hydrology (Amsterdam), v. 96, p. 79–99, doi:10.1016/0022-1694(87)90145-4.

Baker, V.R., 1987b, Dry Falls of the Channeled Scabland, Washington, *in* Hill, M.L., ed., Cordilleran Section of the Geological Society of America: Boulder, Colorado, Geological Society of America, North American Geology, Geological Society of America Centennial Field Guide 1, p. 369–372.

Baker, V.R., 1989, The Grand Coulee and Dry Falls, *in* Breckenridge, R., ed., Glacial Lake Missoula and the Channeled Scabland: Guidebook for Field Trip T310, 28th International Geologic Congress: Washington, D.C., American Geophysical Union, p. 51–56.

Baker, V.R., 1994, Glacial to modern changes in global river fluxes, *in* Material Fluxes on the Surface of the Earth: Washington, D.C., National Academies Press, p. 86–98.

Baker, V.R., 1995, Joseph Thomas Pardee and the Spokane flood controversy: GSA Today, v. 5, no. 9, p. 169–173.

Baker, V.R., 1997, Megafloods and glaciation, *in* Martini, I.P., ed., Late Glacial and Postglacial Environmental Changes: Quaternary, Carboniferous-Permian and Proterozoic: Oxford, UK, Oxford University Press, p. 98–108.

Baker, V.R., 1998, Catastrophism and uniformitarianism: Logical roots and current relevance in geology, *in* Blundell, D.J., and Scott, A.C., eds., Lyell: The Past Is the Key to the Present: Geological Society, London, Special Publication, 143, p. 171–182, doi:10.1144/GSL.SP.1998.143.01.15.

Baker, V.R., 2001, Water and the Martian landscape: Nature, v. 412, p. 228–236, doi:10.1038/35084172.

Baker, V.R., 2002a, The study of superfloods: Science, v. 295, p. 2379–2380, doi:10.1126/science.1068448.

Baker, V.R., 2002b, High-energy megafloods: Planetary settings and sedimentary dynamics, *in* Martini, I.P., Baker, V.R., and Garzon, G., eds., Flood and Megaflood Processes and Deposits: Recent and Ancient Examples: International Association of Sedimentologists, Special Paper No. 32, p. 1–15, doi:10.1002/9781444304299.ch1.

Baker, V.R., 2007, Greatest floods—largest rivers, *in* Gupta, A., ed., Large Rivers: Geomorphology and Management: New York, Wiley, p. 65–74, doi:10.1002/9780470723722.ch5.

Baker, V.R., 2008a, The Spokane Flood debates: Historical background and philosophical perspective, *in* Grapes, R., Oldroyd, D., and Grigelis, A., eds., History of Geomorphology and Quaternary Geology: Geological Society, London, Special Publication 301, p. 33–50, doi:10.1144/SP301.3.

Baker, V.R., 2008b, Paleoflood hydrology: Origin, progress, prospects: Geomorphology, v. 101, p. 1–13, doi:10.1016/j.geomorph.2008.05.016.

Baker, V.R., 2009a, Overview of megaflooding: Earth and Mars, *in* Burr, D.M., Carling, P.A., and Baker, V.R., eds., Megaflooding on Earth and Mars: Cambridge, UK, Cambridge Press, p. 1–12, doi:10.1017/CBO9780511635632.001.

Baker, V.R., 2009b, Megafloods and global paleoenvironmental change on Mars and Earth, *in* Chapman, M.G., and Keszthelyi, L., eds., Preservation of Random Mega-Scale Events on Mars and Earth: Influence on Geologic History: Geological Society of America Special Paper 453, p. 25–36, doi:10.1130/2009.453(03).

Baker, V.R., 2009c, The Channeled Scabland: A retrospective: Annual Reviews of Earth and Planetary Sciences, v. 37, p. 6.1–6.19.

Baker, V.R., 2013, Global late Quaternary fluvial paleohydrology with special emphasis on paleofloods and megafloods, *in* Shroder, J., editor in chief, and Wohl, E.E., ed., Treatise on Geomorphology: Vol. 9, Fluvial Geomorphology: San Diego, California, Academic Press, p. 511–527.

Baker, V.R., and Bunker, R.C., 1985, Cataclysmic late Pleistocene flooding from glacial Lake Missoula: A review: Quaternary Science Reviews, v. 4, p. 1–41, doi:10.1016/0277-3791(85)90027-7.

Baker, V.R., and Costa, J.E., 1987, Flood power, *in* Mayer, L., and Nash, D., eds., Catastrophic Flooding: London, Allen and Unwin, p. 1–24.

Baker, V.R., and Komar, P.D., 1987, Cataclysmic flood processes and landforms, *in* Graf, W.L., ed., Geomorphic Systems of North America: Boulder, Colorado, Geological Society of America, Geology of North America, Centennial Special Volume 2, p. 423–443.

Baker, V.R., and Milton, D.J., 1974, Erosion by catastrophic floods on Mars and Earth: Icarus, v. 23, p. 27–41, doi:10.1016/0019-1035(74)90101-8.

Baker, V.R., and Nummedal, D., eds., 1978, The Channeled Scabland: Planetary Geology Program: Washington, D.C., National Aeronautics and Space Administration, 274 p.

Baker, V.R., and Pickup, G., 1987, Flood geomorphology of the Katherine Gorge, Northern Territory, Australia: Geological Society of America Bulletin, v. 98, p. 635–646, doi:10.1130/0016-7606(1987)98<635:FGOTKG>2.0.CO;2.

Baker, V.R., and Ritter, D.F., 1975, Competence of rivers to transport coarse bedload material: Geological Society of America Bulletin, v. 86, p. 975–978, doi:10.1130/0016-7606(1975)86<975:CORTTC>2.0.CO;2.

Baker, V.R., Bjornstad, B.N., Busacca, A.J., Fecht, K.R., Kiver, E.P., Moody, U.L., Rigby, J.G., Stradling, D.F., and Tallman, A.M., 1991a, The Columbia Plateau, Chapter 3, *in* Morrison, R.B., ed., Quaternary Nonglacial Geology; Conterminous U.S.: Boulder, Colorado, Geological Society of America, Geology of North America, v. K-2, p. 215–250.

Baker, V.R., Strom, R.G., Gulick, V.C., Kargel, J.S., Komatsu, G., and Kale, V.S., 1991b, Ancient oceans, ice sheets and the hydrological cycle on Mars: Nature, v. 352, p. 589–594, doi:10.1038/352589a0.

Baker, V.R., Benito, G., and Rudoy, A.N., 1993, Paleohydrology of late Pleistocene superflooding, Altai Mountains, Siberia: Science, v. 259, p. 348–350, doi:10.1126/science.259.5093.348.

Baker, V.R., Hamilton, C.W., Burr, D.M., Gulick, V., Komatsu, G., Luo, W., Rice, J.W., Jr., and Rodriguez, J.A.P., 2015, Fluvial geomorphology on earth-like planetary surfaces: A review: Geomorphology, v. 245, p. 149–182, doi:10.1016/j.geomorph.2015.05.002.

Barnosky, C.W., 1985, Late Quaternary vegetation in the southwestern Columbia Basin, Washington: Quaternary Research, v. 23, p. 109–122, doi:10.1016/0033-5894(85)90075-4.

Barnosky, C.W., Anderson, P.M., and Bartlein, P.J., 1987, The northwestern U.S. during deglaciation: Vegetational history and paleoclimatic implications, *in* Ruddiman, W.F., and Wright, H.E., Jr., eds., North America and Adjacent

Oceans during the Last Deglaciation: Boulder, Colorado, Geological Society of America, Geology of North America, v. K-3, p. 280–321.
Baulig, H., 1913, Les plateaux del lave du Washington central et la Grand 'Coulee': Annales de Geographie, v. 22, p. 149–159, doi:10.3406/geo.1913.8355.
Benito, G., 1997, Energy expenditure and geomorphic work of the cataclysmic Missoula flooding in the Columbia River Gorge, USA: Earth Surface Processes and Landforms, v. 22, p. 457–472.
Benito, G., and O'Connor, J.E., 2003, Number and size of last-glacial Missoula floods in the Columbia River valley between the Pasco Basin, Washington, and Portland, Oregon: Geological Society of America Bulletin, v. 115, p. 624–638, doi:10.1130/0016-7606(2003)115<0624:NASOLM>2.0.CO;2.
Berg, A.W., 1990, Formation of Mima mounds: A seismic hypothesis: Geology, v. 18, no. 3, p. 281–284, doi:10.1130/0091-7613(1990)018<0281:FOMMAS>2.3.CO;2.
Beverage, J.P., and Culbertson, J.K., 1964, Hyperconcentrations of suspended sediment: American Society of Civil Engineers, Proceedings: Hydraulics Division Journal, v. 90, no. HY6, p. 117–128.
Bjornstad, B.N., 1980, Sedimentology and Depositional Environment of the Touchet Beds, Walla Walla River Basin, Washington: Richland, Washington, Rockwell Hanford Operations, RHO-BWI-SA-44, 104 p.
Bjornstad, B.N., 2006a, On the Trail of the Ice Age Floods: A Geological Field Guide to the Mid-Columbia Basin: Sandpoint, Idaho, Keokee Co. Publishing, Inc., 307 p.
Bjornstad, B.N., 2006b, Past, Present, Future Erosion at Locke Island: Hanford Cultural Resources Project PNNL-15941: Richland, Washington, Pacific Northwest National Laboratory, 17 p.
Bjornstad, B.N., 2014, Ice-rafted erratics and bergmounds from Pleistocene outburst floods, Rattlesnake Mountain, Washington, USA: E&G Quaternary Science Journal, v. 63, no. 1, p. 44–59.
Bjornstad, B.N., and Kiver, E.P., 2012, On the Trail of the Ice Age Floods: The Northern Reaches: Sandpoint, Idaho, Keokee Co. Publishing, Inc., 432 p.
Bjornstad, B.N., Fecht, K.R., and Pluhar, C.J., 2001, Long history of pre-Wisconsin Ice Age floods: Evidence from southeastern Washington State: The Journal of Geology, v. 109, p. 695–713, doi:10.1086/323190.
Bjornstad, B.N., Babcock, R.S., and Last, G.V., 2007, Flood basalts and Ice Age floods: Repeated late Cenozoic cataclysms of southeastern Washington, *in* Stelling, P., and Tucker, D.S., eds., Floods, Faults, and Fire: Geological Field Trips in Washington State and Southwest British Columbia: Geological Society of America Field Guide 9, p. 209–255, doi:10.1130/2007.fld009(10).
Breckenridge, R.M., and Othberg, K.L., 1998, Surficial Geologic Map of the Rathdrum Quadrangle and Part of the Newman Lake Quadrangle, Kootenai County, Idaho: Idaho Geological Survey Surficial Geology Map 6, scale 1:24,000, 1 sheet.
Bretz, J H., 1923, The Channeled Scabland of the Columbia Plateau: The Journal of Geology, v. 31, p. 617–649, doi:10.1086/623053.
Bretz, J H., 1924, The Dalles type of river channel: The Journal of Geology, v. 32, p. 139–149, doi:10.1086/623074.
Bretz, J H., 1925, The Spokane Flood beyond the channeled scablands: The Journal of Geology, v. 33, p. 97–115, 236–259, doi:10.1086/623179.
Bretz, J H., 1927, What caused the Spokane Flood?: Geological Society of America Bulletin, v. 38, p. 107.
Bretz, J H., 1928, Channeled Scabland of eastern Washington: Geographical Review, v. 18, p. 446–477, doi:10.2307/208027.
Bretz, J H., 1929, Valley deposits immediately east of the Channeled Scabland of Washington: The Journal of Geology, v. 37, p. 393–427, 505–554, doi:10.1086/623636.
Bretz, J H., 1930a, Lake Missoula and the Spokane Flood: Geological Society of America Bulletin, v. 41, p. 92–93.
Bretz, J H., 1930b, Valley deposits immediately west of the Channeled Scabland: The Journal of Geology, v. 38, p. 385–422, doi:10.1086/623737.
Bretz, J H., 1932, The Grand Coulee: American Geographical Society Special Publication 15, 89 p.
Bretz, J H., 1959, Washington's Channeled Scabland: Washington Division of Mines and Geology Bulletin 45, 57 p.
Bretz, J H., 1969, The Lake Missoula floods and the Channeled Scabland: The Journal of Geology, v. 77, p. 505–543, doi:10.1086/627452.
Bretz, J H., 1980, Presentation of the Penrose Medal to J Harlen Bretz: Response: Geological Society of America Bulletin, Part II, v. 91, p. 1095, doi:10.1130/GSAB-P2-91-1091.
Bretz, J H., Smith, H.T.U., and Neff, G.E., 1956, Channeled Scabland of Washington: New data and interpretations: Geological Society of America Bulletin, v. 67, p. 957–1049, doi:10.1130/0016-7606(1956)67[957:CSOWND]2.0.CO;2.
Brown, K., McIntosh, J.C., Baker, V.R., and Gosch, D., 2010, Isotopically-depleted late Pleistocene groundwater in Columbia River Basalt aquifers: Evidence for recharge of Glacial Lake Missoula floodwaters?: Geophysical Research Letters, v. 37, L21402, doi:10.1029/2010GL044992.
Bunker, R.C., 1982, Evidence for multiple late-Wisconsin floods from glacial Lake Missoula in Badger Coulee, Washington: Quaternary Research, v. 18, p. 17–31, doi:10.1016/0033-5894(82)90019-9.
Burr, D.M., Caring, P.A., and Baker, V.R., eds., 2009, Megaflooding on Earth and Mars: Cambridge, UK, Cambridge University Press, 319 p.
Busacca, A.J., 1989, Long Quaternary record in eastern Washington, U.S.A. interpreted from multiple buried paleosols in loess: Geoderma, v. 45, p. 105–122, doi:10.1016/0016-7061(89)90045-1.
Busacca, A.J., 1991, Loess deposits and soils of the Palouse and vicinity, *in* Baker, V.R., Bjornstad, B.N., Busacca, A.J., Fecht, K.R., Kiver, E.P., Moody, U.L., Rigby, J.G., Stradling, D.F., and Tallman, A.M., The Columbia Plateau, Ch. 8, *in* Morrison, R.B., ed., Quaternary Non-Glacial Geology of the United States: Boulder, Colorado, Geological Society of America, Geology of North America, K-2, p. 216–228.
Calkins, F.C., 1905, Geology and Water Resources of a Portion of East-Central Washington: U.S. Geological Survey Water-Supply Paper 118, 96 p.
Carling, P.A., 1999, Subaqueous gravel dunes: Journal of Sedimentary Research, v. 69, p. 534–545, doi:10.2110/jsr.69.534.
Carling, P.A., Kirkbride, A.D., Parnachov, S., Borodavko, P.S., and Berger, G.W., 2002, Late Quaternary catastrophic flooding in the Altai Mountains of south-central Siberia: A synoptic overview and introduction to flood deposit sedimentology, *in* Martini, I.P., Baker, V.R., and Garzon, G., eds., Flood and Megaflood Processes and Deposits: Recent and Ancient Examples: Association of Sedimentology Special Publication 32, p. 17–35, doi:10.1002/9781444304299.ch2.
Carrara, P.E., Kiver, E.P., and Stradling, D.F., 1996, The southern limit of Cordilleran ice in the Colville and Pend Oreille valleys of northeastern Washington during the late Wisconsin glaciation: Canadian Journal of Earth Sciences, v. 33, p. 769–778, doi:10.1139/e96-059.
Chambers, R.L., 1971, Sedimentation in glacial Lake Missoula [M.S. thesis]: Missoula, University of Montana, 100 p.
Chambers, R.L., 1984, Sedimentary evidence for multiple glacial lakes Missoula, *in* McBane, J.D., and Garrison, P.B., eds., Northwest Montana and Adjacent Canada: Billings, Montana Geological Society, p. 189–199.
Chatters, J.C., and Hoover, K.A., 1992, Response of the Columbia River fluvial system to Holocene climate change: Quaternary Research, v. 37, p. 42–59, doi:10.1016/0033-5894(92)90005-4.
Chepil, W.S., 1945a, Dynamics of wind erosion: I. Nature of movement of soil by wind: Soil Science, v. 60, p. 305–320, doi:10.1097/00010694-194510000-00004.
Chepil, W.S., 1945b, Dynamics of wind erosion: II. Initiation of soil movement: Soil Science, v. 60, p. 397–411, doi:10.1097/00010694-194511000-00005.
Clague, J.J., 1980, Late Quaternary Geology and Geochronology of British Columbia—Part 1, Radiocarbon Dates: Geological Survey of Canada Paper 80–13, 28 p., doi:10.4095/106640.
Clague, J.J., Barendregt, R., Enkin, R.J., and Foit, F.F., Jr., 2003, Paleomagnetic and tephra evidence for tens of Missoula floods in southern Washington: Geology, v. 31, p. 247–250, doi:10.1130/0091-7613(2003)031<0247:PATEFT>2.0.CO;2.
Clarke, G.K.C., Mathews, W.H., and Pack, R.T., 1984, Outburst floods from glacial Lake Missoula: Quaternary Research, v. 22, p. 289–299, doi:10.1016/0033-5894(84)90023-1.
Clynne, M.A., Calvert, A.T., Wolfe, E.W., Evarts, R.C., Fleck, R.J., and Lanphere, M.A., 2008, The Pleistocene eruptive history of Mount St. Helens, Washington, from 300,000 to 12,800 years before present: U.S. Geological Survey Professional Paper 1750, p. 593–627.
Costa, J.E., 1988, Rheologic, geomorphic, and sedimentologic differentiation of water floods, hyperconcentrated flows, and debris flows, *in* Baker, V.R., Kochel, R.C., and Patton, P.C., eds., Flood Geomorphology: New York, John Wiley and Sons, p. 113–122.
Craig, R.G., 1987, Dynamics of a Missoula flood, *in* Mayer, L., and Nash, D., eds., Catastrophic Flooding: London, Allen & Unwin, p. 305–332.
Curry, A., 2012, Coming to America: Nature, v. 285, p. 30–32.
Dalman, K.A., 2007, Timing, distribution, and climatic implications of Late Quaternary eolian deposition: Northern Columbia Plateau, Washington [M.S. thesis]: Pullman, Washington State University, 132 p.
Dawson, W.L., 1898, Glacial phenomena in Okanogan County, Washington: American Geologist, v. 22, p. 203–217.

Denlinger, R.P., and O'Connell, D.R.H., 2010, Simulations of cataclysmic outburst floods from Pleistocene glacial Lake Missoula: Geological Society of America Bulletin, v. 122, p. 678–689, doi:10.1130/B26454.1.

Department of Energy (DOE), 1988, Consultation Draft: Site Characterization Plan, Reference Repository Location, Hanford Site, Washington, DOE/RW-0164, Volume 1: Washington, D.C., U.S. Department of Energy, 644 p.

Department of Energy (DOE), 2002, Standardized Stratigraphic Nomenclature for Post-Ringold Formation Sediments within the Central Pasco Basin: Richland, Washington: U.S. Department of Energy, Richland Office, DOE/RL-2002–39.

Desilets, D., Zreda, M., Almasi, P.F., and Elmore, D., 2006a, Determination of cosmogenic ^{36}Cl in rocks by isotope dilution: Innovations, validation and error propagation: Chemical Geology, v. 233, p. 185–195, doi:10.1016/j.chemgeo.2006.03.001.

Desilets, D., Zreda, M., and Prabu, T., 2006b, Extended scaling factors for in situ cosmogenic nuclides: New measurements at low latitude: Earth and Planetary Science Letters, v. 246, p. 265–276, doi:10.1016/j.epsl.2006.03.051.

Droser, M.L., and Bottjer, D.J., 1986, A semiquantitative field classification of ichnofabric: Journal of Sedimentary Petrology, v. 56, p. 558–559, doi:10.1306/212F89C2-2B24-11D7-8648000102C1865D.

Dury, G.H., 1965, Theoretical Implication of Underfit Streams: U.S. Geological Survey Paper 452-C, 43 p.

Edgett, K.S., Rice, J.W., and Baker, V.R., eds., 1995, Field trips accompanying the Mars Pathfinder landing site workshop II—Channeled Scabland and Lake Missoula break-out areas in Washington and Idaho, *in* Golombek, M.P., Edgett, K.S., and Rice, J.W., eds., Mars Pathfinder Landing Site Workshop II—Characteristics of the Ares Vallis Region and Field Trips in the Channeled Scabland, Washington: Lunar and Planetary Institute Technical Report 95-01, Part 1, p. 31–63.

Ely, L.L., and Baker, V.R., 1985, Reconstructing paleoflood hydrology with slackwater deposits, Verde River, Arizona: Physical Geography, v. 6, p. 103–126.

Fecht, K.R., 1978, Geology of Gable Mountain: Richland, Washington, Rockwell Hanford Operations, RHO-BWI-LD-5, 70 p.

Fecht, K.R., Marceau, T.E., Bjornstad, B.N., Horton, D.G., Last, G.V., Peterson, R.E., Reidel, S.P., and Valenta, M.M., 2004, Late Pleistocene and Holocene-Age Columbia River Sediments and Bedforms: Hanford Reach Area, Washington, Part 1: Richland, Washington, Bechtel Hanford, Inc., BHI-01648, Rev. 0.

Foley, L.L., 1976, Slack water sediments in the Alpowa Creek drainage, Washington [M.S. thesis]: Pullman, Washington State University, 55 p.

Fryxell, R., 1965, Mazama and Glacier Peak volcanic ash layers: Relative ages: Science, v. 147, p. 1288–1290, doi:10.1126/science.147.3663.1288.

Fuller, R.E., 1932, Tensional surface features of certain basaltic ellipsoids: The Journal of Geology, v. 40, p. 164–170, doi:10.1086/623931.

Gaylord, D.R., and Stetler, L.D., 1994, Eolian-climatic thresholds and sand dunes at the Hanford Site, south-central Washington, USA: Journal of Arid Environments, v. 28, p. 95–116, doi:10.1016/S0140-1963(05)80041-2.

Gaylord, D.R., Foit, F.F., Jr., Schatz, J.K., and Huckleberry, G., 1999, The Sand Hills Coulee dune field, southeastern Washington: Sedimentary and stratigraphic evidence for Late Pleistocene and Holocene eolian-climatic activity: Geological Society of America Abstracts with Programs, v. 31, no. 7, p. 54.

Gaylord, D.R., Foit, F.F., Jr., Schatz, J.K., and Coleman, A.J., 2001, Smith Canyon dune field, Washington, U.S.A.: Relation to glacial outburst floods, the Mazama eruption, and Holocene paleoclimate: Journal of Arid Environments, v. 47, p. 403–424, doi:10.1006/jare.2000.0731.

Gaylord, D.R., Sweeney, M.R., and Busacca, A.J., 2002, Geomorphic development of a late Quaternary paired eolian sequence, Columbia Plateau, Washington: Geological Society of America Abstracts with Programs, v. 34, no. 6, p. 245.

Gaylord, D.R., Busacca, A.J., and Sweeney, M.R., 2003, The Palouse loess and the Channeled Scabland: A paired Ice-Age geologic system, *in* Easterbrook, D.J., ed., Quaternary Geology of the United States: INQUA 2003 Field Guide Volume: Reno, Nevada, Desert Research Institute, p. 123–134.

Gaylord, D.R., Sweeney, M.R., and Busacca, A.J., 2004, Post-LGM eolian history of the northern Columbia Plateau, Washington and relation to glacial outburst flooding: Geological Society of America Abstracts with Programs, v. 36, no. 5, p. 68.

Gaylord, D.R., Pope, M.C., Cabbage, P.R., Glover, J.F., III, Anfinson, O.A., Baar, E.E., and Vervoort, J.D., 2007, Provenance of glacial outburst flood deposits in the Channeled Scabland, WA: Influence of glacial Lake Missoula meltwater, Snake River, and Bonneville Flood sources: Geological Society of America Abstracts with Programs, v. 39, no. 6, p. 82.

Gaylord, D.R., Foit, F.F., Jr., and Anfinson, O., 2011, Tephrochronology of late Pleistocene and Holocene sand dune deposits, Hanford Reach National Monument, WA: Geological Society of America Abstracts with Programs, v. 43, no. 5, p. 272.

Gaylord, D.R., Sweeney, M., Foit, F.F., Jr., McDonald, E.V., and Roberts, H.M., 2014, Overview of the geomorphic, sedimentary, stratigraphic, and paleoclimate history of sand-dominated Quaternary eolian deposits on the Columbia Plateau, WA: Geological Society of America Abstracts with Programs, v. 46, no. 6, p. 591.

Gillette, D.A., Blifford, I.H., and Fryrear, D.W., 1974, The influence of wind velocity on the size distributions of aerosols generated by the wind erosion of soils: Journal of Geophysical Research, v. 79, p. 4068–4075, doi:10.1029/JC079i027p04068.

Glenn, J.L., 1965, Late Quaternary sedimentation and geologic history of the North Willamette Valley, Oregon [Ph.D. thesis]: Corvallis, Oregon, Oregon State University, 231 p.

Gosse, J.C., and Phillips, F.M., 2001, Terrestrial in situ cosmogenic nuclides: Theory and application: Quaternary Science Reviews, v. 20, p. 1475–1560, doi:10.1016/S0277-3791(00)00171-2.

Grolier, M.J., and Bingham, J.W., 1978, Geology of Parts of Grant, Adams, and Franklin Counties, East-Central Washington: Washington Department of Natural Resources, Division of Geology and Earth Resources Bulletin 71, 91 p.

Grosswald, M.G., 1998, New approach to the ice age paleohydrology of northern Eurasia, *in* Benito, G., Baker, V.R., and Gregory, K.J., eds., Palaeohydrology and Environmental Change: New York, John Wiley & Sons, p. 199–214.

Grosswald, M.G., 1999, Cataclysmic Megafloods in Eurasia and the Polar Ice Sheets: An Essay in Geomorphological Analysis of Continental Paleohydrological Systems: Moscow, Scientific World, 120 p. [in Russian].

Grotzinger, J.P., Arvidson, R.E., Bell, J.F., III, Calvin, W., Clark, B.C., Fike, D.A., Golombek, M., Greeley, R., Haldermann, A., Herkenhoff, K.E., Joliff, B.L., Knoll, A.H., McLennan, S.M., Parker, T., Soderblom, L., Sohl-Dickstein, J.N., Squyres, S.W., Tosca, N.J., and Waters, W.A., 2005, Stratigraphy and sedimentology of a dry to wet eolian depositional system, Burns Formation, Meridiani Planum, Mars: Earth and Planetary Science Letters, v. 240, p. 11–72.

Gupta, S., Collier, J.S., Palmer-Felgate, A., and Potter, G., 2007, Catastrophic flooding origin of shelf valley systems in the English Channel: Nature, v. 448, p. 342–345, doi:10.1038/nature06018.

Hallett, D.J., Hills, L.V., and Clague, J.J., 1997, New accelerator mass spectrometry radiocarbon ages for the Mazama tephra layer from Kootenay National Park, British Columbia, Canada: Canadian Journal of Earth Sciences, v. 39, p. 1202–1209.

Hammatt, H.H., 1977, Late Quaternary stratigraphy and archaeological chronology of the lower Granite Reservoir area, lower Snake River, Washington [Ph.D. thesis]: Pullman, Washington, Washington State University, 272 p.

Hanson, M.A., and Clague, J.J., 2016, Record of glacial Lake Missoula flood in glacial Lake Columbia, Washington: Quaternary Science Reviews, v. 133, p. 62–76, doi:10.1016/j.quascirev.2015.12.009.

Hanson, M.A., Lian, O.B., and Clague, J.J., 2012, The sequence and timing of large late Pleistocene floods from glacial Lake Missoula: Quaternary Science Reviews, v. 31, p. 67–81, doi:10.1016/j.quascirev.2011.11.009.

Hays, W.H., and Schuster, R.L., 1987, Maps Showing Ground Failure Hazards in the Columbia River Valley between Richland and Priest Rapids Dam, South-Central Washington: Reston, Virginia, U.S. Geological Survey Miscellaneous Investigation Series Map I-1699, scale 1:100,000.

Hendy, I., 2009, A fresh perspective on the Cordilleran Ice Sheet: Geology, v. 37, p. 95–96, doi:10.1130/focus012009.1.

Hendy, I.L., Taylor, M., Gombiner, J.H., Hemming, S.R., Bryce, J.G., and Blichert-Toft, J., 2014, Cordilleran Ice Sheet meltwater delivery to the coastal waters of the northeast Pacific Ocean: Abstract #PP13B-1417 presented at 2014 Fall Meeting, AGU, San Francisco, California, 15–19 December.

Hickson, C.J., and Vigouroux, N., 2014, Volcanism and glacial interaction in the Wells Gray–Clearwater volcanic field, east-central British Columbia, *in* Dashtgard, S., and Ward, B., eds., Trials and Tribulations of Life on an Active Subduction Zone: Field Trips in and around Vancouver, Canada: Geological Society of America Field Guide 38, p. 169–191, doi:10.1130/2014.0038(08).

Hodges, C.A., 1978, Basaltic ring structures of the Columbia Plateau: Geological Society of America Bulletin, v. 89, p. 1281–1289, doi:10.1130/0016-7606(1978)89<1281:BRSOTC>2.0.CO;2.

Hooper, P.R., 1997, The Columbia River Flood Basalt Province: Current status, *in* Mahoney, J.J., and Coffin, M., eds., Large Igneous Provinces: Conti-

nental, Oceanic, and Planetary Flood Volcanism: American Geophysical Union Geophysical Monograph 100, p. 1–27, doi:10.1029/GM100p0001.
Hunter, R.E., 1977, Terminology of cross-stratified sedimentary layers and climbing-ripple structures: Journal of Sedimentary Petrology, v. 47, p. 697–706.
Ivy-Ochs, S., Schlüchter, C., Kubik, P.W., Synal, H.A., Beer, J., and Kerschner, H., 1996, The exposure age of an Egesen moraine at Julier Pass, Switzerland, measured with the cosmogenic radionuclides: Eclogae Geologicae Helvetiae, v. 89, p. 1049–1063.
Jaeger, W.L., Keszthelyi, L.P., Burr, D.M., McEwen, A.S., Baker, V.R., Miyamoto, H., and Beyer, R.A., 2003, Ring dike structures in the Channeled Scabland as analogs for circular features in Athabasca Valles, Mars: Lunar and Planetary Science Conference XXXIV, abstract #2045.
Joseph, N.L., 1990, Geologic Map of the Spokane 1:100,000 Quadrangle, Washington-Idaho: Washington Division of Geology and Earth Resources Open File Report 90-17, 1 sheet.
Keszthelyi, L., and Jaeger, W., 2015, A field investigation of the basaltic ring structures of the Channeled Scabland and the relevance to Mars: Geomorphology, v. 240, p. 34–43, doi:10.1016/j.geomorph.2014.06.027.
Keszthelyi, L., Thordarson, Th., McEwen, A., Haack, H., Guilbaud, M.-N., Self, S., and Rossi, M., 2004, Icelandic analogs to martian flood lavas: Geochemistry Geophysics Geosystems, v. 5, doi:10.1029/2004GC000758.
Keszthelyi, L., Self, S., and Thordarson, Th., 2006, Flood lavas on Earth, Io, and Mars: Journal of the Geological Society, London, v. 163, p. 253–264, doi:10.1144/0016-764904-503.
Keszthelyi, L.P., Baker, V.R., Jaeger, W.L., Gaylord, D.R., Bjornstad, B.N., Greenbaum, N., Self, S., Thordarson, Th., Porat, N., and Zreda, M.G., 2009, Floods of water and lava in the Columbia River Basin: Analogs for Mars, *in* O'Connor, J.E., Dorsey, R.J., and Madin, I.P., eds., Volcanoes to Vineyards: Geologic Field Trips through the Dynamic Landscape of the Pacific Northwest: Geological Society of America Field Guide 15, p. 845–874, doi:10.1130/2009.fld015(34).
Kiver, E.P., and Stradling, D.F., 1982, Quaternary geology of the Spokane area, *in* Roberts, S., and Fountain, D., eds., 1980 Field Conference Guidebook: Tobacco Root Geological Society, p. 26–44.
Kiver, E.P., Moody, U.L., Rigby, J.G., and Stradling, D.F., 1991, Late Quaternary stratigraphy of the Channeled Scabland and adjacent areas, *in* Baker, V.R., Bjornstad, B.N., Busacca, A.J., Fecht, K.R., Kiver, E.P., Moody, U.L., Rigby, J.G., Stradling, D.F., and Tallman, A.M., authors, Quaternary Geology of the Columbia Plateau, *in* Morrison, R.G., ed., Quaternary Nonglacial Geology; Conterminous U.S.: Boulder, Colorado, Geological Society of America, Geology of North America, v. K-2, p. 238–250.
Kocurek, G., and Dott, R.H., 1981, Distinctions and uses of stratification types in the interpretation of eolian sands: Journal of Sedimentary Petrology, v. 51, p. 579–595.
Komar, P.D., 1980, Modes of sediment transport in channelized flows with ramifications to the erosion of Martian outflow channels: Icarus, v. 42, p. 317–329, doi:10.1016/0019-1035(80)90097-4.
Komar, P.D., 1983, Shape of streamlined islands on Earth and Mars: Experiments and analyses of the minimum drag form: Geology, v. 11, p. 651–654, doi:10.1130/0091-7613(1983)11<651:SOSIOE>2.0.CO;2.
Komar, P.D., 1984, The lemniscate loop-comparisons with the shapes of streamlined landforms: The Journal of Geology, v. 92, p. 133–145, doi:10.1086/628844.
Komar, P.D., 1988, Sediment transport by floods, *in* Baker, V.R., Kochel, R.C., and Patton, P.C., eds., Flood Geomorphology: New York, John Wiley and Sons, p. 97–111.
Kneller, B., and McCaffrey, W., 1999, Depositional effects of flow nonuniformity and stratification within turbidity currents approaching a bounding slope: Deflection, reflection, and facies variation: Journal of Sedimentary Research, v. 69, p. 980–991, doi:10.2110/jsr.69.980.
Komatsu, G., and Baker, V.R., 1997, Paleohydrology and flood geomorphology of Ares Vallis, Mars: Journal of Geophysical Research, v. 102, p. 4151–4160, doi:10.1029/96JE02564.
Komatsu, G., Miyamoto, H., Ito, K., Tosaka, H., and Tokunaga, T., 2000, Back to Bretz?: Comment: Geology, v. 28, p. 573–574, doi:10.1130/0091-7613(2000)28<573:TCSBTB>2.0.CO;2.
Komatsu, G., Arzhannikov, S.G., Gillespie, A.R., Burke, R.M., Miyamoto, H., and Baker, V.R., 2009, Quaternary paleolake formation and cataclysmic flooding along the upper Yenisei River: Geomorphology, v. 104, p. 143–164, doi:10.1016/j.geomorph.2008.08.009.
Komatsu, G., Baker, V.R., Arzhannikov, S.G., Gallagher, R., Arzhannikov, A.V., Murana, A., and Oguchi, T., 2015, Late Quaternary catastrophic flooding related to drainage reorganization and paleolake formation in northern Eurasia: A history of alternative hypotheses and indications for future research: International Geology Review, doi:10.1080/00206814.2015.1048314.
Kovanen, D.J., and Slaymaker, O., 2004, Glacial imprints of the Okanogan Lobe, southern margin of the Cordilleran Ice Sheet: Journal of Quaternary Science, v. 19, p. 547–565, doi:10.1002/jqs.855.
Kuehn, S.C., Froese, D.G., Carrara, P.E., Foit, F.F., Jr., Pearce, N.J.G., and Rotheisler, P., 2009, Major and trace-element characterization, expanded distribution, and a new chronology for the latest Pleistocene Glacier Peak tephras in western North America: Quaternary Research, v. 71, p. 201–216, doi:10.1016/j.yqres.2008.11.003.
Landye, J.J., 1973, Environmental significance of late Quaternary non-marine mollusks from former Lake Bretz, lower Grand Coulee, Washington [M.A. thesis]: Pullman, Washington State University, 117 p.
Lesemann, J.-E., and Brennand, T.A., 2009, Regional reconstruction of subglacial hydrology and glaciodynamic behavior along the southern margin of the Cordilleran Ice Sheet in British Columbia, Canada and northern Washington State, USA: Quaternary Science Reviews, v. 28, p. 2420–2444, doi:10.1016/j.quascirev.2009.04.019.
Levish, D.R., 1997, Late Pleistocene sedimentation in glacial Lake Missoula and revised glacial history of the Flathead Lobe of the Cordilleran Ice Sheet, Mission valley, Montana [Ph.D. diss.]: Boulder, University of Colorado, 191 p.
Lewis, S., 1985, The Corfu landslide: A large-scale prehistoric compound-complex slide in south-central Washington [M.S. thesis]: Tucson, University of Arizona, 48 p.
Lifton, N., Caffee, M., Finkel, R., Marrero, S., Nishizumi, K., Phillips, F.M., Goehring, B., Gosse, J., Stone, J., Schaefer, J., Theriault, B., Jull, A.J., and Fifield, K., 2015, *In situ* nuclide production rate calibration for the CRONUS-Earth project from Lake Bonneville, Utah, shoreline features: Quaternary Geochronology, v. 26, p. 56–69.
Lindsey, K.A., 1996, The Miocene to Pliocene Ringold Formation and Associated Deposits of the Ancestral Columbia River System, South-Central Washington and North-Central Oregon: Olympia, Washington, Washington State Department of Natural Resources Open File Report 96-8, 45 p.
Lindsey, K.A., and Gaylord, D.R., 1990, Lithofacies and sedimentology of the Miocene-Pliocene Ringold Formation, Hanford Site, south-central Washington: Northwest Science, v. 64, p. 165–180.
Livingstone, S.J., Clark, C.D., Piotrowski, J.A., Tranter, M., Bentley, M.J., Hodson, A., Swift, D.A., and Woodward, J., 2012, Theoretical framework and diagnostic criteria for the identification of palaeo-subglacial lakes: Quaternary Science Reviews, v. 53, p. 88–110, doi:10.1016/j.quascirev.2012.08.010.
Livingstone, S.J., Clark, C.D., and Tarasov, L., 2013, Modelling North American palaeo-subglacial lakes and their meltwater drainage pathways: Earth and Planetary Science Letters, v. 375, p. 13–33, doi:10.1016/j.epsl.2013.04.017.
Long, P.E., and Wood, B.J., 1986, Structures, textures, and cooling histories of Columbia River basalt flows: Geological Society of America Bulletin, v. 97, p. 1144–1155, doi:10.1130/0016-7606(1986)97<1144:STACHO>2.0.CO;2.
Lopes, C., and Mix, A.C., 2009, Pleistocene megafloods in the northeast Pacific: Geology, v. 37, p. 79–82, doi:10.1130/G25025A.1.
Lord, M.L., and Kehew, A.E., 1987, Sedimentology and paleohydrology of glacial-lake outburst deposits in southeastern Saskatchewan and northwestern North Dakota: Geological Society of America Bulletin, v. 99, p. 663–673, doi:10.1130/0016-7606(1987)99<663:SAPOGO>2.0.CO;2.
Lowe, D.R., 1982, Sedimentary gravity flows: II. Depositional models with special reference to the deposits of high-density turbidity currents: Journal of Sedimentary Petrology, v. 52, p. 279–297.
Lowe, D.R., 1988, Suspend-load fallout rate as an independent variable in the analysis of current structures: Sedimentology, v. 35, p. 765–776, doi:10.1111/j.1365-3091.1988.tb01250.x.
Lowe, D.J., Green, J.D., Northcote, T.G., and Hall, K.J., 1997, Holocene fluctuations of a meromictic lake in southern British Columbia: Quaternary Research, v. 48, p. 100–113, doi:10.1006/qres.1997.1905.
Maizels, J.K., 1989, Sedimentology, paleoflow dynamics and flood history of jökulhlaup deposits: Paleohydrology of Holocene sediment sequences in southern Iceland sandur deposits: Journal of Sedimentary Petrology, v. 59, p. 204–223.
Malde, H.E., 1968, The Catastrophic Late Pleistocene Bonneville Flood in the Snake River Plain, Idaho: U.S. Geological Survey Professional Paper 596, 52 p.
Mason, J.A., Nter, E.A., Zanner, C.W., and Bell, J.C., 1999, A new model of topographic effects in the distribution of loess: Geomorphology, v. 28, p. 223–236, doi:10.1016/S0169-555X(98)00112-3.

McDonald, E.V., and Busacca, A.J., 1988, Record of pre-late Wisconsin giant floods in the Channeled Scabland interpreted from loess deposits: Geology, v. 16, p. 728–731, doi:10.1130/0091-7613(1988)016<0728:ROPLWG>2.3.CO;2.

McDonald, E.V., and Busacca, A.J., 1992, Late Quaternary stratigraphy of loess in the Channeled Scabland and Palouse regions of Washington State: Quaternary Research, v. 38, p. 141–156, doi:10.1016/0033-5894(92)90052-K.

McDonald, E.V., Sweeney, M.R., and Busacca, A.J., 2012, Glacial outburst floods and loess sedimentation documented during Oxygen Isotope Stage 4 on the Columbia Plateau, Washington State: Quaternary Science Reviews, v. 45, p. 18–30, doi:10.1016/j.quascirev.2012.03.016.

McGee, S.L., and Phillips, F.M., 2005, Comparison of chlorine-36 production rates using the radiocarbon-age-constrained Lake Bonneville shoreline, Utah: American Geophysical Union, Fall Meeting 2005, abstract #U33A-0005.

McKee, B., and Stradling, D., 1970, The sag flowout: A newly described volcanic structure: Geological Society of America Bulletin, v. 81, p. 2035–2044, doi:10.1130/0016-7606(1970)81[2035:TSFAND]2.0.CO;2.

Medley, E., 2012, Ancient cataclysmic floods in the Pacific Northwest: Ancestors to the Missoula floods [M.S. thesis]: Portland, Oregon, Portland State University, 174 p.

Meinzer, O.E., 1918, The glacial history of the Columbia River in the Big Bend Region: Washington Academy of Science Journal, v. 8, p. 411–412.

Meyer, S.E., 1999, Depositional history of pre-late and late Wisconsin outburst flood deposits in northern Washington and Idaho: Analysis of flood paths and provenance [M.S. thesis]: Pullman, Washington, Washington State University, 91 p.

Miyamoto, H., Itoh, K., Komatsu, G., Baker, V.R., Dohm, J.M., Tosaka, H., and Sasaki, S., 2006, Numerical simulations of large-scale cataclysmic floodwater: A simple depth-averaged model and an illustrative application: Geomorphology, v. 76, p. 179–192, doi:10.1016/j.geomorph.2005.11.002.

Miyamoto, H., Komatsu, G., Baker, V.R., Dohm, J.M., Ito, K., and Tosaka, H., 2007, Cataclysmic scabland flooding: Insights from a simple depth-averaged numerical model: Environmental Modelling & Software, v. 22, no. 10, special issue, p. 1400–1408, doi:10.1016/j.envsoft.2006.07.006.

Mullineaux, D.R., Wilcox, R.E., Ebaugh, S.F., Fryxell, R., and Rubin, M., 1978, Age of the last major scabland flood of the Columbia Plateau in eastern Washington: Quaternary Research, v. 10, p. 171–180, doi:10.1016/0033-5894(78)90099-6.

Neff, G.E., 1989, Columbia Basin Project, *in* Engineering Geology in Washington, Volume I: Washington Division of Geology and Earth Resources Bulletin 78, p. 535–564.

Normark, W.R., and Reid, J.A., 2003, Extensive deposits on the Pacific Plate from late Pleistocene North American glacial lake bursts: The Journal of Geology, v. 111, p. 617–637, doi:10.1086/378334.

O'Connor, J.E., 1993, Hydrology, Hydraulics and Sediment Transport of Pleistocene Lake Bonneville Flooding on the Snake River, Idaho: Geological Society of America Special Paper 274, 83 p.

O'Connor, J.E., and Baker, V.R., 1992, Magnitudes and implications of peak discharges from glacial Lake Missoula: Geological Society of America Bulletin, v. 104, p. 267–279, doi:10.1130/0016-7606(1992)104<0267:MAIOPD>2.3.CO;2.

O'Geen, A.T., and Busacca, A.J., 2001, Faunal burrows as indicators of paleo-vegetation in eastern Washington, USA: Palaeogeography, Palaeoclimatology, Palaeoecology, v. 169, p. 23–37, doi:10.1016/S0031-0182(01)00213-9.

Oestreich, K., 1915, Die Grand Coulée, *in* American Geographical Society Memorial Volume of the Transcontinental Excursion of 1912: American Geographical Society Special Publications 1, p. 259–273.

Olmsted, R.K., 1963, Silt mounds of Missoula flood surfaces: Geological Society of America Bulletin, v. 74, p. 47–54, doi:10.1130/0016-7606(1963)74[47:SMOMFS]2.0.CO;2.

Oviatt, C.B., 2015, Chronology of Lake Bonneville, 30,000 to 10,000 yr B.P.: Quaternary Science Reviews, v. 110, p. 166–171, doi:10.1016/j.quascirev.2014.12.016.

Pardee, J.T., 1910, The glacial Lake Missoula, Montana: The Journal of Geology, v. 18, p. 376–386, doi:10.1086/621747.

Pardee, J.T., 1922, Glaciation in the Cordilleran region: Science, v. 56, p. 686–687, doi:10.1126/science.56.1459.686-a.

Pardee, J.T., 1942, Unusual currents in glacial Lake Missoula: Geological Society of America Bulletin, v. 53, p. 1569–1600, doi:10.1130/GSAB-53-1569.

Parker, S., 1838, Journal of an Exploring Tour beyond the Rocky Mountains: Privately published, Albany, New York.

Patton, P.C., and Baker, V.R., 1978a, New evidence for pre-Wisconsin flooding in the Channeled Scabland of eastern Washington: Geology, v. 6, p. 567–571, doi:10.1130/0091-7613(1978)6<567:NEFPFI>2.0.CO;2.

Patton, P.C., and Baker, V.R., 1978b, Origin of the Cheney-Palouse scabland tract, *in* Baker, V.R., and Nummedal, D., eds., The Channeled Scabland: Washington, D.C., National Aeronautics and Space Administration Planetary Geology Program, p. 117–130.

Patton, P.C., Baker, V.R., and Kochel, R.C., 1979, Slackwater deposits: A geomorphic technique for the interpretation of fluvial paleohydrology, *in* Rhodes, D.P., and Williams, G.P., eds., Adjustments of the Fluvial System: Dubuque, Iowa, Kendall/Hunt, p. 225–253.

Petrone, A., 1970, The Moses Lake sand dunes [M.S. thesis]: Pullman, Washington State University, 89 p.

Phillips, F.M., Leavy, B.D., Jannik, N.O., Elmore, D., and Kubik, P.W., 1986, The accumulation of cosmogenic chlorine-36 in rocks: A method for surface exposure dating: Science, v. 231, p. 41–43, doi:10.1126/science.231.4733.41.

Phillips, F.M., Zreda, M.G., Flinsch, M.R., Elmore, D., and Sharma, P., 1996, A reevaluation of cosmogenic ^{36}Cl production rates in terrestrial rocks: Geophysical Research Letters, v. 23, p. 949–952, doi:10.1029/96GL00960.

Phillips, F.M., Zreda, M.G., Plummer, M.A., Elmore, D., and Clark, D.H., 2009, Glacial geology and chronology of Bishop Creek and vicinity, eastern Sierra Nevada, California: Geological Society of America Bulletin, v. 121, p. 1013–1033, doi:10.1130/B26271.1.

Pierson, T.C., and Costa, J.E., 1987, A rheologic classification of subaerial sediment water flows, *in* Costa, J.E., and Wieczorek, G.F., eds., Debris Flows/Avalanches: Process, Recognition, and Mitigation: Geological Society of America Reviews in Engineering Geology, v. VII, p. 1–12, doi:10.1130/REG7-p1.

Pigati, J.S., and Lifton, N.A., 2004, Geomagnetic effects on time-integrated cosmogenic nuclide production rates with emphasis on ^{14}C and ^{10}Be: Earth and Planetary Science Letters, v. 226, p. 193–205, doi:10.1016/j.epsl.2004.07.031.

Pigati, J.S., Zreda, M., Zweck, C., Almasi, P.F., Elmore, D., and Sharp, W., 2008, Ages and inferred causes of Late Pleistocene glaciations on Mauna Kea, Hawai'i: Journal of Quaternary Science, v. 23, p. 683–702, doi:10.1002/jqs.1195.

Pluhar, C.J., Bjornstad, B.N., Reidel, S.P., Coe, R.S., and Nelson, P.B., 2006, Magnetostratigraphic evidence from the Cold Creek bar for onset of ice-age cataclysmic floods in eastern Washington during the early Pleistocene: Quaternary Research, v. 65, p. 123–135, doi:10.1016/j.yqres.2005.06.011.

Pogue, K.R., 1998, Earthquake-generated (?) structures in Missoula flood slackwater sediments (Touchet Beds) of southeastern Washington: Geological Society of America Abstracts with Programs, v. 30, no. 7, p. 398–399.

Pye, K., 1995, The nature, origin and accumulation of loess: Quaternary Science Reviews, v. 14, p. 653–667, doi:10.1016/0277-3791(95)00047-X.

Pye, K., and Tsoar, H., 1990, Aeolian Sand and Sand Dunes: London, Unwin Hyman, 396 p., doi:10.1007/978-94-011-5986-9.

Reidel, S.P., 1984, The Saddle Mountains: The evolution of an anticline in the Yakima fold belt: American Journal of Science, v. 284, p. 942–978, doi:10.2475/ajs.284.8.942.

Reidel, S.P., 2005, A lava flow without a source: The Cohasset Flow and its compositional components, Sentinel Bluffs Member, Columbia River Basalt Group: The Journal of Geology, v. 113, p. 1–21, doi:10.1086/425966.

Reidel, S.P., and Fecht, K.R., 1987, The Huntzinger flow: Evidence of surface mixing of the Columbia River Basalt and its petrogenetic implications: Geological Society of America Bulletin, v. 98, p. 664–677, doi:10.1130/0016-7606(1987)98<664:THFEOS>2.0.CO;2.

Reidel, S.P., and Hooper, P.B., eds., 1989, Volcanism and Tectonism in the Columbia River Flood-Basalt Province: Geologic Society of America Special Paper 239, 386 p.

Reidel, S.P., and Tolan, T.L., 1992, Eruption and emplacement of flood basalt: An example from the large-volume Teepee Butte Member, Columbia River Basalt Group: Geological Society of America Bulletin, v. 104, p. 1650–1671, doi:10.1130/0016-7606(1992)104<1650:EAEOFB>2.3.CO;2.

Reidel, S.P., Fecht, K.R., Hagood, M.C., and Tolan, T.L., 1989, The geologic evolution of the central Columbia Plateau, *in* Reidel, S.P., and Hooper, P.R., eds., Volcanism and Tectonism in the Columbia River Flood-Basalt Province: Geological Society of America Special Paper 239, p. 247–264, doi:10.1130/SPE239-p247.

Reidel, S.P., Lindsey, K.A., and Fecht, K.R., 1992, Field Trip Guide to the Hanford Site: Richland, Washington, Westinghouse Hanford Company, WHC-MR-0391, 50 p.

Reidel, S.P., Camp, V.E., Tolan, T.L., and Martin, B.S., 2013, The Columbia River flood basalt province: Stratigraphy, areal extent, volume, and physical volcanology, *in* Reidel, S.P., Camp, V.E., Ross, M.E., Wolff, J.A., Martin, B.S., Tolan, T.L., and Wells, R.E., eds., The Columbia River Basalt Province: Geological Society of America Special Paper 497, p. 1–43, doi:10.1130/2013.2497(01).

Richardson, K., and Carling, P.A., 2005, A Typology of Sculpted Forms in Open Bedrock Channels: Geological Society of America Special Paper 392, 108 p., doi:10.1130/0-8137-2392-2.1.

Richmond, G.M., Fryxell, R., Neff, G.E., and Weiss, P.L., 1965, The Cordilleran Ice Sheet of the northern Rocky Mountains and related Quaternary history of the Columbia Plateau, *in* Wright, H.E., Jr., and Frey, D.G., eds., The Quaternary of the United States: Princeton, New Jersey, Princeton University Press, p. 231- 242.

Rigby, J.G., 1982, The sedimentology, mineralogy, and depositional environment of a sequence of Quaternary catastrophic flood-derived lacustrine turbidites near Spokane, Washington [M.S. thesis]: Moscow, Idaho, University of Idaho, 132 p.

Russell, A.J., and Knudsen, Ó., 1999a, An ice-contact rhythmite (turbidite) succession deposited during the November 1996 catastrophic outburst flood (jökulhlaup), Skeidarárjökull, Iceland: Sedimentary Geology, v. 127, p. 1–10, doi:10.1016/S0037-0738(99)00024-X.

Russell, A.J., and Knudsen, Ó., 1999b, Controls on the sedimentology of the November jökulhlaup deposits, Skeidarársandur, Iceland, *in* Smith, N.D., and Rogers, J., eds., Fluvial Sedimentology VI: International Association of Sedimentology Special Publication 28, p. 315–329, doi:10.1002/9781444304213.ch23.

Russell, I.C., 1893, Geologic Reconnaissance in Central Washington: U.S. Geological Survey Bulletin 108, 108 p.

Salisbury, R.D., 1901, Glacial work in the western mountains in 1901: The Journal of Geology, v. 9, p. 718–731, doi:10.1086/620970.

Schatz, J.K., 1996, Provenance and depositional histories of the Smith Canyon and Sand Hills Coulee dunes, south-central, Washington [M.S. thesis]: Pullman, Washington State University, 87 p.

Self, S., Thordarson, Th., Keszthelyi, L., Walker, G.P.L., Hon, K., Murphy, M.T., Long, P., and Finnemore, S., 1996, A new model for the emplacement of Columbia River basalts as large inflated pahoehoe flow fields: Geophysical Research Letters, v. 23, p. 2689–2692, doi:10.1029/96GL02450.

Self, S., Thordarson, Th., and Keszthelyi, L., 1997, Emplacement of continental flood basalt lava flows, *in* Mahoney, J.J., and Coffin, M., eds., Large Igneous Provinces: Continental, Oceanic, and Planetary Flood Volcanism: American Geophysical Union Geophysical Monograph 100, p. 381–410, doi:10.1029/GM100p0381.

Shao, Y., Raupach, M.R., and Findlater, P.A., 1993, Effect of saltation bombardment on the entrainment of dust by wind: Journal of Geophysical Research, v. 98, no. D7, p. 12,719–12,726, doi:10.1029/93JD00396.

Shaw, H.R., and Swanson, D.A., 1970, Eruption and flow rates of flood basalt, *in* Gilmore, E.H., and Stradling, D.F., eds., Proceedings of the Second Columbia River Basalt Symposium, East: Cheney, Washington State College Press, p. 271–299.

Shaw, J., Munro-Stasiuk, M., Sawyer, B., Beaney, C., Lesemann, J.E., Musacchio, A., Rains, B., and Young, R.R., 1999, The Channeled Scabland: Back to Bretz?: Geology, v. 27, p. 605–608, doi:10.1130/0091-7613(1999)027<0605:TCSBTB>2.3.CO;2.

Shaw, J., Munro-Stasiuk, M., Sawyer, B., Beaney, C., Lesemann, J.E., Musacchio, A., Rains, B., and Young, R.R., 2000, The Channeled Scabland: Back to Bretz?: Comment and Reply: Geology, v. 27, p. 576.

Simons, D.B., Richardson, E.V., and Nordin, C.F., 1965, Sedimentary structures generated by flow in alluvial channels, *in* Middleton, G.V., ed., Primary Sedimentary Structures and Their Hydrodynamic Interpretation: Society for Sedimentary Geology (SEPM) Special Publication 12, p. 34–52, doi:10.2110/pec.65.08.0034.

Smith, G.A., 1986, Coarse-grained nonmarine volcaniclastic sediment: Terminology and depositional process: Geological Society of America Bulletin, v. 97, p. 1–10, doi:10.1130/0016-7606(1986)97<1:CNVSTA>2.0.CO;2.

Smith, G.A., 1993, Missoula flood dynamics and magnitudes inferred from sedimentology of slackwater deposits on the Columbia Plateau, Washington: Geological Society of America Bulletin, v. 105, p. 77–100, doi:10.1130/0016-7606(1993)105<0077:MFDAMI>2.3.CO;2.

Smith, G.A., and Lowe, D.R., 1991, Lahars: Volcano-hydrologic events and deposition in the debris flow-hyperconcentrated flow continuum, *in* Fisher, R.V., and Smith, G.A., eds., Sedimentation in Volcanic Settings: Society for Sedimentary Geology (SEPM) Special Publication 45, p. 59–70, doi:10.2110/pec.91.45.0059.

Smith, G.D., 1992, Sedimentology, stratigraphy, and geoarcheology of the Tsulim site, on the Hanford Site, Washington [M.S. thesis]: Pullman, Washington State University, 169 p.

Smith, L.N., 2006, Stratigraphic evidence for multiple drainings of glacial Lake Missoula along the Clark Fork River, Montana, USA: Quaternary Research, v. 66, p. 311–322, doi:10.1016/j.yqres.2006.05.009.

Smith, L.N., and Hanson, M.A., 2014, Sedimentary record of glacial Lake Missoula along the Clark Fork River from deep to shallow positions in the former lakes: St. Regis to near Drummond, Montana, *in* Shaw, C.A., and Tikoff, B., eds., Exploring the Northern Rocky Mountains: Geological Society of America Field Guide 37, p. 51–63, doi:10.1130/2014.0037(02).

Stetler, L.D., and Gaylord, D.R., 1996, Evaluating eolian-climatic interactions using a regional climate model from Hanford, Washington (USA): Geomorphology, v. 17, p. 99–113, doi:10.1016/0169-555X(95)00097-O.

Stoffel, K.L., Joseph, N.L., Waggoner, S.Z., Gulick, C.W., Korosec, M.A., and Bunning, B.B., 1991, Geologic Map of Washington—Northeast Quadrant: Washington Division of Geology and Earth Resources Geologic Map GM-39, scale 1:250,000.

Stradling, D.F., and Kiver, E.P., 1986, The significance of volcanic ash as a stratigraphic marker for the late Pleistocene in northeastern Washington, *in* Keller, S.A.C., ed., Mount St. Helens: Five Years After: Cheney, Washington, Eastern Washington University Press, p. 120–126.

Swanson, D.A., Wright, T.L., and Helz, R.T., 1975, Linear vent systems and estimated rates of magma production and eruption for the Yakima Basalt on the Columbia Plateau: American Journal of Science, v. 275, p. 877–905, doi:10.2475/ajs.275.8.877.

Sweeney, M.R., Busacca, A.J., and Gaylord, D.R., 2000, Eolian facies of the Palouse region, Pacific Northwest: Clues to controls on thick loess accumulation: Geological Society of America Abstracts with Programs, v. 32, no. 7, p. 22.

Sweeney, M.R., Busacca, A.J., and Gaylord, D.R., 2005, Topographic and climatic influences on accelerated loess accumulation since the last glacial maximum in the Palouse, Pacific Northwest, USA: Quaternary Research, v. 63, p. 261–273, doi:10.1016/j.yqres.2005.02.001.

Sweeney, M.R., Gaylord, D.R., and Busacca, A.J., 2007, Evolution of Eureka Flat: A dust-producing engine of the Palouse loess, USA: Quaternary International, v. 162–163, p. 76–96, doi:10.1016/j.quaint.2006.10.034.

Symons, T.W., 1882, Report of an Examination of the Upper Columbia River: U.S. Congress, Senate, 47th Congress, First Session, Senate Document, no. 186.

Thordarson, Th., and Self, S., 1998, The Roza Member, Columbia River Basalt Group: A gigantic pahoehoe lava flow field formed by endogenous processes?: Journal of Geophysical Research, v. 103, p. 27,411–27,445, doi:10.1029/98JB01355.

Tinkler, K.J., and Wohl, E.E., eds., 1998, Rivers over Rock: Fluvial Processes in Bedrock Channels: Washington, D.C., American Geophysical Union Monograph 107, 322 p., doi:10.1029/GM107.

Tolan, T.L., Reidel, S.P., Beeson, M.H., Anderson, J.L., Fecht, K.R., and Swanson, D., 1989, Revisions to the estimates of the areal extent and volume of the Columbia River Flood Basalt Province, *in* Reidel, S.P., and Hooper, P.R., eds., Volcanism and Tectonism in the Columbia River Flood-Basalt Province: Geological Society of America Special Paper 239, p. 1–20, doi:10.1130/SPE239-p1.

TUFLOW, 2016, TUFLOW User Manual: Build 2016-03-AA, 663 p., online at http://www.tuflow.com/Download/TUFLOW/Releases/2016-03/AA/Doc/TUFLOW%20Manual.2016-03-AA.pdf (accessed 30 March 2016).

Waitt, R.B., 1980, About forty last-glacial Lake Missoula jökulhlaups through southern Washington: The Journal of Geology, v. 88, p. 653–679, doi:10.1086/628553.

Waitt, R.B., 1982, Surficial geology, *in* Geologic Map of the Wenatchee 1:100,000 Quadrangle, Washington: U.S. Geological Survey Miscellaneous Investigations Map I-1311.

Waitt, R.B., Jr., 1984, Periodic jökulhlaups from Pleistocene glacial Lake Missoula; New evidence from varved sediment in northern Idaho and Washington: Quaternary Research, v. 22, p. 46–58, doi:10.1016/0033-5894(84)90005-X.

Waitt, R.B., 1985, Case for periodic, colossal jökulhlaups from Pleistocene glacial Lake Missoula: Geological Society of America Bulletin, v. 96, p. 1271–1286, doi:10.1130/0016-7606(1985)96<1271:CFPCJF>2.0.CO;2.

Waitt, R.B., 1987, Erosional landscape and surficial deposits, *in* Tabor, R.W., Frizzell, V.A., Jr., Whetten, J.T., Waitt, R.B., Swanson, D.A., Byerly, G.R.,

Booth, D.B., Hetherington, M.J., and Zartman, R.E., Geologic Map of the Chelan 30-Minute by 60-Minute Quadrangle, Washington: U.S. Geological Survey Miscellaneous Investigations Map I-1661 scale 1:100,000, 29 p.

Waitt, R.B., 1994, Scores of gigantic, successively smaller Lake Missoula floods through Channeled Scabland and Columbia valley, *in* Swanson, D.A., and Haugerud, R.A., eds., Geologic Field Trips in the Pacific Northwest: Seattle, Department of Geological Sciences, University of Washington (Geological Society of America, 1994 Annual Meeting), v. 1, Chapter 1K, 88 p.

Waitt, R.G., Jr., and Thorson, R.M., 1983, The Cordilleran Ice Sheet in Washington, Idaho, and Montana, *in* Wright, H.E., Jr., ed., Late Quaternary Environments of the United States; Volume I, The Late Pleistocene: Minneapolis, University of Minnesota Press, p. 53–70.

Waitt, R.B., Denlinger, R.P., and O'Connor, J.E., 2009, Many monstrous Missoula floods down Channeled Scabland and Columbia Valley, *in* O'Connor, J.E., Dorsey, R.J., and Madin, I.P., eds., Volcanoes to Vineyards: Geologic Field Trips through the Dynamic Landscape of the Pacific Northwest: Geological Society of America Field Guide 15, p. 775–844, doi:10.1130/2009.fld015(33).

Washburn, A.L., 1988, Mima Mounds, an Evaluation of Proposed Origins with Special Reference to the Puget Lowland: Washington Division of Geology and Earth Resources Report of Investigations 29, 53 p.

Webster, G.D., Baker, V.R., and Gustafson, C., 1976, Channeled Scablands of Southeastern Washington: Pullman, Washington, Washington State University, Geological Society of America Cordilleran Section Meeting, Field Trip Guide No. 2, 25 p.

Whipple, K.X., Hancock, G.S., and Anderson, R.S., 2000, River incision into bedrock: Mechanics and relative efficacy of plucking, abrasion and cavitation: Geological Society of America Bulletin, v. 112, p. 490–503, doi: 10.1130/0016-7606(2000)112<490:RIIBMA>2.0.CO;2.

Whitlock, C., and Bartlein, P.J., 1997, Vegetation and climate change in northwest America during the past 125 kyr: Nature, v. 388, p. 57–61, doi:10.1038/40380.

Zreda, M., England, J., Phillips, F., Elmore, D., and Sharma, P., 1999, Unblocking of the Nares Strait by Greenland and Ellesmere ice-sheet retreat 10,000 years ago: Nature, v. 398, p. 139–142, doi:10.1038/18197.

Manuscript Accepted by the Society 18 March 2016